

**ABSORPTION OF CARBON DIOXIDE  
IN A SPRAY COLUMN**

**A Thesis**

**Submitted to the Faculty of Graduate Studies and Research**

**In Partial Fulfillment of the Requirements**

**for the Degree of**

**Master of Applied Science**

**In Industrial Systems Engineering**

**University of Regina**

**by**

**Jeffery Kuntz**

**Regina, Saskatchewan**

**July 2006**

**Copyright 2006: J. Kuntz**



Library and  
Archives Canada

Bibliothèque et  
Archives Canada

Published Heritage  
Branch

Direction du  
Patrimoine de l'édition

395 Wellington Street  
Ottawa ON K1A 0N4  
Canada

395, rue Wellington  
Ottawa ON K1A 0N4  
Canada

*Your file* *Votre référence*  
*ISBN: 978-0-494-20219-7*  
*Our file* *Notre référence*  
*ISBN: 978-0-494-20219-7*

**NOTICE:**

The author has granted a non-exclusive license allowing Library and Archives Canada to reproduce, publish, archive, preserve, conserve, communicate to the public by telecommunication or on the Internet, loan, distribute and sell theses worldwide, for commercial or non-commercial purposes, in microform, paper, electronic and/or any other formats.

The author retains copyright ownership and moral rights in this thesis. Neither the thesis nor substantial extracts from it may be printed or otherwise reproduced without the author's permission.

**AVIS:**

L'auteur a accordé une licence non exclusive permettant à la Bibliothèque et Archives Canada de reproduire, publier, archiver, sauvegarder, conserver, transmettre au public par télécommunication ou par l'Internet, prêter, distribuer et vendre des thèses partout dans le monde, à des fins commerciales ou autres, sur support microforme, papier, électronique et/ou autres formats.

L'auteur conserve la propriété du droit d'auteur et des droits moraux qui protègent cette thèse. Ni la thèse ni des extraits substantiels de celle-ci ne doivent être imprimés ou autrement reproduits sans son autorisation.

---

In compliance with the Canadian Privacy Act some supporting forms may have been removed from this thesis.

Conformément à la loi canadienne sur la protection de la vie privée, quelques formulaires secondaires ont été enlevés de cette thèse.

While these forms may be included in the document page count, their removal does not represent any loss of content from the thesis.

Bien que ces formulaires aient inclus dans la pagination, il n'y aura aucun contenu manquant.

  
**Canada**

**UNIVERSITY OF REGINA**

**FACULTY OF GRADUATE STUDIES AND RESEARCH**

**SUPERVISORY AND EXAMINING COMMITTEE**

Jeffery Kuntz, candidate for the degree of Master of Applied Science, has presented a thesis titled, ***Absorption of Carbon Dioxide in a Spray Column***, in an oral examination held on April 27, 2006. The following committee members have found the thesis acceptable in form and content, and that the candidate demonstrated satisfactory knowledge of the subject material.

External Examiner:        Dr. Mingzhe Dong, Faculty of Engineering

Supervisor:                 Dr. Adisorn Aroonwilas, Faculty of Engineering

Committee Member:        Dr. Muhammad Ayub, Faculty of Engineering

Committee Member:        Dr. Liming Dai, Faculty of Engineering

Chair of Defense:            Dr. Daryl Hepting, Department of Computer Science

## Abstract

The capture of carbon dioxide (CO<sub>2</sub>) from industrial gas streams is considered to be one of the potential approaches to reduce the greenhouse gas emissions and alleviate the problem of global warming. The CO<sub>2</sub> capture can be achieved through several techniques, including gas absorption into a liquid solvent. The performance of the CO<sub>2</sub> absorption process relies on efficient mass transfer characteristics of gas-liquid contacting devices. The most common contacting device in CO<sub>2</sub> absorption application is the packed column filled with a variety of packing materials such as random-type and structured-type packing. The spray column is an alternative contacting device capable of providing a great extent of gas-liquid contact. The spray column has been commonly used in applications to remove sulfur dioxide (SO<sub>2</sub>) from flue gas. There is however little knowledge and published data on the performance of the spray column for the removal of CO<sub>2</sub>.

This thesis provides a better understanding of mass transfer performance of the spray column used in CO<sub>2</sub> absorption application. The performance was tested experimentally for the removal of CO<sub>2</sub> from a simulated gas stream by using an aqueous solution of monoethanolamine (MEA) as the absorption solvent. More than 400 experimental runs were carried out in two 10-cm diameter absorption columns under wide ranges of process conditions. The overall rate of mass transfer was measured by collecting and analyzing samples of the simulated gas and liquid solvent, entering and leaving the columns. The performance of the spray was evaluated from the measured mass transfer rate and presented in terms of the volumetric overall mass transfer coefficient ( $K_G a_e$ ) as a function of process variables. Such variables include the gas flow

rate (15 – 764 m<sup>3</sup>/m<sup>2</sup>\*h), liquid flow rate (1.3 – 10.3 m<sup>3</sup>/m<sup>2</sup>\*h), gas-phase CO<sub>2</sub> concentration (5 – 15%), MEA concentration of the liquid (3 – 7 kmol/m<sup>3</sup>), CO<sub>2</sub> loading of the liquid (0.00 – 0.45 mol/mol), and spray nozzle type. It was found that the mass transfer performance of the spray column varies significantly with the tested variables. The effect of each variable was quantified. The results produced have also been further analyzed to arrive at the fundamental mass transfer characteristics, especially the effective mass transfer area ( $a_e$ ) and the gas-phase mass transfer coefficient ( $k_G$ ).

The mass transfer performance of the spray column was directly compared to the performance of a packed column (Mellapak 500Y, Switzerland), which was also tested under identical conditions as the reference in this thesis. The superior performance of the spray column was evident from the comparison, demonstrating the potential of using the spray column in the CO<sub>2</sub> removal application.

## **Acknowledgements**

I wish to express my gratitude to Dr. Adisorn Aroonwilas, my supervisor, for his endless support and guidance. I am very grateful for the opportunity he has provided me in my pursuit of my Master of Applied Science degree. I am also grateful to all of the assistance provided by the members of the CO<sub>2</sub> research group at the University of Regina.

The financial support provided to me by Dr. Aroonwilas and the Faculty of Engineering at the University of Regina is gratefully appreciated. I also acknowledge the support of Sulzer Brothers Ltd. (Switzerland), who provided the structured packing at no cost.

Finally, I wish to thank my parents, brothers and girlfriend for their support of my graduate education.

## Table of Contents

	Page
<b>Abstract</b> .....	i
<b>Acknowledgements</b> .....	iii
<b>Table of Contents</b> .....	iv
<b>List of Tables</b> .....	vii
<b>List of Figures</b> .....	viii
<b>Nomenclature</b> .....	xi
<b>Chapter One: Introduction</b> .....	1
<b>1.1 Global Climate Change and Carbon Dioxide Emissions</b> .....	1
<b>1.2 Current Policies for CO<sub>2</sub> Emission Reduction</b> .....	4
<b>1.2.1 United Nations Framework Convention on Climate Change</b> .....	4
<b>1.2.2 Kyoto Protocol and Canada</b> .....	5
<b>1.2.3 Greenhouse Gas Protocol Initiative</b> .....	6
<b>1.3 CO<sub>2</sub> Capture Technology</b> .....	6
<b>1.3.1 CO<sub>2</sub> Absorption Process</b> .....	8
<b>1.3.2 Performance of CO<sub>2</sub> Absorption</b> .....	9
<b>1.4 Limitation of Knowledge</b> .....	10
<b>1.5 Research Objectives</b> .....	14
<b>Chapter Two: Literature Review and Fundamentals</b> .....	15
<b>2.1 Mass Transfer Principles</b> .....	15
<b>2.1.1 Mass Transfer with Chemical Reaction</b> .....	20
<b>2.1.2 Determination of Overall Mass Transfer Coefficient</b> .....	23

<b>2.2 CO<sub>2</sub> Absorption Reactions</b> .....	25
<b>2.3 General Thermodynamic Framework</b> .....	27
<b>2.4 Gas Liquid Contactors</b> .....	28
<b>2.4.1 Packed Column</b> .....	28
<b>2.4.2 Tray Column</b> .....	31
<b>2.4.3 Spray Column</b> .....	33
<b>2.4.4 Comparison of Spray, Packed and Tray Columns</b> .....	35
<b>2.4.5 Limitations of the Previous Studies on CO<sub>2</sub> Absorption using Spray         Column</b> .....	35
<b>Chapter Three: Experimental Apparatus and Procedures</b> .....	41
<b>3.1 Experimental Apparatus</b> .....	41
<b>3.1.1 Absorption Columns</b> .....	41
<b>3.1.2 Auxiliary Equipment</b> .....	42
<b>3.2 Absorption Experiment Procedures</b> .....	54
<b>3.3 Sample Analysis</b> .....	55
<b>Chapter Four: Results and Discussion</b> .....	61
<b>4.1 Effects of Process Parameters on Mass Transfer Coefficient</b> .....	63
<b>4.1.1 Effect of CO<sub>2</sub> Partial Pressure</b> .....	63
<b>4.1.2 Effect of Gas Flow Rate</b> .....	66
<b>4.1.3 Effect of Liquid Flow Rate</b> .....	70
<b>4.1.4 Effect of MEA Concentration</b> .....	74
<b>4.1.5 Effect of CO<sub>2</sub> Loading</b> .....	75
<b>4.1.6 Effect of Nozzle Size</b> .....	75

<b>4.2 Spray versus Packed Column</b> .....	81
<b>Chapter Five: Theoretical Analysis of Data</b> .....	84
<b>5.1 Effective Mass Transfer Area</b> .....	84
<b>5.2 Gas-Phase Mass Transfer Coefficient (<math>k_G</math>)</b> .....	90
<b>Chapter Six: Conclusion and Future Work</b> .....	98
<b>6.1 Conclusions</b> .....	98
<b>6.2 Recommendations for Future Work</b> .....	100
<b>References</b> .....	101
<b>Appendix A: Data from spray column and packed column</b> .....	105
<b>Appendix A1 – P-20 Nozzle Data</b> .....	106
<b>Appendix A2 – P-28 Nozzle Data</b> .....	111
<b>Appendix A3 – P-40 Nozzle Data</b> .....	114
<b>Appendix A4 – Packed Column Data</b> .....	115
<b>Appendix B: Economics of spray and packed column.</b> .....	116

## List of Tables

<b>Table 2.1:</b>	Comparison of packed, tray and spray columns .....	37
<b>Table 2.2:</b>	Previous work with spray columns .....	38
<b>Table 3.1:</b>	Specifications of spray nozzles used in the present study .....	50
<b>Table 3.2:</b>	Geometric features of the structured packing .....	52
<b>Table 3.3:</b>	Operating conditions of spray and packed columns .....	59
<b>Table 4.1:</b>	Typical results from an experimental run .....	62
<b>Table 4.2:</b>	Operating ranges of spray nozzles tested .....	79
<b>Table 5.1:</b>	Comparison of packed column and spray column with [MEA] = 5 kmol/m <sup>3</sup> , gas flowrate = 382 m <sup>3</sup> /m <sup>2</sup> *h, 15 kPa CO <sub>2</sub> .....	94

## List of Figures

<b>Figure 1.1:</b>	Process flow diagram of CO <sub>2</sub> absorption unit.....	11
<b>Figure 1.2:</b>	Physical and chemical solvents for acid gas removal .....	12
<b>Figure 2.1:</b>	Concentration profiles of diffusing component A in gas and liquid phases (Treybal, 1980) .....	17
<b>Figure 2.2:</b>	Film Theory (modified from Astarita et al., 1983) .....	21
<b>Figure 2.3:</b>	Gas-phase and liquid phase concentration profiles for different kinetic regimes. (Levenspiel, 1999).....	24
<b>Figure 2.4:</b>	Schematic sketches of columns .....	29
<b>Figure 3.1:</b>	Schematic drawing of CO <sub>2</sub> absorption apparatus .....	44
<b>Figure 3.2:</b>	Photograph of the experimental apparatus.....	45
<b>Figure 3.3:</b>	Photograph of spray column .....	46
<b>Figure 3.4:</b>	Scale drawing of spray column.....	47
<b>Figure 3.5:</b>	Photograph of packed column .....	48
<b>Figure 3.6:</b>	Scale drawing of packed column .....	49
<b>Figure 3.7:</b>	Photograph of spray nozzles used in the present study.....	51
<b>Figure 3.8:</b>	Photograph of structured packing used in the present study.....	53
<b>Figure 3.9:</b>	Packed column liquid distributor .....	57
<b>Figure 3.10:</b>	Scale drawing of packed column top .....	58
<b>Figure 3.11:</b>	Gas Measuring Apparatus for CO <sub>2</sub> loading determination .....	60
<b>Figure 4.1:</b>	Effect of CO <sub>2</sub> partial pressure and gas flow rate on overall mass transfer at CO <sub>2</sub> loading of 0.0 and 0.25 mole/mole. (Nozzle = P-20, Liquid flow rate = 1.53 m <sup>3</sup> /m <sup>2</sup> -h).....	64

<b>Figure 4.2:</b>	Effect of CO <sub>2</sub> partial pressure on overall mass transfer. (Nozzle = P-20, Liquid flow rate = 1.53 m <sup>3</sup> /m <sup>2</sup> -h, Gas flow rate = 382 – 764 m <sup>3</sup> /m <sup>2</sup> -h)....	65
<b>Figure 4.3:</b>	Effect of gas flow rate on overall mass transfer at different CO <sub>2</sub> loadings (Nozzle = P-20, Liquid flow rate = 1.53 m <sup>3</sup> /m <sup>2</sup> -h, [MEA]=3M).....	68
<b>Figure 4.4:</b>	Effect of gas flow rate on overall mass transfer at different liquid flow rates (Nozzle = P-28, P <sub>CO2</sub> =15 kPa, [MEA]=5M) .....	69
<b>Figure 4.5:</b>	Effect of liquid flow rate on overall mass transfer of P-20 nozzle at different CO <sub>2</sub> loadings (P <sub>CO2</sub> =15 kPa, [MEA] =3M, Gas flow rate=76 m <sup>3</sup> /m <sup>2</sup> -h).....	71
<b>Figure 4.6:</b>	Effect of liquid flow rate on overall mass transfer of P-28 nozzle at different CO <sub>2</sub> loadings (P <sub>CO2</sub> =15 kPa, [MEA] =5M, Gas flow rate=382 m <sup>3</sup> /m <sup>2</sup> -h).....	72
<b>Figure 4.7:</b>	Effect of liquid flow rate on overall mass transfer of P-40 nozzle at different CO <sub>2</sub> loadings (P <sub>CO2</sub> =15 kPa, [MEA] =5M, Gas flow rate=382 m <sup>3</sup> /m <sup>2</sup> -h).....	73
<b>Figure 4.8:</b>	Effect of the concentration of the MEA on overall mass transfer at CO <sub>2</sub> loadings of 0.00 and 0.25 mole/mole respectively (Nozzle=P-20, P <sub>CO2</sub> =15 kPa) .....	77
<b>Figure 4.9:</b>	Effect of CO <sub>2</sub> loading on overall mass transfer for different nozzles (for P-20 nozzle, P <sub>CO2</sub> =15 kPa, [MEA] =3M, Gas flow rate=76 m <sup>3</sup> /m <sup>2</sup> -h, Liquid flow rate = 1.53 m <sup>3</sup> /m <sup>2</sup> -h; for P-28 nozzle, P <sub>CO2</sub> =15 kPa, [MEA] =5M, Gas flow rate=382 m <sup>3</sup> /m <sup>2</sup> -h, Liquid flow rate = 4.59 m <sup>3</sup> /m <sup>2</sup> -h; and for P-40	

	nozzle, $P_{CO_2}=15$ kPa, $[MEA] =5M$ , Gas flow rate= $382$ $m^3/m^2-h$ , Liquid flow rate= $10.32$ $m^3/m^2-h$ ) ..... 78	78
<b>Figure 4.10:</b>	Effect of the nozzle size on overall mass transfer and liquid flow rate (Gas flow rate= $382$ $m^3/m^2-h$ , $P_{CO_2}=15\%$ $CO_2$ , $[MEA]=5$ $kmol/m^3$ )..... 80	80
<b>Figure 4.11:</b>	Mass transfer performance comparison between the packed column and spray column at the same operating conditions ..... 83	83
<b>Figure 5.1:</b>	Linear relationship between $(1/K_G a_e)$ and $(H/k_L)$ for analysis of effective mass transfer area..... 86	86
<b>Figure 5.2:</b>	An increase in effective mass transfer area with liquid flow rate for P-28 nozzle (Gas flow rate= $382$ $m^3/m^2-h$ , $P_{CO_2}=15\%$ $CO_2$ , $[MEA] =3$ $kmol/m^3$ ) ..... 89	89
<b>Figure 5.3:</b>	Contribution of reduction in droplet size and number of spray droplet to effective mass transfer area..... 91	91
<b>Figure 5.4:</b>	Effective mass transfer area at different MEA concentrations (Nozzle P- 28, Gas flow rate= $382$ $m^3/m^2-h$ , $P_{CO_2}=15\%$ ). ..... 92	92
<b>Figure 5.5:</b>	Effect of nozzle size on effective mass transfer area (Gas flow rate= $382$ $m^3/m^2-h$ , $P_{CO_2}=15\%$ ). ..... 93	93
<b>Figure 5.6:</b>	Gas-phase mass transfer coefficient of P-28 nozzle. .... 96	96
<b>Figure 5.7:</b>	Gas-phase mass transfer coefficient and Onda et al correlation. .... 97	97

## Nomenclature

$a_e$	effective interfacial area, $m^2/m^3$
$a_t$	surface area of packing
$C_1$	constant for equation
$C_A$	concentration of component A, $kmol/m^3$
$C_{A,1}$	concentration of component A at beginning of transfer path, $kmol/m^3$
$C_{A,2}$	concentration of component A at beginning of transfer path, $kmol/m^3$
$C_{A,i}$	concentration of component A at gas-liquid interface, $kmol/m^3$
$C_{A,L}$	concentration of component A in liquid bulk, $kmol/m^3$
$C_{B,L}$	concentration of reactant B in liquid bulk, $kmol/m^3$
$C_{MEA}$	concentration of active MEA in aqueous solution
$C_{solution}$	concentration of active MEA in solution
$CO_2$	carbon dioxide
$CO_3^{2-}$	carbonate ion
$D_{A,L}$	diffusion coefficient of component A in liquid, $m^2/s$
$D_{A,solvent}$	diffusion coefficient of component A in solvent, $m^2/s$
$D_{A,water}$	diffusion coefficient of component A in water, $m^2/s$
$D_{CO_2,L}$	diffusion coefficient of $CO_2$ in aqueous solution
$D_{CO_2,Water}$	diffusion coefficient of $CO_2$ in water
DEA	Diethanolamine
$D_G$	gas-phase diffusion coefficient
$D_m$	maximum drop diameter in spray, ft
$D_p$	equivalent diameter of packing

$d_0$	nozzle orifice diameter, ft
$G$	gas flow rate
$G_I$	inert gas velocity, $\text{kmol/m}^2\text{-s}$
$H$	Henry's constant, $\text{kPa}\cdot\text{m}^3/\text{kmol}$
$\text{H}^+$	hydrogen ion
$\text{H}_3\text{O}^+$	hydronium ion
$\text{HCO}_3^-$	bicarbonate ion
$H'_i$	Henry constant for pure components
$h_+$	van Krevelen coefficient for cation
$h_-$	van Krevelen coefficient for anion
$h_g$	coefficient for dissolving gas
$I$	enhancement factor
$K_G$	overall gas mass transfer coefficient, $\text{kmol/m}^2\text{-s}\cdot\text{kPa}$
$K_L$	overall liquid mass transfer coefficient, $\text{m/s}$
$k_G$	gas mass transfer coefficient, $\text{kmol/m}^2\text{-s}\cdot\text{kPa}$
$k_L$	chemical liquid mass transfer coefficient, $\text{m/s}$
$k_L^\circ$	physical liquid mass transfer coefficient, $\text{m/s}$
$k_2$	second-order reaction rate constant, $\text{m}^3/\text{kmol}\cdot\text{s}$
MEA	monoethanolamine
$m$	meter
mm	millimeter
$m_i$	mass fraction of water or amine
$N_A$	mass transfer flux of component A, $\text{kmol/m}^2\text{-s}$

NaOH	sodium hydroxide
OH <sup>-</sup>	hydroxide ion
P	total pressure, kPa
P <sub>CO2</sub>	partial pressure of CO <sub>2</sub> , kPa
RR'NCOO <sup>-</sup>	carbamate ion
RR'NH	amine
RR'NH <sub>2</sub> <sup>+</sup>	protonated amine ion
RR'NH <sup>+</sup> COO <sup>-</sup>	zwitterions
r	rate of chemical reaction, kmol/m <sup>3</sup> -s
T	absolute temperature, K
u <sub>r</sub>	relative velocity of liquid with respect to the gas, ft/s
w	MEA weight percent concentration
x	distance from gas-liquid interface
Y <sub>A</sub>	mole fraction of component A in gas phase
Y <sub>A,G</sub>	mole ratio of component A in bulk gas
y <sub>A</sub> <sup>*</sup>	mole fraction of component A in equilibrium with liquid bulk concentration
Y <sub>A,G</sub>	mole fraction of component A in gas bulk
Y <sub>A,i</sub>	mole fraction of component A at gas-liquid interface
Z	total column height

**Greek Letters**

α <sub>CO2</sub>	CO <sub>2</sub> loading of liquid solution, mol CO <sub>2</sub> /mol amine
------------------	--

$\lambda$	thickness of liquid film boundary, m
$\mu$	viscosity, Pa-s or lb/ft*s
$\rho$	density, lb/ft <sup>3</sup>
$\sigma$	surface tension, lb/s

**Subscripts**

G	gas phase
L	liquid phase

# **Chapter One**

## **Introduction**

### **1.1 Global Climate Change and Carbon Dioxide Emissions**

Global climate change has become a very important area of study in recent years. The introduction of the Kyoto agreement has brought Greenhouse Gases (GHGs) such as methane (CH<sub>4</sub>), carbon dioxide (CO<sub>2</sub>), nitrous oxide (N<sub>2</sub>O), and halogens to the front line of strategies to control climate change. The goal of the agreement is to reduce global emissions of those gases that are harmful to human and the environment. There has been a large amount of data published on the increase in the earth's temperature (EPA, 2006; DOE, 2006; Overview of Climate Change Research, 2005). It is noted that during the twentieth century the average temperature of the earth's surface has increased about  $0.6 \pm 0.2^\circ \text{C}$  (Overview of Climate Change Research, 2005). The increase is attributed largely to human activities such as the consumption of fossil fuels at the present rate. The production of large amounts of CO<sub>2</sub> is mostly to blame as it traps heat energy from the sun near the surface of the earth. The warming of the earth's surface is believed to have caused a reduction in snow cover and floating ice in the Northern hemisphere (Overview of Climate Change Research, 2005). This has led to a rise in the sea level of about 4 to 8 inches over the past century. It is also responsible for the more frequent extreme rainfalls that are taking place through much of the United States. At present, researchers believe that in the next century the temperature could rise as much as 1.4 to 5.8°C which would lead to higher water evaporation, resulting in more intense rainstorms, a decrease in soil

moisture and quality and the sea level is expected to rise two feet along coast lines (EPA: Global Warming: Climate, 2006).

The increased amount of CO<sub>2</sub> can be analyzed in regards to four different but interconnected areas of the earth, i.e. atmosphere, hydrosphere, cryosphere, and biosphere (Overview of Climate Change Research, 2005). The atmosphere is the earth portion where the greenhouse effect is most prevalent. The earth receives energy from the sun, and some of the energy is absorbed by greenhouse gases such as CO<sub>2</sub> while the remaining energy is reflected back to the space. This energy absorption process is necessary as it allows the earth to maintain an average temperature of about 15°C. However, with the increase in concentration of these greenhouse gases, there is more energy being trapped in the atmosphere causing the temperature to rise. A large portion of these gases is produced from the burning of fossil fuels. It is believed that the increase in the temperature of the atmosphere has led to the changes in weather patterns, resulting in flooding, drought and increased storm strength.

The hydrosphere will also be affected by the global warming problem. The ocean, capable of storing much larger amounts of energy compared to the atmosphere, is responsible for transporting heat around the world, i.e. from the equatorial regions to the poles. This transfer of heat keeps areas in the north and the south at a livable temperature. For instance, the Gulf Stream carries heat from the Gulf of Mexico to northwest Europe, providing a milder climate for Europe when compared to areas of the same latitude. The Gulf Stream travels north due to the evaporation of water near the European region causing colder waters to exist. The colder water sinks due to density and the warmer surface water flows in to take its place. If global warming causes the

ocean temperature to rise, it is possible that this ocean current could end and local climates will change.

The cryosphere is another important element affected by global warming. The areas that are covered with ice and snow are responsible for reflecting a large amount of the solar energy back to space. With the rising surface temperature, the ice and snow will melt in a faster rate which will lead to a smaller reflective surface and less reflected solar energy, thus resulting in a warming trend. This change in snow and ice cover affects air temperature, ocean currents, storm patterns and the sea level. The simulation results from several climate models demonstrate that the Arctic region has already been impacted (Overview of Climate Change Research, 2005). Temperatures taken in the Arctic show that it is at the warmest temperature recorded in the last 400 years (Overview of Climate Change Research, 2005).

The effects of global warming on the biosphere (or the world of plants and animals) are difficult to measure. However, it is realized that certain species inhabiting certain areas around the world would become extinct if the climate begins to alternate too drastically. When disruptions occur in the food chain, it is then very difficult to trace all the problems that will arise from the climate change.

The excessive emissions of CO<sub>2</sub> from human activities are considered to be the major contributor to the global warming problem. The main source of the emissions is from the utilization of liquid fuels and the combustion of coal for power generation. The increase has been dated back to 1950. According to Marland et al, (2005), from 1950 to 1974 the total CO<sub>2</sub> emissions in Canada have increased by a factor of 2.4. The emissions continued to grow and then there was a level off period in the early 1980's. After 1987,

the emissions continued to grow at a constant rate and reached their peak in 2002 at a level of 140 million metric tons of carbon. In 2002, the Canadian coal industry produced 20 percent of the total fossil fuel CO<sub>2</sub> emissions, 50 percent was derived from the consumption of liquid fuels, and the natural gas industry contributed about 28 percent of the total. It was estimated that each Canadian was producing 4.49 metric tons of carbon, which is considered to be one of the highest averages among the leaders of the fossil fuel CO<sub>2</sub> emitting nations (Marland et al, 2005).

## **1.2 Current Policies for CO<sub>2</sub> Emission Reduction**

Recently, many policies for the reduction of CO<sub>2</sub> emissions have been developed. Canada has committed to a number of these international policies, including the United Nations Framework Convention on Climate Change, the Kyoto Protocol, and the Greenhouse Gas Protocol Initiative.

### **1.2.1 United Nations Framework Convention on Climate Change**

The United Nations formed a committee to deal with climate change in 1988. The committee is called the United Nations Intergovernmental Panel on Climate Change (IPCC). They are recognized as the most authoritative scientific body on climate change. The IPCC periodically assesses the effects of climate change with the help from experts around the world. To date, there have been three comprehensive reports filed on the subject (Greenhouse Gases, Climate Change and the Canadian EPA, 1999). Through these reports, strong evidence in the need to reduce emissions of greenhouse gases has been demonstrated. It shows that climate change has become a serious environmental

issue that needs a global attempt to eliminate it. Recently, the IPCC has published a special report on CO<sub>2</sub> capture and storage, mapping out the ways in which the technology can be a key contributor in reaching reduction goals for emissions.

### **1.2.2 Kyoto Protocol and Canada**

Countries from around the world have all realized the need to take action in an attempt to reduce greenhouse gas emissions and address climate change issues. In 1997, more than 160 countries including Canada met in Kyoto Japan, and agreed that greenhouse gas controls needed to be implemented. The agreement is commonly known as the Kyoto Protocol that became legally binding when 55 countries and 55 per cent of the emissions were addressed (Canada and the Kyoto Protocol, 2001). Canada has been given an emission target to reach. The target is to reduce its greenhouse gas emissions to 6% below 1990 levels by the period between 2008 and 2012. To date, 61.6 per cent of the emissions have been addressed. The agreement is constantly being redefined and more mechanisms are being added in an effort to make it more probable that countries will be able to meet their targets. There are three major mechanisms that Canada is hoping to add to the Kyoto agreement. They are market-based instruments that will allow a country to earn or buy credits by helping other countries meet their targets. Credits can be earned by assisting developing countries in emission control or by partaking in emission reduction projects with countries that have already taken on a Kyoto target. Another option is also to buy or sell credits with developed countries that have taken on a Kyoto target. This allows countries that need more credits to easily obtain them, and also countries that have excess credits to make a profit.

### **1.2.3 Greenhouse Gas Protocol Initiative**

The Greenhouse Gas (GHG) Protocol Initiative is a tool that is attempting to organize GHG accounting and reporting standards internationally. This initiative will ensure that all of the different trading schemes and alternate climate related initiatives have a consistent approach to GHG accounting principles. It will simplify the comparison between trading schemes that are present within and outside of the Kyoto framework. The GHG Protocol is an international assembly of business, government organizations, non-government organizations that are all under the watch of the World Business Council for Sustainable Development (WBCSD) and the World Resource Institute (WRI). This assembly brings together leading experts on GHG emissions in an attempt to produce acceptable accounting procedures and reporting standards (The GHG Protocol Initiative, 2005). The GHG Protocol has two models that are followed. They are the Corporate GHG Accounting and Reporting Standard and the Project GHG Accounting and Reporting Standard. The corporate model is for use by companies and organizations to help them to be able to accurately report all of their emissions. The project model has been produced for use as a guideline in emissions reduction and land use as well as land use change and forestry.

### **1.3 CO<sub>2</sub> Capture Technology**

The CO<sub>2</sub> capture and sequestration is considered to be one of the potential approaches to reduce the total emissions and meet Kyoto targets that have been set out. The goal of the program is to collect the CO<sub>2</sub> emissions from industrial point sources and inject the collected CO<sub>2</sub> underground for storage. The injection sites include geological

caverns, coal deposits, and active or depleted oil reservoirs. The caverns are natural formations such as coal seams and aquifers that are capable of retaining the gas. The CO<sub>2</sub> could be injected into coal deposits for storage and at the same time for recovery of methane gas. In enhanced oil recovery application, the CO<sub>2</sub> could be injected into an oil reservoir in order to drive the oil out through the production wells. When the reservoir is completely depleted of oil, it would be capped and the injected CO<sub>2</sub> would be trapped underground (The Capture and Storage of Carbon Dioxide Emissions, 2001). The reason that the flue gas should not be injected directly into the ground is because of the volume of the flue gas, which is mainly nitrogen, and the amount of area it takes up. Since nitrogen does not harm the environment it is more beneficial to remove it and store only the captured CO<sub>2</sub> underground. This will allow for a much larger amount of CO<sub>2</sub> to be stored in the reservoirs or caverns.

The capture of CO<sub>2</sub> can be achieved through several techniques, including gas absorption into a liquid, adsorption on a solid, permeation through a membrane, and cryogenic separation. Gas absorption refers to the transfer of a selected gas component from a gas phase to a liquid phase in which it is soluble. Gas adsorption is a process by which a selected component in a gas phase is adsorbed by attractive forces onto a solid surface or into pores of a solid and is therefore separated (Geankoplis, 1993). Membrane permeation is a process where the selected gas component is transported across a thin membrane layer from one side to the other side. The thickness and selectivity of the membrane control the rate and quality of the separation. Cryogenic separation takes place when the gas stream is cooled to a temperature at which a gaseous component having a relatively higher boiling point is condensed and separated from the main gas

stream. These techniques have all been proven to work. However, the biggest challenge to be overcome is the high cost of the capture that prevents the implementation in the actual application.

### **1.3.1 CO<sub>2</sub> Absorption Process**

Among these techniques, gas absorption at this point and time is the most economical technique for removal of CO<sub>2</sub> from high-volume gas streams (DOE: Carbon Capture and Separation, 2006). Figure 1.1 shows a typical process flow diagram of a CO<sub>2</sub> absorption plant, which includes the gas absorption section as well as the solvent regeneration section. The basic operation of the process starts by introducing a gas stream containing CO<sub>2</sub> into the bottom of the absorption column. Once in the column the gas travels up against the counter-current flow of the absorbing liquid that is introduced to the top of the column from the liquid holding tank. As the liquid travels down the column, the liquid is broken apart into rivulets or small drops depending on the internals of the column. This promotes the contact between gas and liquid phases, causing the transfer of CO<sub>2</sub> from the gas to the liquid. The CO<sub>2</sub> lean gas proceeds up the column where it is released as clean gas with trace CO<sub>2</sub>. The CO<sub>2</sub> rich liquid then travels out of the bottom of the absorption column where it is collected and pumped through a heat exchanger so as to receive heat energy from a stream of hot CO<sub>2</sub> lean liquid prior to the feed into the stripping column. The heated CO<sub>2</sub> rich liquid travels down the stripping column against the upward flow of vapor mixture generated from a re-boiler. The CO<sub>2</sub> rich liquid travels further through the re-boiler where the rich liquid is heated to boiling and the absorbed CO<sub>2</sub> is released and then carried by the vapor mixture stream traveling

back into the stripping column. As traveling up the column, the vapor stream picks up more CO<sub>2</sub> released from the rich liquid, and leaves out of the top of the stripping column. At that point, the vapor stream containing mainly H<sub>2</sub>O and CO<sub>2</sub> is passed through a reflux condenser where the majority of water is knocked out and separated, providing a gas stream of 98 +% CO<sub>2</sub> leaving the process. The CO<sub>2</sub> lean liquid from the re-boiler is pumped through a heat exchanger and a cooler before its return to the absorption column to complete the process cycle.

### **1.3.2 Performance of CO<sub>2</sub> Absorption**

To make the CO<sub>2</sub> absorption process affordable, greater performance of the process must be achieved. This could be done by improving the two main factors that have the most impact on the process performance, i.e. the liquid solvent used and the design of column internals. The solvents used can be classified into physical and chemical categories as shown in Figure 1.2. The chemical is preferred as it offers high absorption at low CO<sub>2</sub> partial pressures. The most commonly used chemical solvents are aqueous solutions of alkanolamines. The alkanolamines can then be separated into three groups: primary, secondary and tertiary types. Primary amines include monoethanolamine (MEA) and diglycolamine (DGA), secondary amines include Diethanolamine (DEA) and diisopropanolamine (DIPA), and the tertiary amines include triethanolamine (TEA) and methyldiethanolamine (MDEA). There are also other classes of chemical solvents that are being researched and they are the sterically hindered amines and the formulated solvents. The sterically hindered amines include the 2-amino-2-methyl-1-propanol (AMP) amine, which has become very popular. The formulated

solvents are solvents that contain a variety of amines with different additives to produce favorable characteristics that help in gas treating. The most popular solvent is the primary amine, MEA (DuPart et al, 1993, IEA Greenhouse Gas R&D Program, Year, 2001). It is widely used because of its high reactivity with CO<sub>2</sub> and its high cyclic capacity.

The design of column internals also plays a very important role in CO<sub>2</sub> absorption. The three types of gas-liquid contactors that have been compared are the packed, tray and spray columns. The packed column uses either random or structured packing as the method to increase the contact area between gas stream and liquid solvent. There are several types of packing such as Raschig rings, Berl saddle and Mellapak structured packing. The tray column utilizes a tray system that transports the liquid solvent down the column against the upward flow of the gas stream. The trays have holes in them to allow the gas to bubble through the liquid pools on each tray. Some trays utilize bubble caps to help transport the gas through each tray. The spray column utilizes a series of spray nozzles that atomize the liquid solvent and provides the largest area of contact for the gas. The nozzles come in various sizes to allow for different liquid flow rates to pass through them. In general, the spray column offers the lowest pressure drop through the column and the lowest cost of column construction among the three contactors. The use of spray column therefore presents a great potential in reducing the total cost of CO<sub>2</sub> capture. However, the efficiency of spray column for CO<sub>2</sub> capture should be investigated and compared with the efficiency of conventional packed column.

#### **1.4 Limitation of Knowledge**

The removal of CO<sub>2</sub> from gas streams has been well documented and many

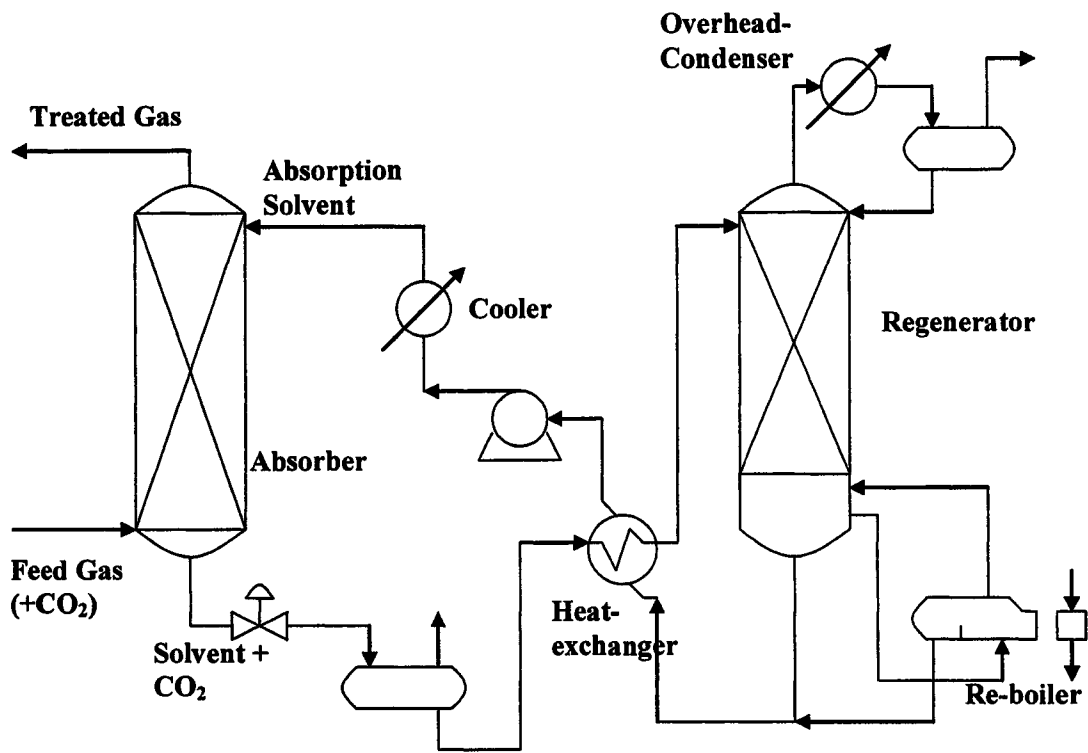


**Figure 1.1:** Process flow diagram of CO<sub>2</sub> absorption unit.

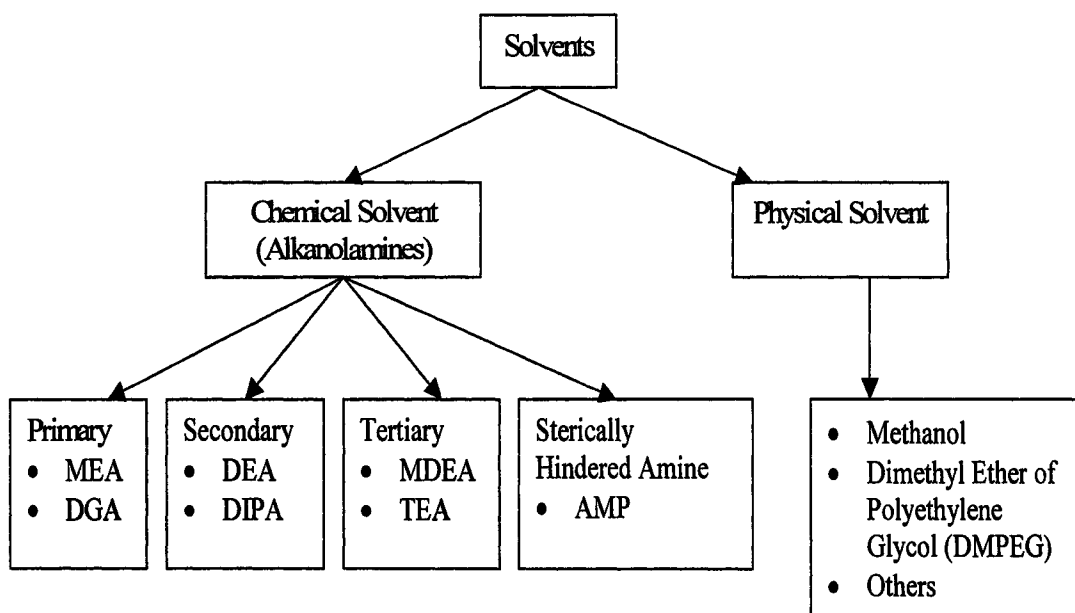


**Figure 1.2:** Physical and chemical solvents for acid gas removal.  
(Information from Kohl and Nielsen, 1997)

techniques have been studied. The absorption of CO<sub>2</sub> using packed and tray columns have produced a large amount of published data with many types of solvents and column internals being tested (Aroonwilas, 1996; Bravo, 1997; Treybal, 1980). In contrary, the spray column has been studied by few and to date there has been little data produced in the area of CO<sub>2</sub> removal (Yeh, 2003).

The main use of the spray column has been for the removal of SO<sub>2</sub> from flue gas streams. Specific areas of study are the design of the scrubber, orientation of the nozzles and solvents used (Feldkamp et al., 2003; Weiss et al., 1990; Nguyen and Spink, 1993). To the best of my knowledge there has not been any direct comparison in SO<sub>2</sub> removal efficiency that has been made between the packed and the spray columns. There have been a few attempts at CO<sub>2</sub> removal utilizing a spray column and the focus was on using sodium hydroxide (NaOH) as the solvent (Taniguchi et al., 1997; Fukunaka, 1992). It has been published that the general perception of the spray column producing lower efficiencies in mass transfer when compared to that of a packed column is false (Mehta and Sharma, 1970). The specific case of the CO<sub>2</sub> – MEA system in a spray column to date has no data published. This provides no information for comparison of solvents as well as various types of nozzles and their performance. There is a need for further study in this area to examine the feasibility of such systems. The use of amines for CO<sub>2</sub> removal has been proved to work in packed and tray columns so by using it in the spray column comparisons can be made.

## 1.5 Research Objectives

The primary objective of the present study was to explore the feasibility of using a spray column for the removal of CO<sub>2</sub> from gas streams by the conventional absorption solvent MEA. Along with the primary objective, this study was carried out with specific objectives that were (i) to determine the mass-transfer performance of spray column in capturing CO<sub>2</sub>, (ii) to reveal how such performance of the spray column was affected by the variation in operating and design parameters of the absorption process, and (iii) to provide a performance comparison between the spray column and a conventional packed column. The mass transfer performance was determined experimentally under wide ranges of process parameters, including CO<sub>2</sub> partial pressure in gas phase, gas flow rate, liquid flow rate, concentration of absorption solvent, CO<sub>2</sub> loading of absorption solvent, and type of spray nozzle.

This thesis is divided into six chapters. Introduction and research objectives are presented in this chapter. Chapter 2 contains basic principles of mass transfer with chemical reactions and a literature review of gas-liquid contacting devices including packed-, tray-, and spray columns for CO<sub>2</sub> removal. Details of the apparatus and procedures for the CO<sub>2</sub> absorption experiments are given in Chapter 3. In Chapter 4, the experimental results presented in terms of the volumetric overall mass transfer coefficient ( $K_G a_e$ ) are reported as a function of operating and design parameters of the CO<sub>2</sub> absorption process. Chapter 5 presents a theoretical analysis of the experimental data, providing the knowledge on fundamental parameters for mass transfer in spray column. Finally, conclusions drawn from the study and recommendations for future work are given in Chapter 6.

## Chapter Two

### Literature Review and Fundamentals

This chapter reviews the fundamentals of mass transfer taking place in gas absorption process, in particular CO<sub>2</sub> absorption process. The kinetics of CO<sub>2</sub> absorption system into aqueous amine solutions is included to provide knowledge for theoretical analysis. The literature on the gas-liquid contactors, i.e. packed column, tray column, and spray column, is also reviewed in this chapter.

#### 2.1 Mass Transfer Principles

Mass transfer takes place when one component is transferred from one phase into another distinct phase or through a single phase. The basic mechanism for mass transfer, whether through gas, liquid, or solid is the same. The following general equation can be used to express the mass transfer phenomena (Geankoplis, 1993; Treybal, 1980):

$$\text{Rate of a transfer process} = \frac{\text{driving force}}{\text{resistance}} = (\text{coefficient})(\text{driving force}) \quad (2.1)$$

The process takes place through the diffusion driven by a difference in concentration of the transferring component. The rate of transfer process is the mass-transfer flux, and the driving force is the concentration gradient. The flux of a component *A* in a single phase can also be written as the following:

$$N_A = k_L^\circ (C_{A,1} - C_{A,2}) \quad (2.2)$$

where  $N_A$  = mass transfer flux of the component A

$k_L^\circ$  = individual liquid-phase mass transfer coefficient

$C_{A,1}$  = concentration of component A at beginning of transfer path

$C_{A,2}$  = concentration of component A at end of transfer path

In most cases of mass transfer operation, there are two insoluble phases that are brought in contact with each other in order to allow mass transfer of a third component to occur between them. An example is in gas absorption where a component  $A$  in the gas phase is transferred to the liquid phase during the contact. To simplify the process, it is assumed that there is no chemical reaction associated with the transfer process. The diffusion of component  $A$  across the gas-liquid interface takes place due to a non-equilibrium condition being present (Figure 2.1). In the figure, the concentration of  $A$  in the main body of the gas is  $y_{A,G}$  mole fraction, and falls to  $y_{A,i}$  at the gas liquid interface. In the liquid, the concentration of  $A$  drops from  $C_{A,i}$  at the interface to  $C_{A,L}$  in the liquid main body. The only resistances to component diffusion are those within the fluids themselves, there is no resistance to the transfer across the interface (Treybal, 1980). This statement suggests that the concentration  $y_{A,i}$  in the gas phase and the concentration  $C_{A,i}$  in the liquid phase are in equilibrium. The equilibrium can be represented by Henry's Law (Perry and Green, 1984):

$$Py_{A,i} = HC_{A,i} \quad (2.3)$$

where  $P$  is the total system pressure and  $H$  is Henry's law coefficient.

Figure 2.1 shows that the mass flux of component  $A$  across the interface can be written in the form:

$$N_A = k_G P(y_{A,G} - y_{A,i}) = k_L (C_{A,i} - C_{A,L}) \quad (2.4)$$

where  $k_G$  is the individual gas-phase mass transfer coefficient. The concentration of  $A$  in the bulk of the fluids is possible to obtain by sampling and analyzing. The concentration at the interface however is practically impossible to determine.

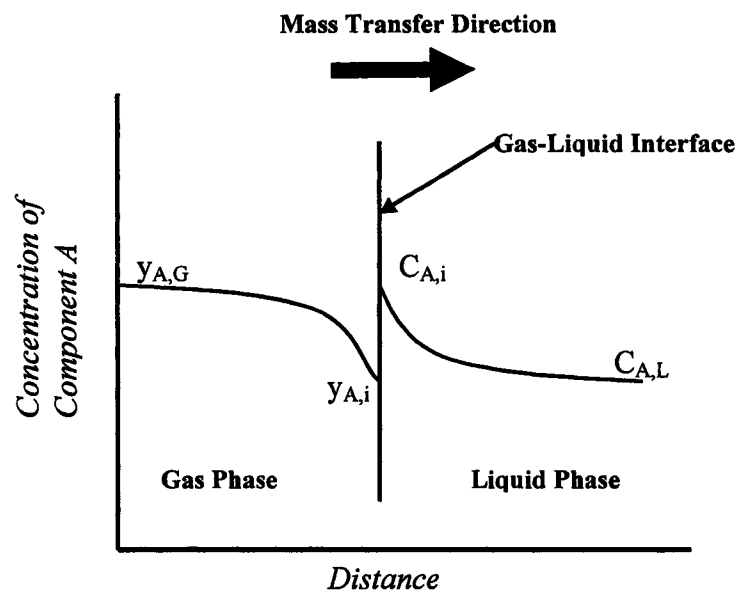


**Figure 2.1:** Concentration profiles of diffusing component  $A$  in gas and liquid phases (Treybal, 1980).

The concentration gradients  $(y_{A,G} - y_{A,i})$  and  $(C_{A,i} - C_{A,L})$  take place over extremely small distances which make it difficult to obtain a measure of each. Under these circumstances, it is more practical to express the mass flux in the terms of overall mass transfer coefficients,  $K_G$  or  $K_L$  along with the overall driving force across both phases:

$$N_A = K_G (Py_{A,G} - HC_{A,L}) = K_L \left( \frac{Py_{A,G}}{H} - C_{A,L} \right) \quad (2.5)$$

The relationship between the overall mass transfer coefficients and the individual phase coefficients can be given as the following (Perry and Green, 1984):

$$\frac{1}{K_G} = \frac{1}{k_G} + \frac{H}{k_L} \quad (2.6)$$

$$\frac{1}{K_L} = \frac{1}{k_L} + \frac{1}{Hk_G} \quad (2.7)$$

In most operations, the mass transfer takes place under turbulent flow conditions. There are several theories that have been established to explain the differences in the coefficients. The oldest and most obvious picture of the meaning of mass transfer is the Film theory model (Treybal, 1980). The film theory assumes that there is an existence of a stagnant film of liquid near the gas-liquid interface through which mass transfer takes place by molecular diffusion. The rest of the liquid is assumed to be perfectly mixed. The concept of the film theory is shown in Figure 2.2. In the film theory, mass is only transferred through the film under steady state conditions and the concentration profile of the transferred component is linear (Astarita et al., 1983). In the case where no chemical reaction is present, the differential equation for steady-state mass transfer can be written as:

$$D_{A,L} \frac{d^2 C_A}{dx^2} = 0 \quad (2.8)$$

Based on the boundary conditions in Figure 2.2, the mass transfer flux ( $N_A$ ) is:

$$N_A = D_{A,L} \frac{C_{A,i} - C_{A,L}}{\lambda} \quad (2.9)$$

where  $D_{A,L}$  is the diffusion coefficient of  $A$  in the liquid and  $\lambda$  is the thickness of the liquid film. A comparison of Equations 2.4 and 2.9 shows that the mass transfer coefficient is proportional to the diffusion coefficient:

$$k_L^\circ = \frac{D_{A,L}}{\lambda} \quad (2.10)$$

According to Astarita et al. (1983), mass transfer predictions based on the film theory model are questionable because empirical correlations available in literature for a liquid in contact with a gas consistently produce the mass transfer coefficient  $k_L^\circ$  proportional to the square root of the diffusion coefficient  $D_{A,L}$ .

One of the most reliable models used in mass transfer area is the Penetration theory proposed by Higbie in 1935. This model involves the movement of the liquid at the gas-liquid interface. It is assumed that small liquid elements from the bulk liquid are continuously brought to the interface through which mass transfer takes place for a specific time period referred to as the contact time ( $\tau$ ) before the elements are circulated back to the bulk liquid. The contact time in this case is so short that the concentration gradient of transferred component within the liquid elements would not have time to fully develop, thus causing mass transfer to proceed under unsteady state conditions. In the absence of chemical reaction, the mass transfer coefficient  $k_L^\circ$  in this case is given by (Drew and Hoopes, 1956):

$$k_L^\circ = 2\sqrt{\frac{D_{A,L}}{\pi\tau}} \quad (2.11)$$

### 2.1.1 Mass Transfer with Chemical Reaction

Chemical reactions can play an important role in the mass transfer process. The reactions take place when the gas is brought into contact with the liquid and component  $B$  in the liquid reacts with the diffusing component  $A$ . All reactions proceed only in the liquid side if component  $B$  is non-volatile. According to Levenspiel (1999) there are eight kinetic regimes to consider, going from extremely fast reactions to infinitely slow reactions. The eight regimes are summarized below along with concentration profiles for each case (Figure 2.3).

- Regimes A and B: Instantaneous reaction

The instantaneous reaction takes place so quickly that it occurs at a reaction plane within the liquid film at the gas-liquid interface. The liquid film at every point can contain either component  $A$  or  $B$  but it cannot contain both.

- Regimes C and D: Fast reaction

The slower reaction rate when compared to Regimes  $A$  and  $B$  has the reaction plane spreading into a reaction zone where both components  $A$  and  $B$  can be present at the same time. The reaction is fast enough to take place entirely within the liquid film. Thus, there is no component  $A$  entering the main body of the liquid.

- Regimes E and F: Intermediate reaction

The reaction is slow enough that some of component  $A$  diffuses through the reaction zone into the main body of the liquid. Component  $A$  reacts within both

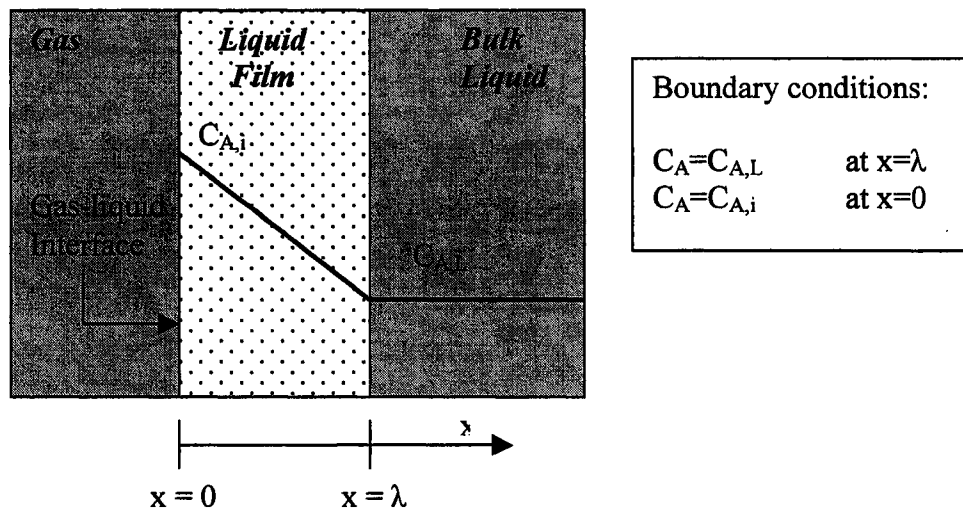


**Figure 2.2:** Film Theory (modified from Astarita et al., 1983).

the liquid film as well as the main body of the liquid.

- Regimes G and H: Slow reaction

The reaction takes place so slow that it takes place almost exclusively in the body of the liquid. The film still provides a resistance to component  $A$  as it transfers into the main body of the liquid.

The chemical reaction affects the rate of mass transfer in two ways. First, the transferred component  $A$  is consumed by the chemical reaction in the liquid, resulting in a low concentration of  $A$  in the liquid main body. The chemical reaction produces a higher driving force for the mass transfer to take place when compared to a case without chemical reaction. Second, at a given level of the driving force, the actual rate of mass transfer may be considerably higher than without chemical reaction (Aroonwilas, 2001). According to Astarita et al. (1983), the ratio of the actual rate with chemical reaction to the rate that would be observed under the same driving force in the absence of chemical reactions can be defined as the enhancement factor,  $I$ . The following equation shows the relationship:

$$I = \frac{k_L}{k_L^\circ} \geq 1 \quad (2.12)$$

where  $k_L$  is the liquid mass transfer coefficient with chemical reaction and  $k_L^\circ$  is the liquid mass transfer coefficient without chemical reaction. The rate of mass transfer with chemical reaction can be written as follows:

$$N_A = Ik_L^\circ (C_{A,i} - C_{A,L}) \quad (2.13)$$

Then, Equations (2.6) and (2.7) can be rewritten as:

$$\frac{1}{K_G} = \frac{1}{k_G} + \frac{H}{Ik_L^\circ} \quad (2.14)$$

$$\frac{1}{K_L} = \frac{1}{Ik_L^{\circ}} + \frac{1}{Hk_G} \quad (2.15)$$

A number of equations for calculating the enhancement factor  $I$  in different reaction scenarios can be found in the literature (Astarita et al., 1983; Perry and Green, 1984; DeCoursey and Thring, 1989).

### 2.1.2 Determination of Overall Mass Transfer Coefficient

The volumetric overall mass transfer coefficient ( $K_G a_e$ ) was commonly used for analyzing the mass transfer performance of gas-liquid contactors. The  $K_G a_e$  is a lumped parameter that includes not only the thermodynamic and kinetic contributions of the transferred component across the gas-liquid interfacial area but also the hydrodynamics of gas-liquid contactor presented as the degree of the interfacial area per unit volume. The value of  $K_G a_e$  is performance based term presented per unit of mass transfer driving force. It was used in common practice for the reason that the interfacial area provided by the contactor cannot be accurately measured. Therefore, it is more useful to present mass transfer performance based on a unit volume of the contactor, rather than on an interfacial area unit as follows:

$$\frac{1}{K_G a_e} = \left( \frac{1}{k_G a_e} \right) + \left( \frac{H}{Ik_L^{\circ} a_e} \right) \quad (2.16)$$

A practical approach for obtaining the volumetric overall mass transfer coefficient is to perform gas absorption experiments where the concentration profile of the absorbed component in the gas phase is measured along the test column. Considering a section of absorption column with height  $dZ$ , the mass balance of absorbed component  $A$  can be written as:

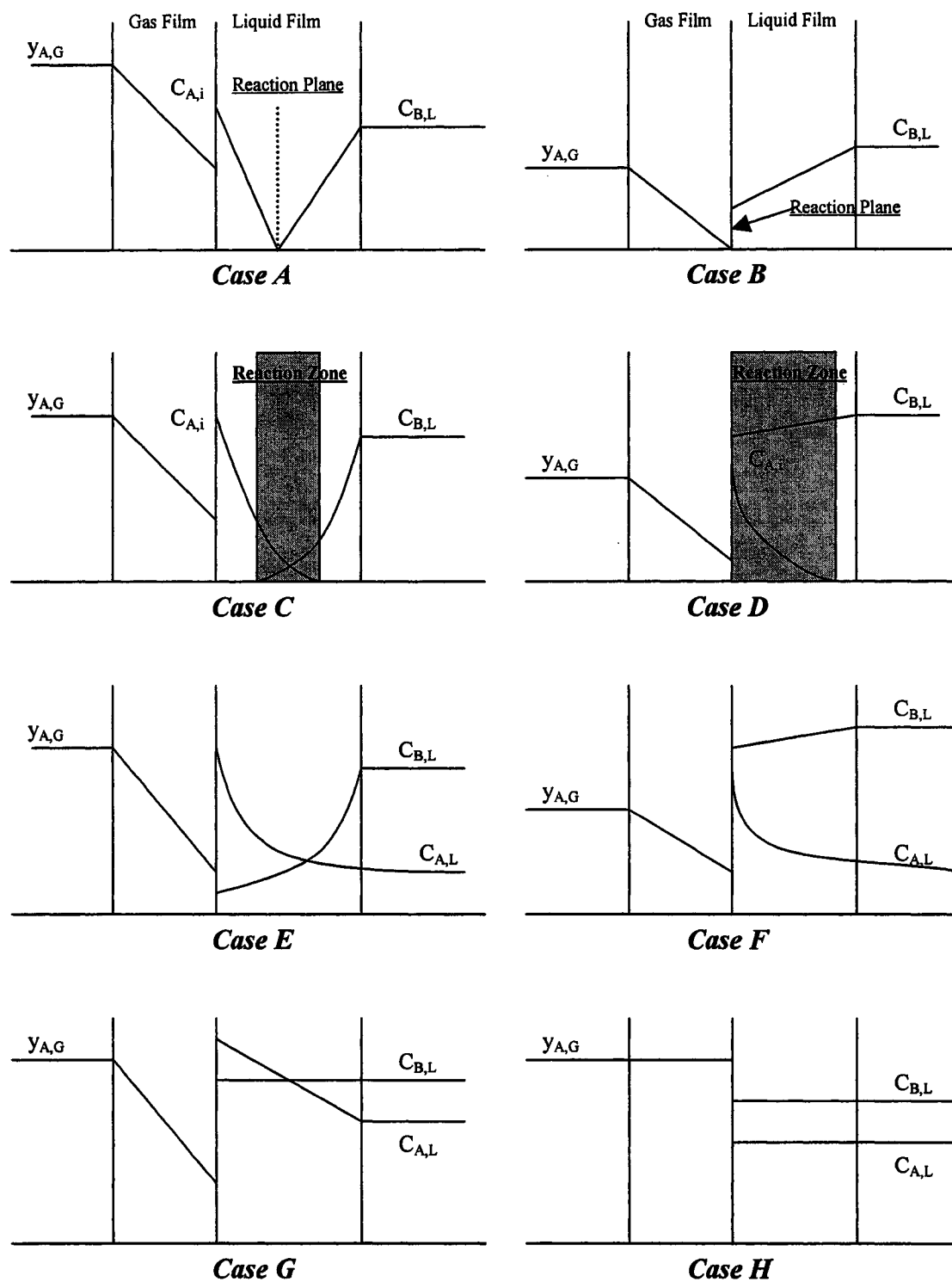


**Figure 2.3:** Gas-phase and liquid phase concentration profiles for different kinetic regimes. (Levenspiel, 1999)

$$N_A a_e dZ = G_I d \left[ \frac{y_A}{(1 - y_A)} \right] \quad (2.17)$$

$$K_G a_e P (y_A - y_A^*) dZ = G_I dY_A \quad (2.18)$$

- where  $a_e$  = the gas-liquid interfacial area,  
 $G_I$  = the molar flow rate of inert gas,  
 $y_A$  = mole fraction of A in gas phase,  
 $y_A^*$  = mole fraction of A in equilibrium with liquid bulk concentration,  
 $Y_A$  = mole ratio of A in gas phase, and  
 $P$  = pressure of the absorber.

From Equation (2.18), the volumetric overall mass transfer coefficient can be defined as:

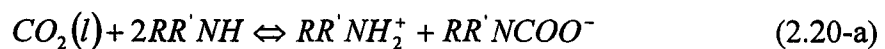
$$K_G a_e = \left\{ \frac{G_I}{P(y_A - y_A^*)} \right\} \left\{ \frac{dY_A}{dZ} \right\} \quad (2.19)$$

## 2.2 CO<sub>2</sub> Absorption Reactions

Aqueous solutions of amines are extensively used as an absorption solvent in the removal of CO<sub>2</sub> from gas streams. In this study the amine used was Monoethanolamine (MEA) and it is important to understand the mechanism of the reaction with CO<sub>2</sub> as well as the rate at which it proceeds. The following section briefly describes the reaction kinetics.

The reaction between CO<sub>2</sub> and amine solutions is very complex. The following three main reactions, according to Astarita et al. (1983), need to be considered.

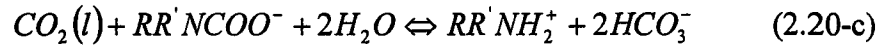
### **Carbamate formation:**



**Bicarbonate formation:**

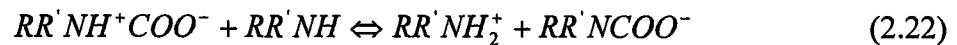


**Carbamate reversion:**



where  $R$  stands for  $-C_2H_4OH$  and  $R'$  represents  $-H$  and  $-C_2H_4OH$  for primary and secondary amines, respectively. The importance of the above three reactions is dependent upon their rate constants and reactant concentrations. The carbamate formation reaction generally predominates when the  $CO_2$  loading is less than 0.5 moles of  $CO_2$ /mole of amine, and the carbamate reversion plays the major role when the  $CO_2$  loading exceeds 0.5 moles of  $CO_2$ /mole of amine. The significance of the bicarbonate formation is inversely proportional to the stability of carbamate ( $RR'NCOO^-$ ) (Astarita et al., 1983).

For the  $CO_2$ -MEA system that is used in this study, the carbamate formation is considered to be the main reaction since the MEA carbamate is quite stable (Sartori and Savage, 1983). The formation mechanism is believed to be made up of two steps (Astarita et al., 1983):



Reaction (2.21) is the rate determining step and therefore the reaction rate is first order with respect to both  $CO_2$  and  $RR'NH$ :

$$r = k_2 [CO_2] [RR'NH] \quad (2.23)$$

where  $k_2$  is the second order rate constant. There have been several different experimental techniques used by a number of different researchers to determine values

for  $k_2$  for the CO<sub>2</sub>-MEA system. According to Blauwhoff et al. (1984), the kinetic data can be characterized by the expression produced by Hikita et al. (1977):

$$\log(k_2) = 10.99 - \frac{2152}{T} \quad (2.24)$$

The Hikita expression when compared to previous rate constants produced can be found to be in good agreement (Aroonwilas, 1999 & 2001).

### **2.3 General Thermodynamic Framework**

There is a very important relationship that must be understood for the design of absorption units. This relationship is the one between the concentration of CO<sub>2</sub> in an amine solution and its partial pressure in the gas phase under the equilibrium. This is because the equilibrium will establish the driving force for the mass transfer process. There are several approaches to model the experimental data. For the present case of CO<sub>2</sub>-amine system, the most advanced and thermodynamically rigorous model is the electrolyte NRTL model proposed by Austgen et al. in 1989.

The Austgen et al. model is based on the evaluation of activity coefficients for all of the chemical species present in the absorption system. The activity coefficients were obtained by differentiating the excess Gibbs free energy with respect to the mole number of a given species. When dealing with an electrolyte solution, the excess Gibbs free energy consists of three parts. They are the long-range contribution represented by the Pitzer-Debye-Huckel (PDH) expression. The PDH accounts for the electrostatic forces among ions. The second part is accounted for by the Born expression which accounts for the excess Gibbs free energy from the difference in the dielectric constants between the pure water and aqueous solution. The third part relates to the short-range interaction

forces among all species. The NRTL model accounts for local ion-molecule, ion-ion, molecule-molecule interactions that exist in the area of any species (Aroonwilas, 2001).

The NRTL equation is a complex model that goes beyond the scope of this work. There are several equations that all interlink to produce the final results. These equations can be seen more in depth in Austgen et al. (1989).

## **2.4 Gas Liquid Contactors**

There are three main types of gas-liquid contactors that are used for the absorption process, i.e. packed column, tray column and the spray column (Figure 2.4). They all have unique advantages and disadvantages associated with them. The general information on each system was taken largely from Treybal (1980), and Perry and Green (1997).

### **2.4.1 Packed Column**

The packed column is commonly used for continuous contact of liquid and gas in either co-current or counter-current modes of operation. In general, the vertical column is filled with a type of packing made from a variety of materials such as ceramic, plastic or metal to promote the degree of contact between liquid and gas. The common operation of the packed column is that the liquid is introduced at the top of the column and at the same time the gas is fed at the bottom. As the liquid trickles down through the packing by gravity, it is constantly being broken apart into small rivulets and droplets, allowing a large degree of contact with the continuous gas phase. The greater the gas-liquid contact,

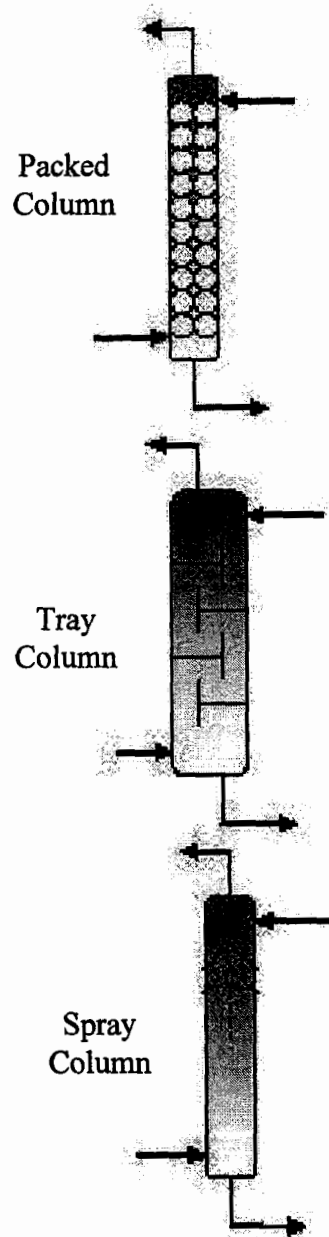


**Figure 2.4:** Schematic sketches of columns.

the greater the performance of gas absorption process. The packing must possess the following five traits to ensure the success of operation (Treybal, 1980).

1. The packing must not react with the chemical being used.
2. The packing must represent a low cost to the operation.
3. The packing must be structurally strong for ease of installation and handling.
4. The packing must provide desirable fluid flow characteristics. It must allow for a large amount of fluid to flow through a cross section without flooding or over loading the column and also offer a low pressure-drop.
5. The packing must provide a large interfacial area for the contacting of the gas and the liquid.

The packing in the column can be classified into two different types, i.e. random or structured. The random packing is packed in the column in a random arrangement, usually by dumping. There are several types of random packing available in the market, including Raschig rings, Berl saddle, Pall rings, and Intalox Metal Tower Packing (IMTP). Each offers different sizes ranging from 6 to 90 mm. Unlike the random packing, the structured packing having a regular geometric structure is manufactured as elements and fitted carefully to the cross section of the column. There are many different types of structured packing as it is named for the configuration pattern of the packing sheets. In general, structured packing provides a very large surface area for contact as well as a much lower gas pressure drop compared to the random packing. The packing within the column constantly splits the initial liquid stream into smaller and smaller

streams or rivulets as the liquid proceeds down the column which always produces more surface area for the gas to contact.

There are several operational issues arising when the packed column is in use. One such issue is the flooding condition that limits the hydrodynamic capacity or throughput of the column. The packed column is flooded when the liquid rate and/or the gas rate increase to the point where there are slugs of flowing gas being formed and the liquid is unable to flow smoothly and steadily through the column. The flooding results in the significant reduction in gas-liquid contact area provided by the column. Another operational issue of packed column is the entrainment of liquid in the exiting gas stream. At high gas velocities, liquid particles can become entrained in the gas stream and be carried out of the column. This problem is rectified by installing a mist eliminator at the gas outlet. The packing can also cause concern with maintenance of the column. If the liquid used is dirty, the packing can overtime become plugged. There is no cost-effective way to clean the system, except to remove all of the packing and replace it with new packing. This leads to a great expense in both labour and material as well as down time for the plant while the column is in service.

The packed column is a well-researched topic in the area of CO<sub>2</sub> capture. It has proven to be effective and technology is constantly improving the system. One problem that is yet to be overcome is the costs associated with the size of the column needed and the packing to fill it.

#### **2.4.2 Tray Column**

The tray column is a vertical tower that uses trays to transport the liquid from the

top of the column to the bottom. The trays are setup as a series of equilibrium stages where the liquid is introduced into the column on the top or first stage. In general, the liquid accumulates on the tray to the level set by a weir where the liquid departs from the first tray and enters a down-comer leading to the next tray below. The liquid continues to travel the trays in the same manner until it reaches the bottom of the column. At the same time, the gas enters the bottom of the column and passes through the bottom of each tray. At each tray, the gas bubbles through the liquid pool on the tray and froths up to where it is released and travels to the next tray above it. The gas travels up the column and through all the trays to the top where it is released. The trays are either of a sieve, valve, or bubble cap arrangement to allow the gas to transfer through the liquid that travels across them. The number of trays that are present in the column is based on material balances and the separation target to be achieved. The absorption in the tray column is dependent upon highly turbulent conditions being present to obtain high mass-transfer. The liquid pool on each tray needs to be fairly deep to offer longer contact time for mass transfer to take place. The combination of the deep liquid pool and the high gas flow rate can produce the high rate of mass transfer (Treybal, 1980).

The trays in the column can be manufactured from a number of different materials. The materials include glass, glass-lined metals, plastics or wood but generally the trays are made of metal. The tray thickness is dependent upon the corrosiveness of fluids used in the column. The trays in the column must be well secured to the shell of the column as to withstand the weight of liquid pool pressing down and the force of the gas attempting to get through the tray and the liquid pool (Treybal, 1980).

There are several operational issues associated with the tray column. The tray column produces a high pressure-drop as the gas passes through. This high pressure-drop may lead to column flooding, which causes the mass transfer efficiency of the column to drop significantly. The column is also prone to corrosion problem as the liquid pools on the trays. The corners of the trays that are in constant contact with the liquid are considered to be the main locations of the corrosion. The maintenance cost is also very high in the tray column. The trays need to be replaced once corrosion begins. This involves in the shut down of the process so as to remove the trays from the internals of the column, thus providing expensive labour costs for the maintenance and repair.

### **2.4.3 Spray Column**

The spray column is a vertical tower that uses spray nozzles to break the absorbing liquid into small droplets that are then contacted by the continuous gas phase. The flow in the column is countercurrent as the spray is projected from the top of the column and the gas is introduced into the bottom of the column.

The spray column offers a very low pressure-drop for the gas. It also offers a very basic operation and equipment. The liquid is pumped to the nozzles where it is then forced through small orifices. The nozzle used can produce many different spray patterns, which include a hollow cone, full cone, and flat fan with a variety of spray angles ranging from 20° to 120°. The nozzles provide several design features that make them unique. For instance, they are manufactured with one-piece construction with no vanes or internal parts that can be damaged. In some cases, they produce a highly

efficient laminar jet that hits a target pin and produce a fine fog (Bete Industrial Spray Nozzles).

The advantage of the spray nozzle is that a very large interfacial area for gas liquid contact can be generated. The drops produced according to the Bete Industrial Spray Nozzles are in the range of 25 to 400 microns. The nozzle is also easily interchangeable as it connects via tubing or piping connection. The main advantage though is the cost. It is much cheaper and quicker to replace the nozzle when it needs to be replaced (See Appendix B). The cost of one of the nozzles that was used in the project was US\$ 25-40. Other advantages are the size of the column needed to operate with spray nozzles. The spray column can be significantly smaller than other gas-liquid contactors while still providing excellent results and a high efficiency for the process. One of the operational advantages of using spray column is that there is no limit to flooding or excessive foaming in the column.

A disadvantage of the spray nozzle is the additional pumping cost needed to get the liquid through the nozzle. However, this additional cost would be outweighed by the cost saving due to the empty spray column containing no internal devices. Another disadvantage is if the fluid becomes dirty the nozzle will easily plug but this can be rectified by adding in-line filters to remove particulates that may be present. There is also a problem with a large amount of the spray becoming entrained in the gas stream as they come into contact with each other. This can be solved by adding a mist eliminator at the gas outlet to remove the liquid.

There is very little data that has been published about the spray column. When the specific case of CO<sub>2</sub>-MEA system is looked at there has been no reported data. There

is very little utilization of the spray column in such instances. This makes comparison difficult to other systems.

#### **2.4.4 Comparison of Spray, Packed and Tray Columns**

The three contactors can be compared in a variety of aspects as summarized in Table 2.1. The following highlights the favorable characteristics of the spray column.

1. Spray column offers the lowest pressure drop through the column.
2. The spray column offers little to no liquid hold as long as the discharge on the liquid side is adequate.
3. Spray column produces no foaming that causes problems in the operation.
4. Spray column with suitable material for nozzle production is likely to be most cost effective.
5. Spray column can be cleaned much easier than packed and tray columns.
6. Large temperature fluctuation is a non-issue for spray column with proper construction materials.
7. Spray column provides low capital cost on construction of column and internals.

These characteristics present a great potential of spray column in reducing the cost of CO<sub>2</sub> capture.

#### **2.4.5 Limitations of the Previous Studies on CO<sub>2</sub> Absorption using Spray Column**

There is very little data that has been published about the spray column. When the specific case of CO<sub>2</sub>-MEA absorption system is looked at, there has been no reported

data. There is very little utilization of the spray column in such instances for CO<sub>2</sub> absorption in general. This makes comparison difficult to other systems. Table 2.2 shows a list of previous work that uses a spray column for different gas separation applications.

**Table 2.1:** Comparison of packed, tray and spray columns (Modified from Treybal, 1980)

<b>Condition</b>	<b>Packed Column</b>	<b>Tray Column</b>	<b>Spray Column</b>
Gas-pressure drop	Small pressure drop.	Large pressure drop.	Smallest pressure drop through system.
Liquid holdup	Small liquid holdup.	Large liquid holdup.	Smallest liquid holdup. This is an important issue for the system with a concern for liquid degradation.
Liquid/Gas ratio	Better than spray but not as good as tray.	Capable of handling very low liquid/gas ratios.	Watch ratio to ensure liquid is large enough to fall through rising gas.
Liquid Cooling/Side streams	Not easy to remove liquid once in packing	Cooling coils are readily built into tray towers. Liquid more easily removed from system.	Cannot be done until one pass through the column.
Foaming Systems	Operate with less gas bubbling through liquid which produces less foam.	Lots of bubbling producing foam. Foaming can be a problem.	Foaming in a non-issue. Short contact time means no foam.
Solids Present	Not well handled. Best to remove solids before they enter column in both gas and liquid streams.	Not well handled. Best to remove solids before they enter column in both gas and liquid streams.	Not well handled. Orifice on nozzle very small easily plugged. Can be rectified by inline filters before liquid gets into column.
Corrosion	Less costly to replace than a tray column but still high expense associated with packing.	Costly to replace trays.	Spray nozzles very cheap when compared to other options. Also offers least labour time to replace.
Cleaning	Cleaning difficult because all packing has to be removed.	Frequent cleaning easier than packed column.	Cleaning easiest of group. Just have to spin off nozzle and rinse.
Large Temperature Fluctuation	Metal packing satisfactory.	Metal trays satisfactory.	Metal nozzles satisfactory.

**Table 2.2:** Previous work with spray columns

<b>References</b>	<b>Apparatus Used &amp; Application</b>	<b>Experiment and Variables Tested</b>	<b>Findings</b>
Skarupa et al. (1995)	Spray Tower used for flue gas desulphurization with limestone  (SO <sub>2</sub> removal with lime.)	Experiment involved increasing gas velocity from 10 to 15 ft/s and the effect on SO <sub>2</sub> removal. Also different nozzle tested which include spiral-high and low pressure, tangential nozzles.	At a constant liquid rate the SO <sub>2</sub> removal efficiency decreased as the gas velocity increased to 12 ft/s. When the gas velocity was greater than 12 ft/s there was no additional decrease in efficiency. Data also showed that gas-phase mass transfer coefficient and/or mass transfer area increased sufficiently at high gas rates. This resulted in decrease in operating cost because of the lower liquid-to-gas ratio is partially offset by increase in pressure drop through the absorber.
Weiss et al. (1989)	Flue Gas Desulphurization in wet spray absorption.  (SO <sub>2</sub> removal with lime)	Spray tower design discussed with spray zone, demister and oxidation zone as well as theoretical calculation and fluid mechanics of the spray zone.	Flue gas desulphurization in wet absorber is a fully developed technology. Possible that optimization of spray nozzle placement may lead to cost savings. Dry spray absorption an option if initial SO <sub>2</sub> concentration low.
Fukunaka et al. (1992)	Absorption column where drops produced by injector needles.  (CO <sub>2</sub> -NaOH)	Absorption rate of CO <sub>2</sub> gas in to droplets of NaOH. Samples were taken to determine amount of CO <sub>2</sub> removed and determined by Warder Method. The rate of the CO <sub>2</sub> and N <sub>2</sub> mixtures were 30 and 60 mm/s.	The CO <sub>2</sub> gas absorption into NaOH solution is significantly mixed in the absorption tower and the absorption rate is controlled by liquid film mass transfer.

**Table 2.2:** Previous work with spray columns (Continued)

<b>References</b>	<b>Apparatus Used &amp; Application</b>	<b>Experiment and Variables Tested</b>	<b>Findings</b>
Nicholls et al. (1998)	Co-current spray gas-liquid contacting stage.  (Air-H <sub>2</sub> O)	Column used includes entraining and dis-entraining sections. This case utilized air as the gas and water as the liquid. Air travels through entraining tube, collects water passes through dis-entraining sections and some water collects on the plates and falls back down the column. The humidity of the gas is then analyzed as it leaves the column. The spray column is directly compared to a packed column.	The spray column can be used at much higher superficial gas velocities than the packed columns without entrainment or flooding problems. However, there is a greater pressure drop in this instance due to plates that gas travels through.
Nguyen et al. (1993)	Fine spray in duct line for SO <sub>2</sub> removal.  (SO <sub>2</sub> -NaOH, SO <sub>2</sub> -NH <sub>3</sub> , SO <sub>2</sub> -dolime, SO <sub>2</sub> -amines)	There were various liquids used in test. They include ammonia, dolime, NaOH and proprietary amines. Liquid was sprayed into duct and then loaded amine was removed. The nozzles were placed in parallel with either a 1 or 2 stage process utilized.	The process works well and can be used as a pre-scrubber to less expensive materials can be used following the scrubber. Data on amine trials show that a two stage process is of better use.
Mehta et al. (1970)	Spray column used in mass transfer  (CO <sub>2</sub> - H <sub>2</sub> O and CO <sub>2</sub> -NaOH)	Utilized a single spray nozzle in a column where gas introduced at the bottom of column. Column operated at atmospheric pressure and 32°C. Gases were either pure CO <sub>2</sub> or air-CO <sub>2</sub> mixture. The liquid was water. Spray nozzle were solid cone design.	Provides for a low pressure drop in the gas phase. The wall effect is very minor in the absorption. The liquid drops produced must be large enough to fall through the rising gas but small enough to produce a larger interfacial area.

**Table 2.2:** Previous work with spray columns (Continued)

References	Apparatus Used & Application	Experiment and Variables Tested	Findings
Taniguchi et al. (1997)	Gas absorption in a spray column.  (CO <sub>2</sub> -NaOH and CO <sub>2</sub> -H <sub>2</sub> O)	Process used CO <sub>2</sub> -air mixture as the gas and NaOH as the absorption liquid. The nozzle was a full cone nozzle.	In the column there is no collision of drops. An empirical correlation was produced for the volume mean diameter averaged over a cross sectional area of the column. The rates of absorption in the CO <sub>2</sub> -NaOH case could be well predicted using a solid sphere model.
Taniguchi et al. (1999)	Small spray column for absorption of lean gas.  (NH <sub>3</sub> -H <sub>2</sub> O)	Process used lean NH <sub>3</sub> as the gas and water as the absorption liquid. The nozzle was a full cone nozzle.	Produced an accurate model on amount of NH <sub>3</sub> with water spray.

## **Chapter Three**

### **Experimental Apparatus and Procedures**

This chapter describes the details of the experimental apparatus and the experimental procedures that were used to carry out the absorption experiments. The contents have been broken into the following areas for discussion; experimental apparatus, procedure for absorption experiments and sampling analysis.

#### **3.1 Experimental Apparatus**

The apparatus used in the absorption experiments is shown in Figure 3.1. Figure 3.2 shows a photograph of the actual setup located in the Process Engineering Laboratory at the University of Regina. The details of the columns used as well as the associated equipment utilized are given in the subsections.

##### **3.1.1 Absorption Columns**

The absorption experiments were conducted in two separate columns, i.e. spray column and packed column. The spray column was constructed of acrylic plastic that was 0.552 m high and had an ID of 0.10 m. A photograph and dimensions of the spray column are given in Figures 3.3 and 3.4, respectively. The packed column was also constructed of acrylic plastic with an ID of 0.10 m but had a height of 0.803 m. A photograph and dimensions of the packed column are given in Figures 3.5 and 3.6, respectively. The spray column was operated with one of three nozzles installed. The three nozzles were manufactured by BETE Industrial Spray Nozzles and they are models P-20, P-28, and P-40. The nozzles were constructed of 316 Stainless Steel material. The

specifications and a photograph of the nozzles used can be found in Table 3.1 and Figure 3.7, respectively. The nozzles were operated through a range of liquid flows and pressures to test the capacity and effectiveness of each nozzle utilized. The packed column was fitted with Mellapak 500Y structured packing provided by Sulzer Brothers Limited, Winterthur, Switzerland. The Mellapak 500Y was utilized because it is shown in literature to be the best structured packing available for the absorption of CO<sub>2</sub> (Aroonwilas, 2001). There were two sections of the packing used that provided a height of 0.4 m. The packing was installed with each layer rotated by 90° with respect to the previous one (Installation and operating instructions for Sulzer columns C-803). Table 3.2 provides the specifications of the packing and Figure 3.8 shows a photograph of a section of the packing.

The CO<sub>2</sub> concentrations in both feed and exit gas streams were needed so that the overall mass transfer coefficient ( $K_{Ga_e}$ ) could be calculated by Equation (2.19). For this reason there was a sampling point before the gas entered the column and at the point where the gas exited the column. The CO<sub>2</sub> concentrations were measured in the gas phase using an infrared spectroscopy, which is reliable, easy to use and readily available. The details of the specific analyzer used are given in Section 3.3.

### **3.1.2 Auxiliary Equipment**

Auxiliary equipment such as a liquid pump, liquid feed and storage tanks and gas flow meters were used in this work. A gear pump that is magnetically driven by a 0.1 Hp electric motor was purchased from Cole-Parmer and used to deliver the liquid to the top

of the spray and packed columns. The liquid feed and storage tanks were made of high density polyethylene and each had a maximum capacity of 20 L. Two Cole-Parmer gas

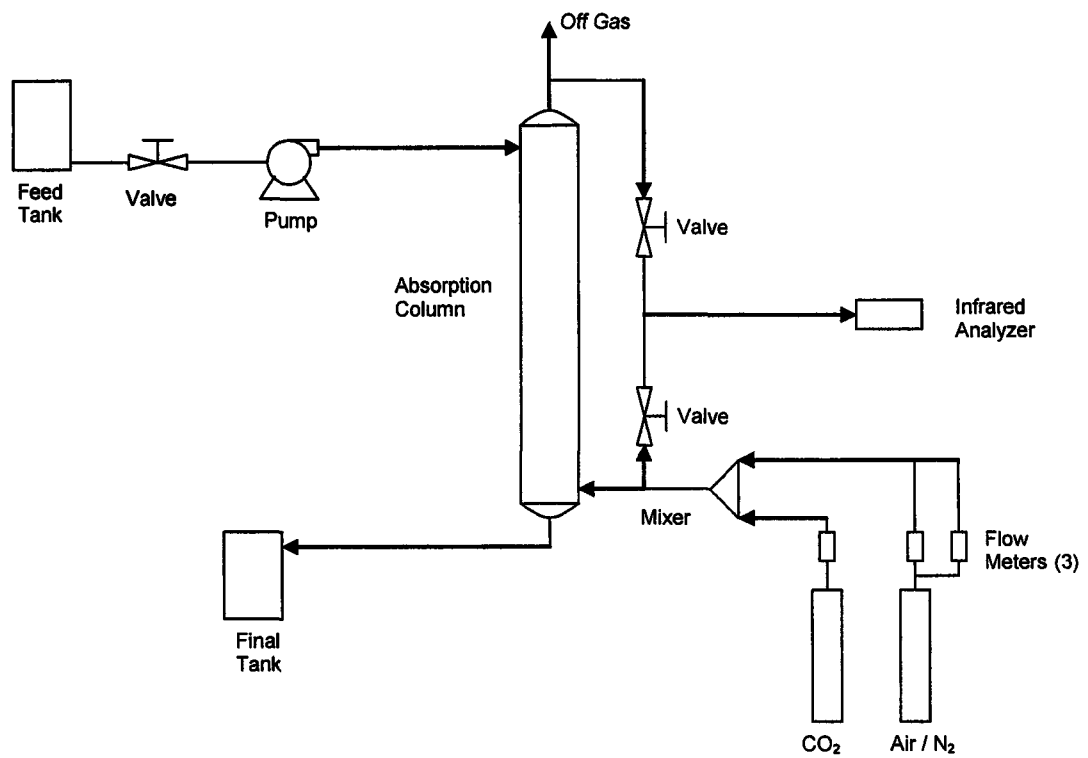


**Figure 3.1:** Schematic drawing of CO<sub>2</sub> absorption apparatus.

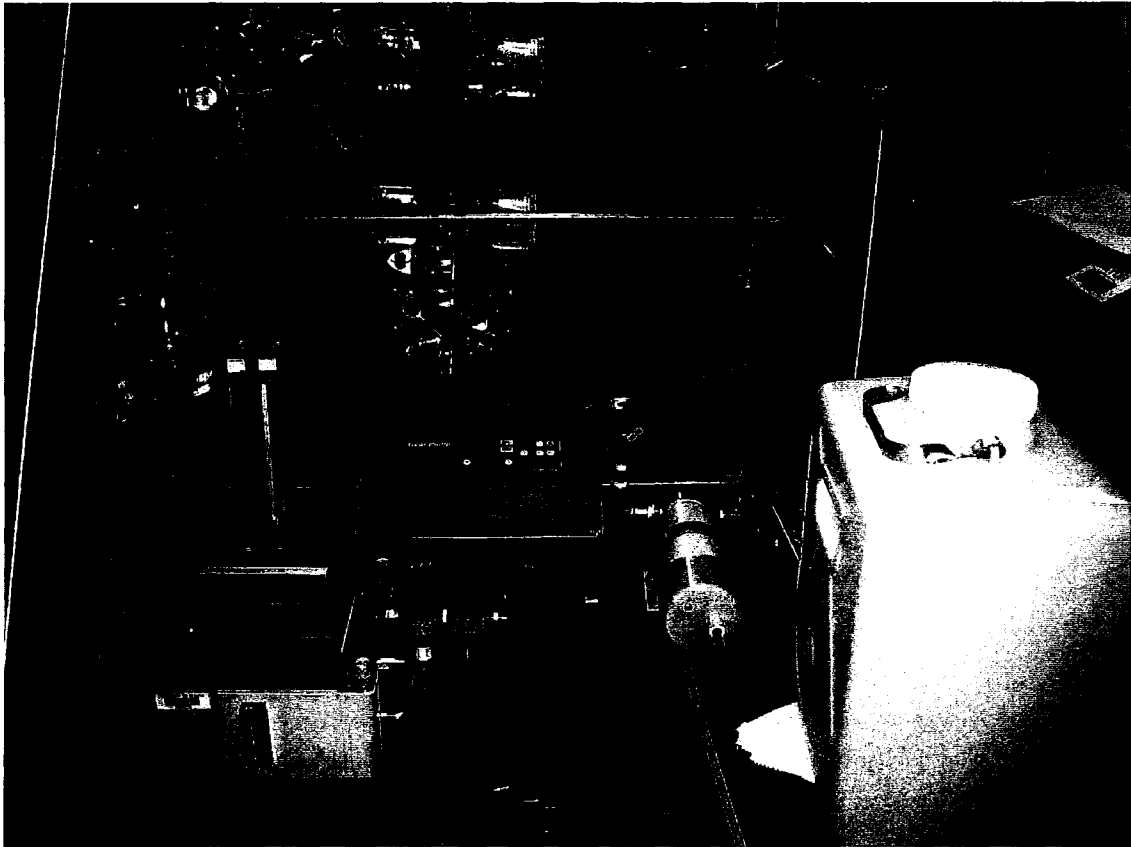


**Figure 3.2:** Photograph of the experimental apparatus.  
(Original in color)

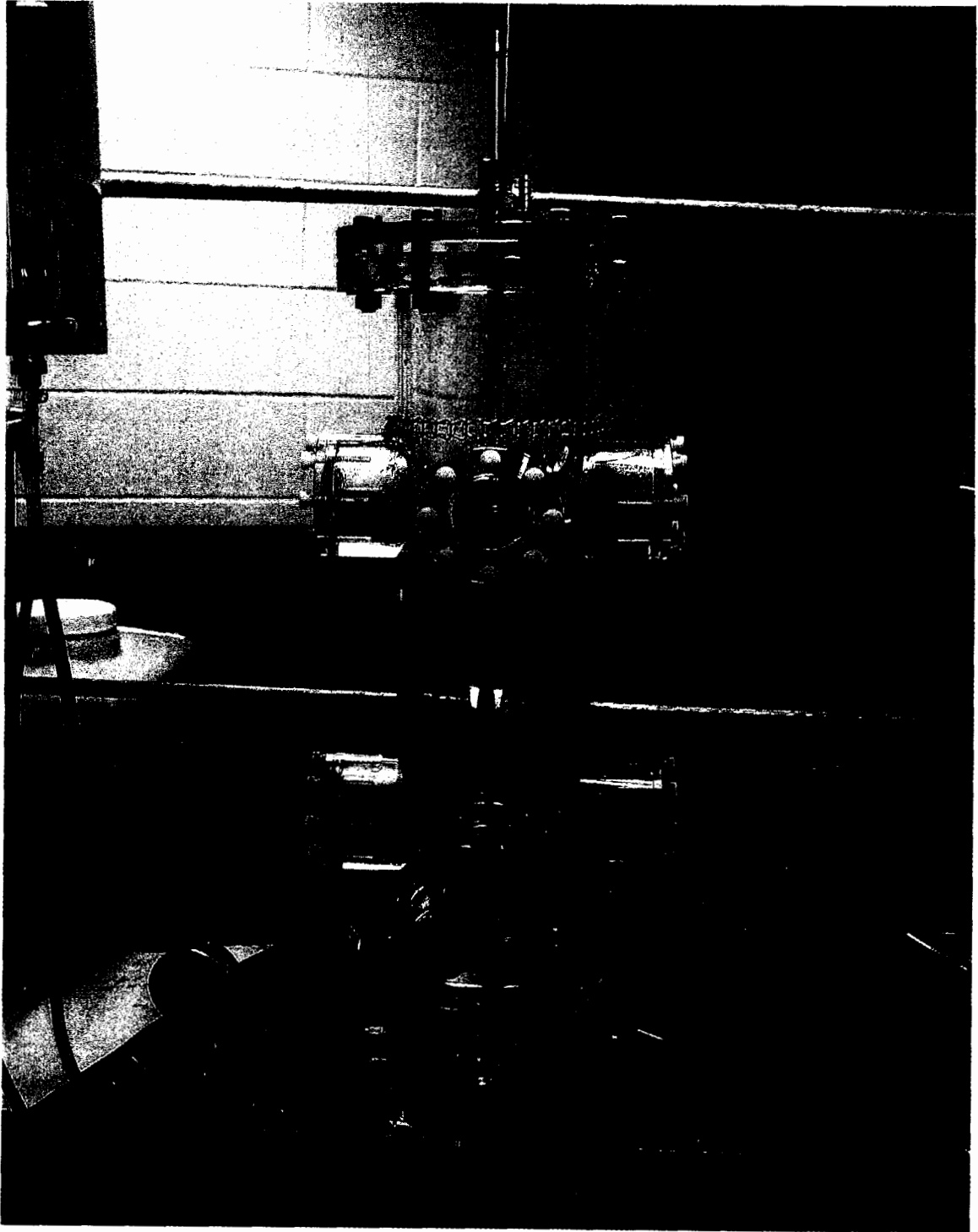
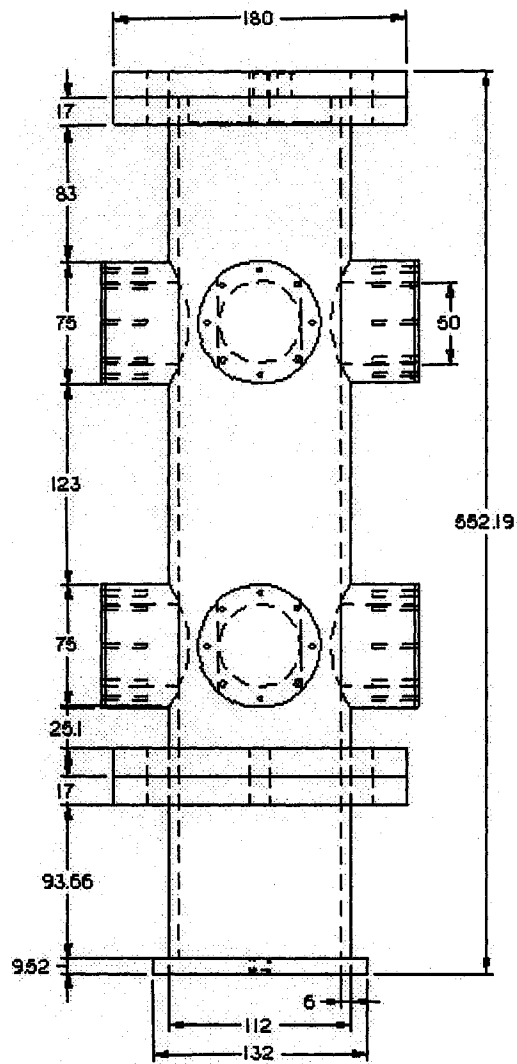


**Figure 3.3:** Photograph of spray column.  
(Original in color)



Units = mm

**Figure 3.4:** Scale drawing of spray column.

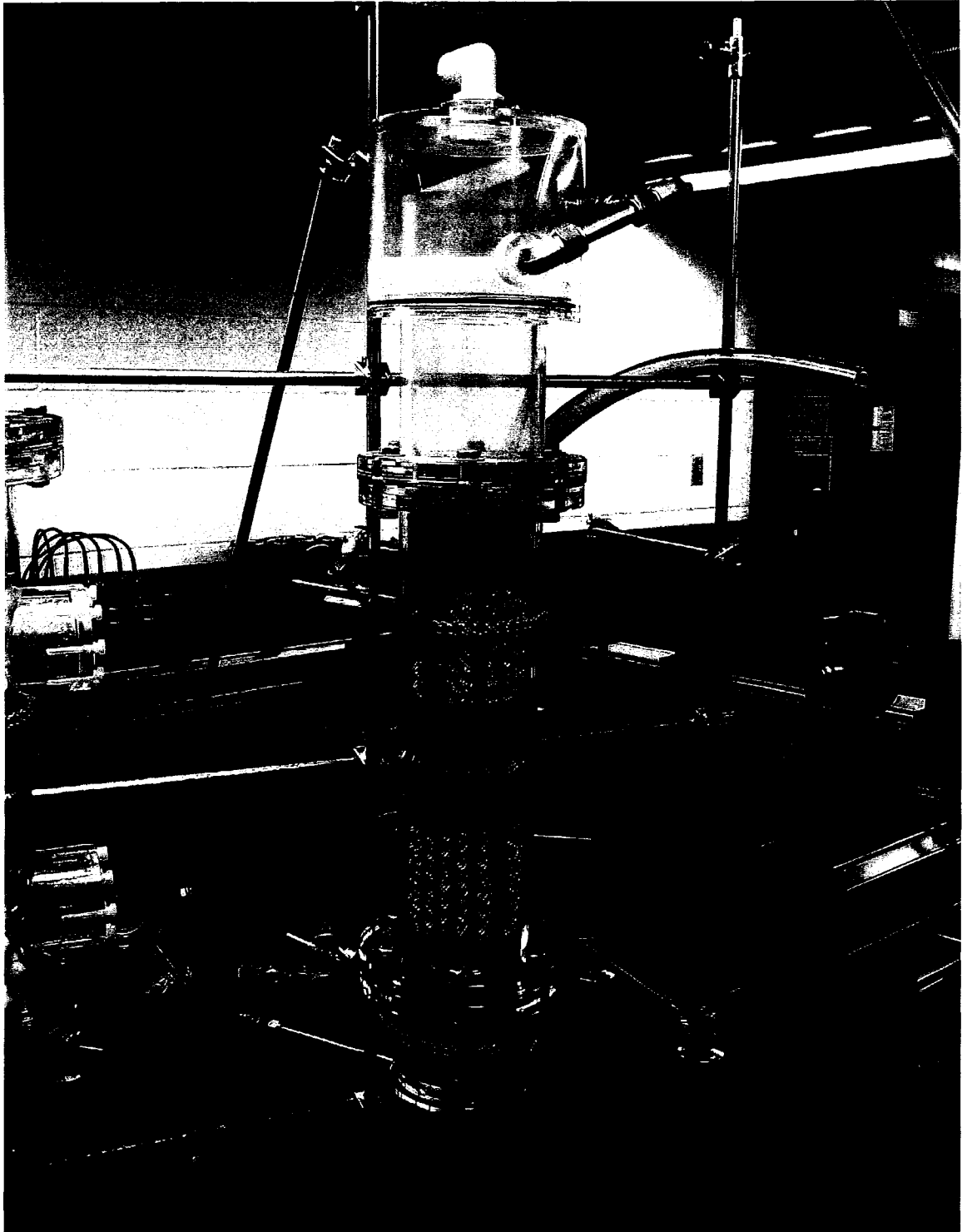
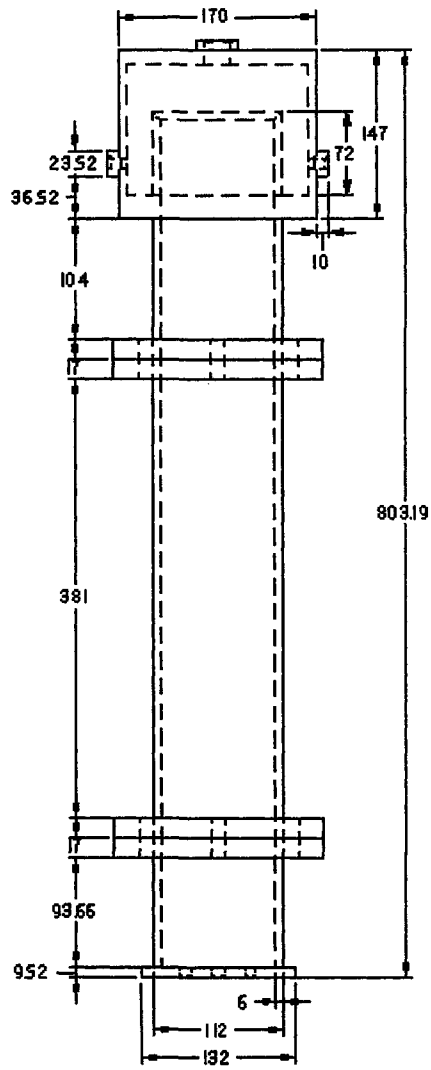


**Figure 3.5:** Photograph of packed column.  
(Original in color)



Units = mm

**Figure 3.6:** Scale drawing of packed column.

**Table 3.1:** Specifications of spray nozzles used in the present study.

Nozzle	Liquid Flow Rate (L/min) @ Pressure					Approx. Orifice Dia. (mm)
	1 bar	2 bar	3 bar	5 bar	7 bar	
P-20	0.153	0.216	0.264	0.341	0.404	0.508
P-28	0.296	0.419	0.513	0.662	0.784	0.711
P-40	0.638	0.902	1.11	1.43	1.69	1.02

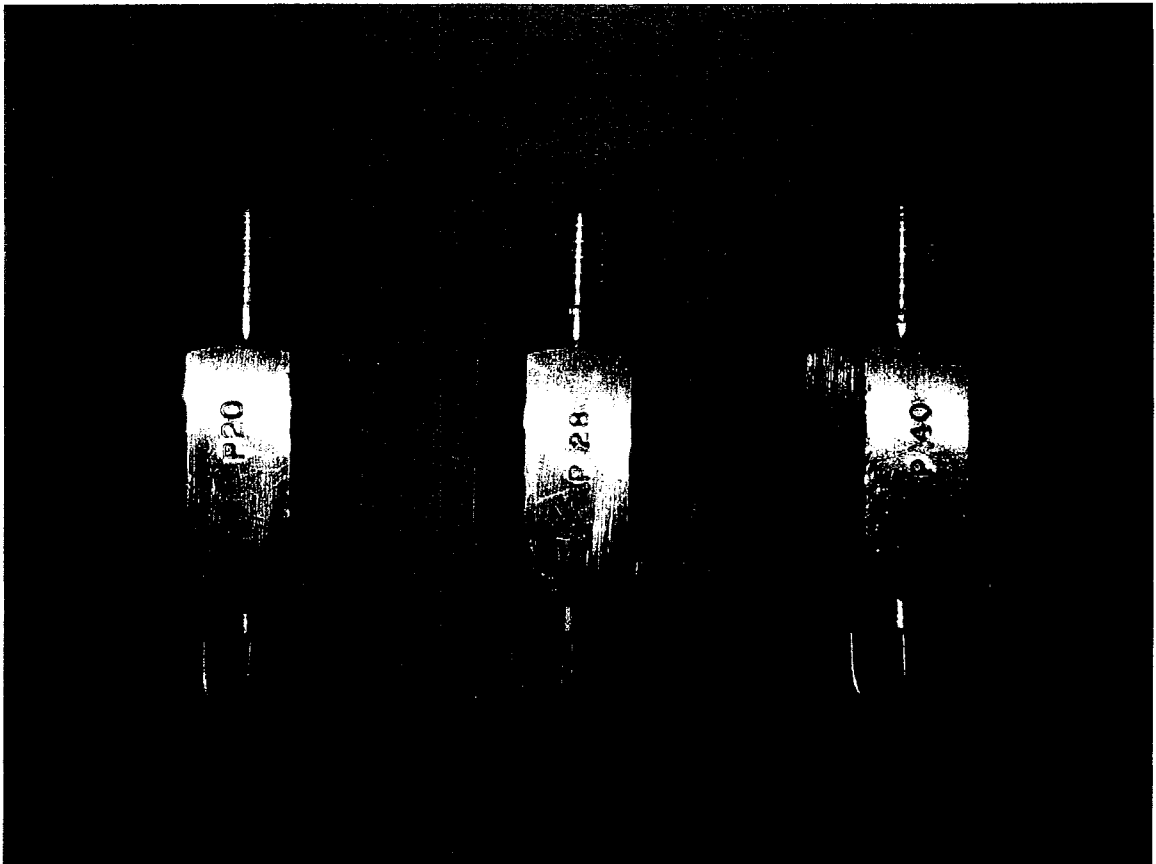


**Figure 3.7:** Photograph of spray nozzles used in the present study.  
(Original in color)

**Table 3.2:** Geometric features of the structured packing.

<b><i>Feature</i></b>	<b><i>Mellapak 500Y</i></b>
Packing Material	Stainless Steel
Element Height (m)	0.205
Specific Area (m <sup>2</sup> /m <sup>3</sup> )	500
Void Fraction	0.91
Corrugation Angle (°)	45
Crimp Height (m)	6.53x10 <sup>-3</sup>
Corrugation Base (m)	9.60x10 <sup>-3</sup>

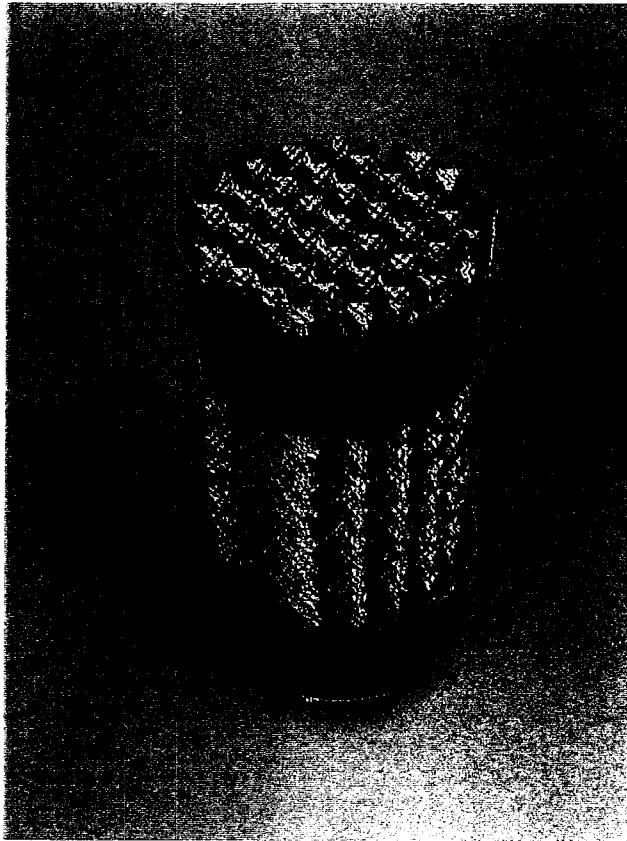


**Figure 3.8:** Photograph of structured packing used in the present study.  
(Original in color)

flow meters were used to regulate the flow of the air and CO<sub>2</sub>. They were scaled meters and were calibrated using a Humonics OptiFlow 650 soap flow meter. The maximum flow was 32 L/min for N<sub>2</sub> and 20 L/min for CO<sub>2</sub>. There was also another flow meter used when the air flow rate of more than 32 L/min was required for the experiments. The third flow meter was manufactured by King Instrument Company. The N<sub>2</sub> was used for the inert gas when the velocity was less than 32 L/min and when the velocity was greater air from a major supply line was used. This was because the maximum velocity for the N<sub>2</sub> from the cylinder was 32 L/min.

### **3.2 Absorption Experiment Procedures**

The CO<sub>2</sub> absorption experiments began by preparing the feed solution at the desired concentration of MEA and CO<sub>2</sub> loading for each experimental run being done. Air from a major supply line or N<sub>2</sub> from a cylinder depending on the velocity required and CO<sub>2</sub> from a cylinder were introduced and regulated by flow meters to the desired rate and concentration. They were then mixed and introduced into the bottom of the column through a single line. The gas once in the column passed through a dispersion outlet to fully disperse the gas throughout the column. At the same time, the previously prepared solution from the feed tank was pumped to the top of the column where it entered the column through either a spray nozzle or the liquid distributor (Figure 3.9 and Figure 3.10) for the packed column. This brought the gas and liquid into contact counter-currently, and the CO<sub>2</sub> in the gas phase was absorbed. The gas then carried out through the top of the column while the CO<sub>2</sub> rich solution was collected out of the bottom of the column in a storage tank. During the operation liquid samples were taken out of the bottom of the column and the gas concentration was recorded as it left the top of the column.

To obtain reliable experimental results, the absorption process was operated until steady state conditions were reached. The steady state condition was indicated when the concentration of the off gas held constant. The time for the spray column to reach steady state was approximately 7-10 minutes while the time for the packed column was approximately 15 minutes. It was at these times that the concentration of the off gas was measured and a liquid sample was collected out of the bottom of the column. The liquid sample was used to verify the CO<sub>2</sub> absorption rates that were calculated from the gas phase data. The CO<sub>2</sub> content in the liquid samples was determined by the method described in Section 3.3.

The absorption experiments that were carried out were all conducted with MEA as the solvent used. The spray column was the main focus of the study to evaluate the feasibility of the operation. The packed column was tested under some of the same conditions in an attempt to produce two sets of data that could easily be compared and analyzed against each other. The operating conditions used in this experiment for both the spray and the packed column can be found in Table 3.3.

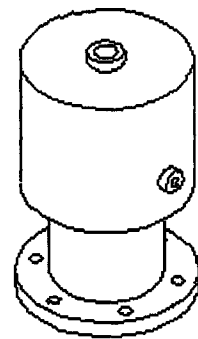
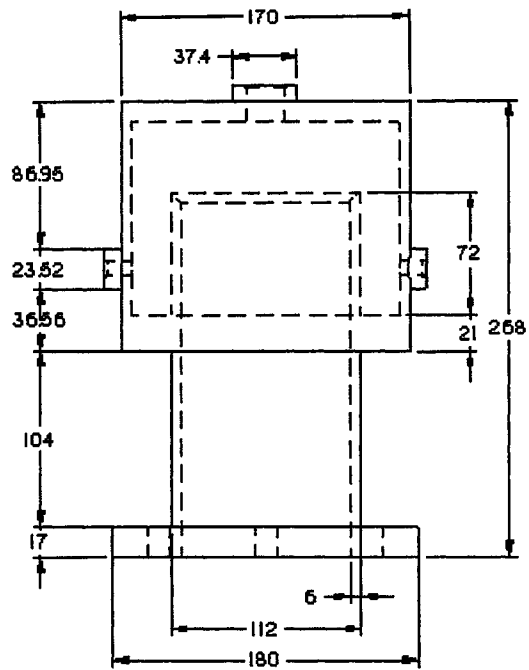
### **3.3 Sample Analysis**

The CO<sub>2</sub> concentration in the gas phase as it entered and left the columns was measured with the infrared gas analyzer (Model 302WP, Nova Analytical Systems Inc.). The reading range was 0.0 to 20.0 % of CO<sub>2</sub> by volume and the accuracy was within  $\pm 2\%$  of the full scale reading. During the experiments once steady state had been reached within the columns a reading was taken at the top of the column.

The analysis of the liquid sample that contained the captured CO<sub>2</sub> gas was done using the standard method given by the Association of Official Analytical Chemists (AOAC). The total amine concentration was determined by titration with standard 1.0 N hydrochloric acid (HCl) solutions using methyl orange as the indicator. Then, the determination of CO<sub>2</sub> content in the liquid involved acidifying a precisely measured quantity of the sample by adding excess HCl solution. The CO<sub>2</sub> gas was released and it was captured by a precision gas burette. The amount of released CO<sub>2</sub> was then used to calculate the loading of the amine solution. The titration apparatus is shown in Figure 3.11.



**Figure 3.9:** Packed column liquid distributor.  
(Original in color)



Units = mm

**Figure 3.10:** Scale drawing of packed column top.

**Table 3.3:** Operating conditions of spray and packed columns.

<b>Parameter</b>	<b>Conditions</b>
<ul style="list-style-type: none"><li>• Absorption Solvent</li></ul>	Monoethanolamine (MEA)
<ul style="list-style-type: none"><li>• Gas Phase<ol style="list-style-type: none"><li>1. Gas Velocity</li><li>2. Feed CO<sub>2</sub> Concentration</li></ol></li></ul>	Up to 764 m <sup>3</sup> /m <sup>2</sup> -h 5, 10, 15%
<ul style="list-style-type: none"><li>• Liquid Phase<ol style="list-style-type: none"><li>1. Liquid Velocity</li><li>2. MEA Concentration</li><li>3. CO<sub>2</sub> Loading</li><li>4. Temperature</li></ol></li></ul>	Up to 10.3 m <sup>3</sup> /m <sup>2</sup> -h 3,5,7 kmol/m <sup>3</sup> 0, 0.15, 0.25, 0.35, 0.45 mol/mol 25°C

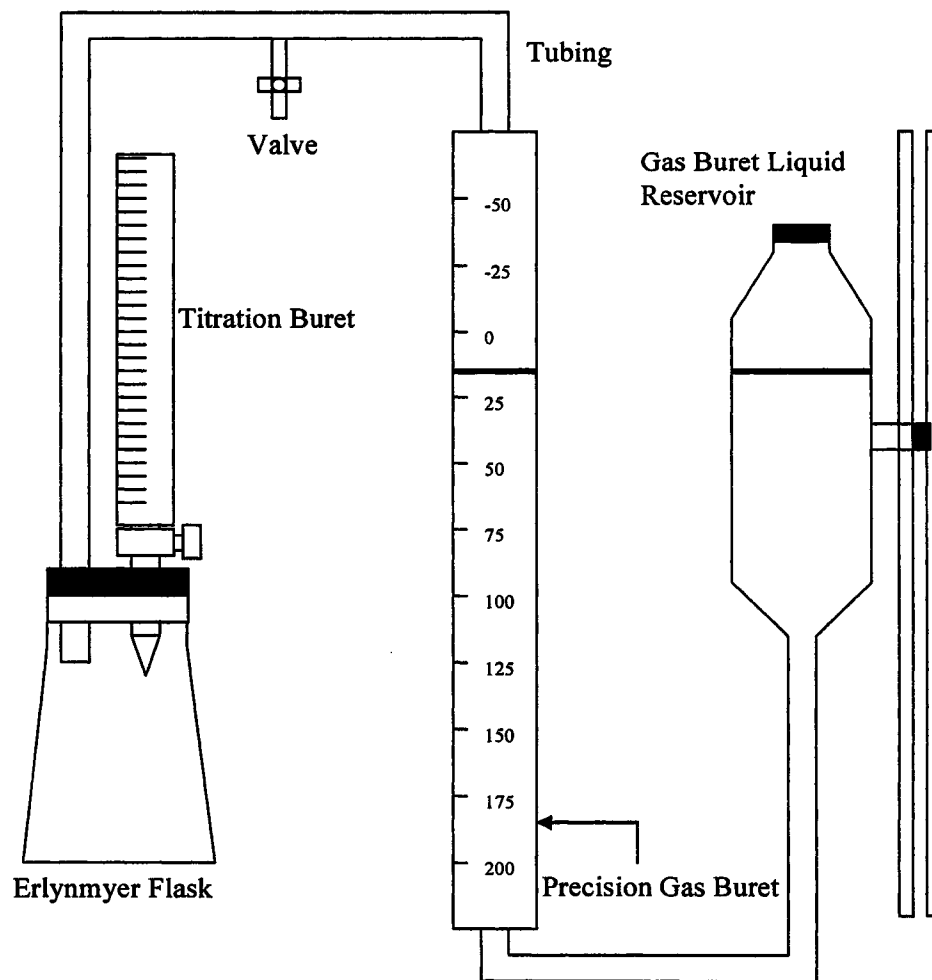


**Figure 3.11:** Gas Measuring Apparatus for CO<sub>2</sub> loading determination.

## Chapter Four

### Results and Discussion

The main objective of this chapter is to provide a set of experimental results for the chemical absorption of CO<sub>2</sub> into an aqueous solution of MEA in the pilot scale columns that included both the spray nozzle and packing as the column internals. The results have been presented in terms of the volumetric overall mass transfer coefficient,  $K_G a_e$ , and are reported as functions of the process parameters that were tested. The absorption experiments were conducted over the ranges of the operating and design parameters previously listed in Table 3.3. The results compiled, from more than 420 experimental runs, of which an example is given in Table 4.1, includes measured data of CO<sub>2</sub> concentration in the gas and liquid phase, liquid composition and gas and liquid flow rates. The rest of the experimental results are given in Appendix A.

The experimental data was then manipulated and put into Equation (2.19) that was defined earlier as:

$$K_G a_e = \left\{ \frac{G_I}{P(y_A - y_A^*)} \right\} \left\{ \frac{dY_A}{dZ} \right\} \quad (2.19)$$

where  $Y_A$  denotes the mole ratio of CO<sub>2</sub> (in the gas phase) to the inert gas. The first term on the right hand side of Equation (2.19) was determined from the values of the operating conditions (gas load and pressure) of the absorption experiment. The second term of the equation,  $dY_A/dZ$ , the concentration gradient, was obtained by taking the difference in the inlet and outlet gas concentration and dividing it by the height in the spray column that the spray covered. The height of the spray zone or the packing section was measured for

**Table 4.1:** Typical results from an experimental run

Run #		10-23	10-24	10-25	10-26
<b>GAS SIDE</b>					
<b>INLET</b>	N <sub>2</sub> flow rate (L/min)	4.55	9.42	14.43	20.72
	CO <sub>2</sub> flow rate (L/min)	0.50	1.07	1.63	2.29
	CO <sub>2</sub> concentration (%)	10.33	10.33	10.33	10.33
	CO <sub>2</sub> in feed gas (Mole/min)	0.023	0.048	0.074	0.107
	N <sub>2</sub> in feed gas (Mole/min)	0.203	0.420	0.644	0.925
	Temperature (K)	298.15	298.15	298.15	298.15
<b>OUTLET</b>	CO <sub>2</sub> concentration (%)	2.31	4.01	5.60	6.45
	CO <sub>2</sub> in treated gas (Mole/min)	0.005	0.018	0.038	0.064
	Absorbed CO <sub>2</sub> (Mole/min)	0.0186	0.0309	0.0360	0.0427
<b>LIQUID SIDE</b>					
<b>INLET</b>	Liquid Flow Rate (L/min)	0.20	0.20	0.20	0.20
	MEA concentration (kmol/m <sup>3</sup> )	3.0	3.0	3.0	3.0
	CO <sub>2</sub> Loading (Mole CO <sub>2</sub> /Mole MEA)	0.0099	0.0099	0.0099	0.0099
<b>OUTLET</b>	CO <sub>2</sub> Loading (Mole CO <sub>2</sub> /Mole MEA)	0.0397	0.0595	0.0694	0.0793
	Absorbed CO <sub>2</sub> (Mole/min)	0.0178	0.0297	0.0357	0.0416
<b>Mass Balance</b>		-3.96	-3.67	-0.85	-2.54
Nozzle		P-20	P-20	P-20	P-20
G <sub>in</sub> (kmol/m <sup>2</sup> *h)		1.501	3.111	4.765	6.842
K <sub>Ga<sub>e</sub></sub> (kmol/m <sup>3</sup> *h*kPa)		0.275	0.403	0.423	0.477

**Note:** A full listing of the results can be found in Appendix A.

each run that was done. This chapter shows the effects of the tested parameters on the efficiency of absorption within the spray column.

#### **4.1 Effects of Process Parameters on Mass Transfer Coefficient**

##### **4.1.1 Effect of CO<sub>2</sub> Partial Pressure**

In the gas absorption application, the gas-phase CO<sub>2</sub> concentration varies considerably as the gas stream travels through the absorption column. The variation in the CO<sub>2</sub> concentration defines the change in CO<sub>2</sub> partial pressure prevailing along the height of the column. It was found in this study that the CO<sub>2</sub> partial pressure has a great impact on the overall mass transfer performance of the spray column. As the partial pressure increased from 5 kPa to 15 kPa, the  $K_{Ga_e}$  decreased as shown in Figure 4.1. The effect of CO<sub>2</sub> partial pressure can be illustrated more clearly in Figure 4.2 where the  $K_{Ga_e}$  coefficient was plotted directly against the partial pressure. The reduction in  $K_{Ga_e}$  value holds true at different liquid flow rates and the different CO<sub>2</sub> loadings that were run for the experiments. This follows the overall mass transfer equation (Equation 2.19) that the  $K_{Ga_e}$  decreases as the mass-transfer driving force  $P(y_A - y_A^*)$  in the gas phase increases. It can also be observed from Figure 4.2 that the effect of partial pressure became less especially at the CO<sub>2</sub> loading of more than 0.25 mole/mole and the partial pressure of more than 10 kPa. The restricted diffusion of relative amine in the liquid phase is speculated to be the cause of this behavior. Mass transfer phenomena under the high CO<sub>2</sub> loading condition was mainly controlled by the CO<sub>2</sub> reaction in the liquid, thus resulting in only a small change in the amount of CO<sub>2</sub> absorbed as the partial pressure increased.

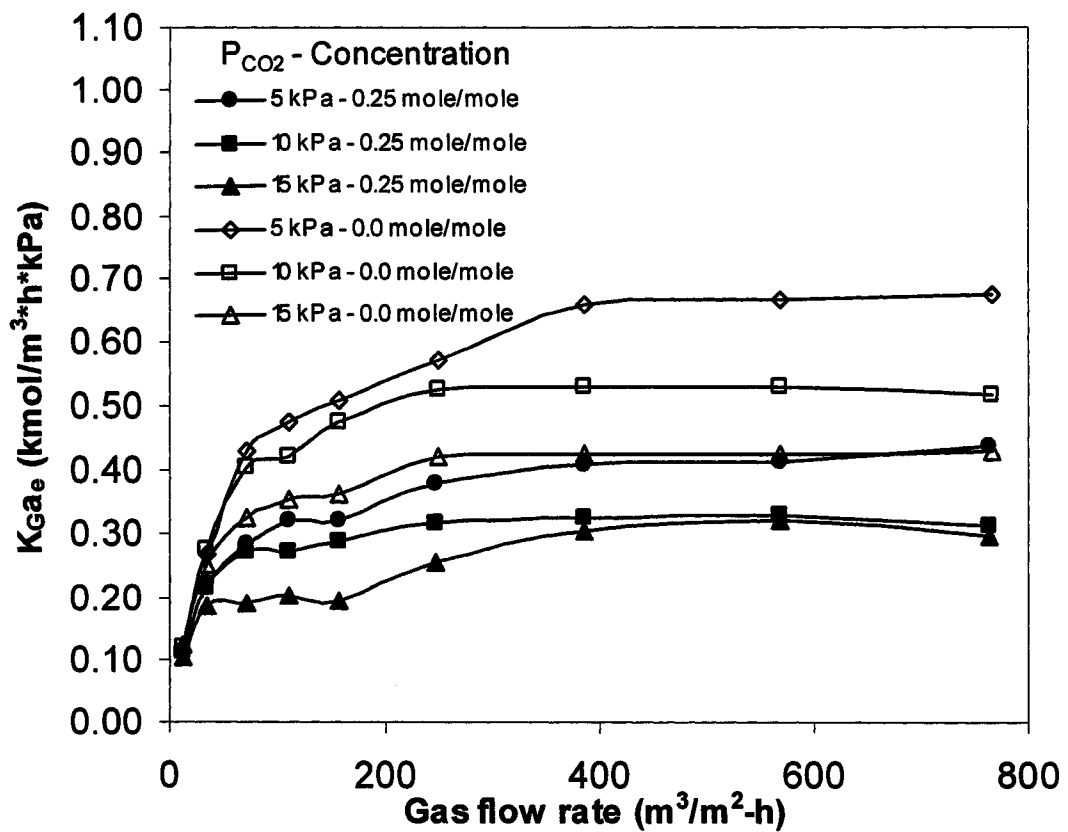


**Figure 4.1:** Effect of CO<sub>2</sub> partial pressure and gas flow rate on overall mass transfer at CO<sub>2</sub> loading of 0.0 mole/mole and 0.25 mole/mole. (Nozzle = P-20, Liquid flow rate = 1.53 m<sup>3</sup>/m<sup>2</sup>-h).

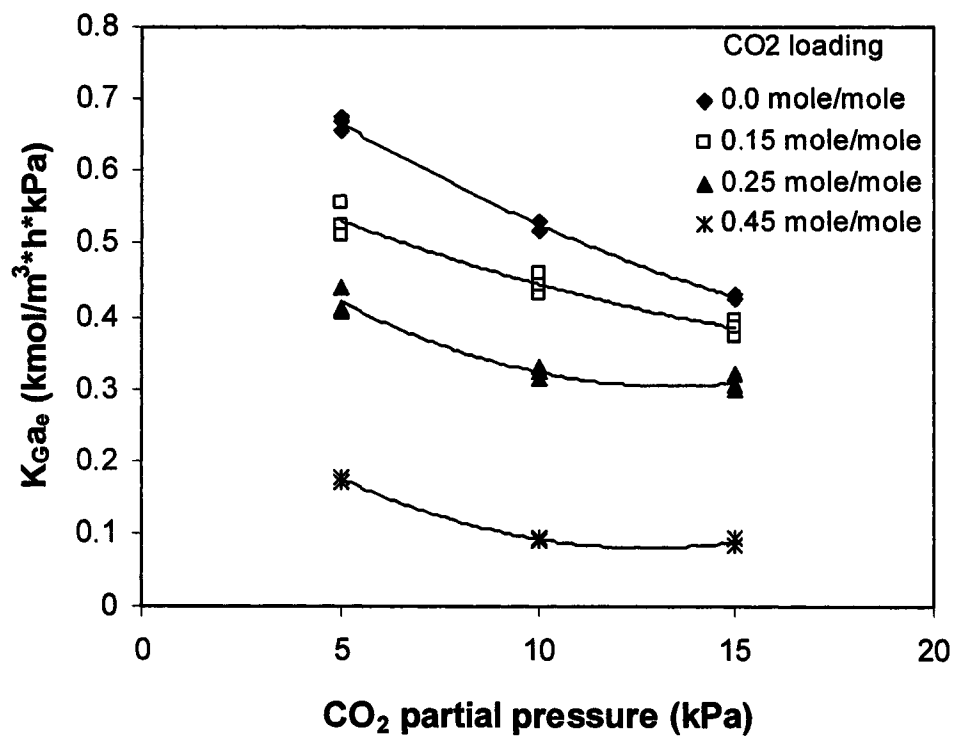


**Figure 4.2:** Effect of CO<sub>2</sub> partial pressure on overall mass transfer. (Nozzle = P-20, Liquid flow rate = 1.53 m<sup>3</sup>/m<sup>2</sup>-h, Gas flow rate = 382 – 764 m<sup>3</sup>/m<sup>2</sup>-h).

#### 4.1.2 Effect of Gas Flow Rate

The gas flow rate affected the overall mass transfer coefficient but only to a certain point. As the gas flow rate increased so to did the  $K_G a_e$ . This behavior illustrates the gas-phase controlled mass transfer, taking place within the low range of the gas flow rate. When the gas flow rate exceeded  $300 \text{ m}^3/\text{m}^2\text{-h}$ , the  $K_G a_e$  tends to remain constant. The mass transfer at this point shifts from the gas-phase controlling mechanism to the liquid-phase controlling mechanism. It can be seen that the shape of the curve is consistent as the loading is varied as well (Figure 4.3). It is also shown in Figure 4.4 that at different liquid flow rates the same holds true that at about a gas flow rate of  $300 \text{ m}^3/\text{m}^2\text{-h}$  the curve again levels off. This data shows that as the gas flow rate increases the mass transfer coefficient increases simultaneously to a point where the liquid phase mass transfer takes over and becomes the main driving force for  $\text{CO}_2$  absorption. In general, as the gas flow increases the amount of  $\text{CO}_2$  molecules available for absorption increases. This would lead to a higher mass transfer performance. However, the overall rate of gas absorption is not fully dependent upon the gas flow rate though. It is also dependent upon the liquid flow rate and availability of reactive amine in the liquid which as seen in this case controls the rate of mass transfer after the gas flow rate reaches the point of  $300 \text{ m}^3/\text{m}^2\text{-h}$  (Aroonwilas, 2001).

In the actual application, the conventional absorber such as packed column is designed at the rate of gas flow much greater than  $300 \text{ m}^3/\text{m}^2\text{-h}$ , therefore the  $K_G a_e$  is always unaffected by the gas rate. In contrary, the spray column could be designed to have a large cross-sectional area, resulting in a much lower gas rate. To avoid the

undesirably low CO<sub>2</sub> absorption performance, one should keep in mind the minimum gas rate of 300 m<sup>3</sup>/m<sup>2</sup>-h as one of the design criteria for spray column.

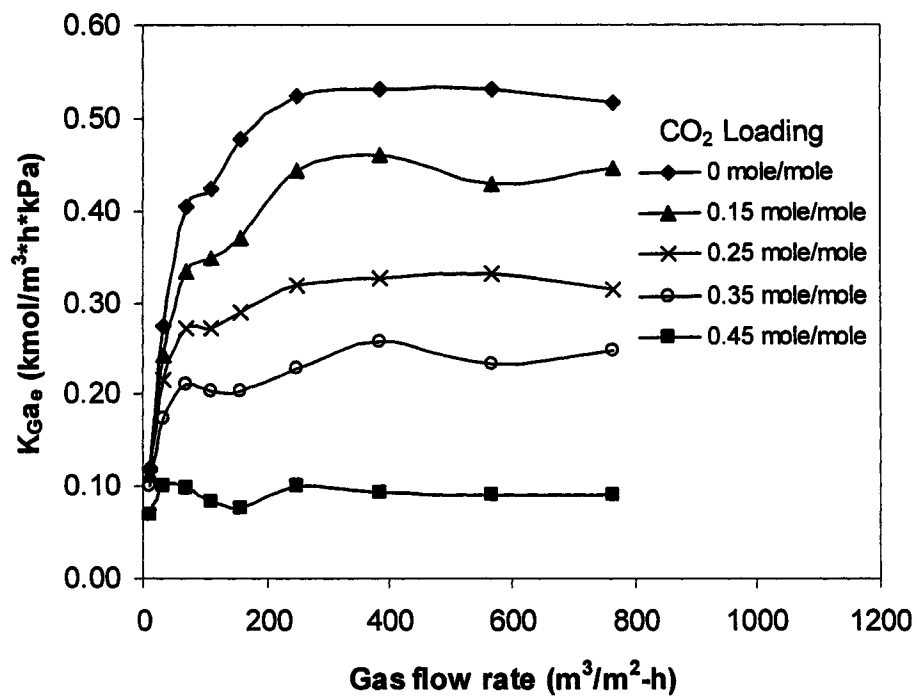


**Figure 4.3:** Effect of gas flow rate on overall mass transfer at different CO<sub>2</sub> loadings (Nozzle = P-20, Liquid flow rate = 1.53 m<sup>3</sup>/m<sup>2</sup>-h, [MEA] = 3M).

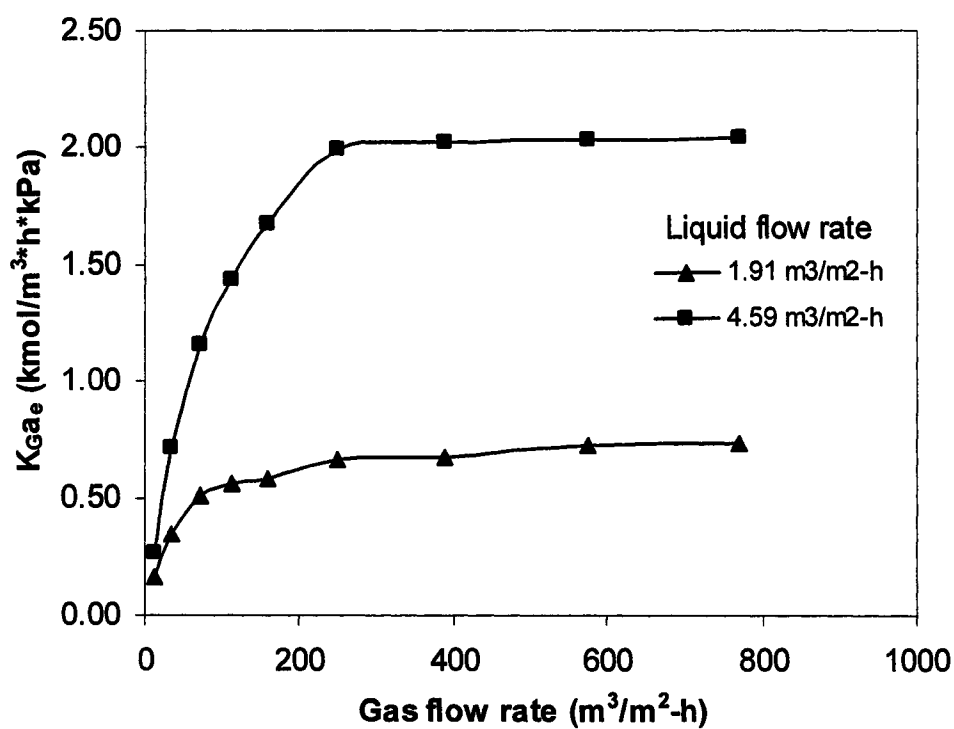


**Figure 4.4:** Effect of gas flow rate on overall mass transfer at different liquid flow rates (Nozzle = P-28,  $P_{CO_2}=15$  kPa,  $[MEA] = 5M$ ).

### 4.1.3 Effect of Liquid Flow Rate

Liquid flow rate has a great impact on the overall mass transfer performance of spray column. Figures 4.5, 4.6 and 4.7 show that as the liquid flow rate increased the  $K_G a_e$  increased and this held true for the entire range of liquid flow rate that was tested. As the liquid flow increases more effective interfacial area ( $a_e$ ), between the liquid and the gas was formed producing a higher overall mass transfer to take place between the two. The figures also show that the increase in  $K_G a_e$  was observed for the entire range of CO<sub>2</sub> loading tested.

For the individual spray nozzle, the increase in liquid flow rate caused the  $K_G a_e$  to rise in two different manners. At the low range of liquid flow, the  $K_G a_e$  tends to increase with the liquid flow rate in the exponential manner. The increase in  $K_G a_e$  then appears to be proportional at the higher range of liquid flow. The exponential increase was caused by two phenomena, taking place in parallel. First, the increase in liquid flow rate led to a reduction in size of spray droplets from large to small, thus resulting in an increase in droplet surface area per unit volume of liquid. Second, as the liquid flow rate increased so did the amount of droplets produced by the nozzle and also the surface area available for mass transfer. The combined effect of the two phenomena therefore provided the exponential increase in  $K_G a_e$ . At the high range of liquid flow rate, the reduction in droplet size by the increasing liquid flow however became insignificant, leaving the increasing amount of spray droplets to be the primary factor that defined the proportional increase in mass transfer performance.

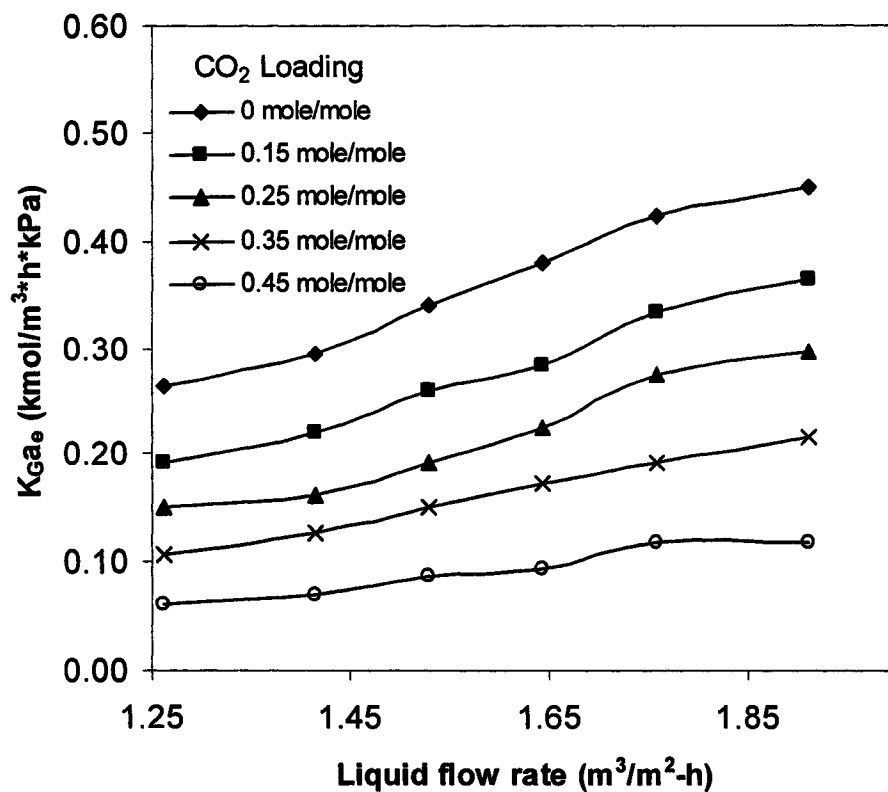


**Figure 4.5:** Effect of liquid flow rate on overall mass transfer of P-20 nozzle at different CO<sub>2</sub> loadings ( $P_{CO_2}=15$  kPa,  $[MEA] =3M$ , Gas flow rate= $76$  m<sup>3</sup>/m<sup>2</sup>-h).

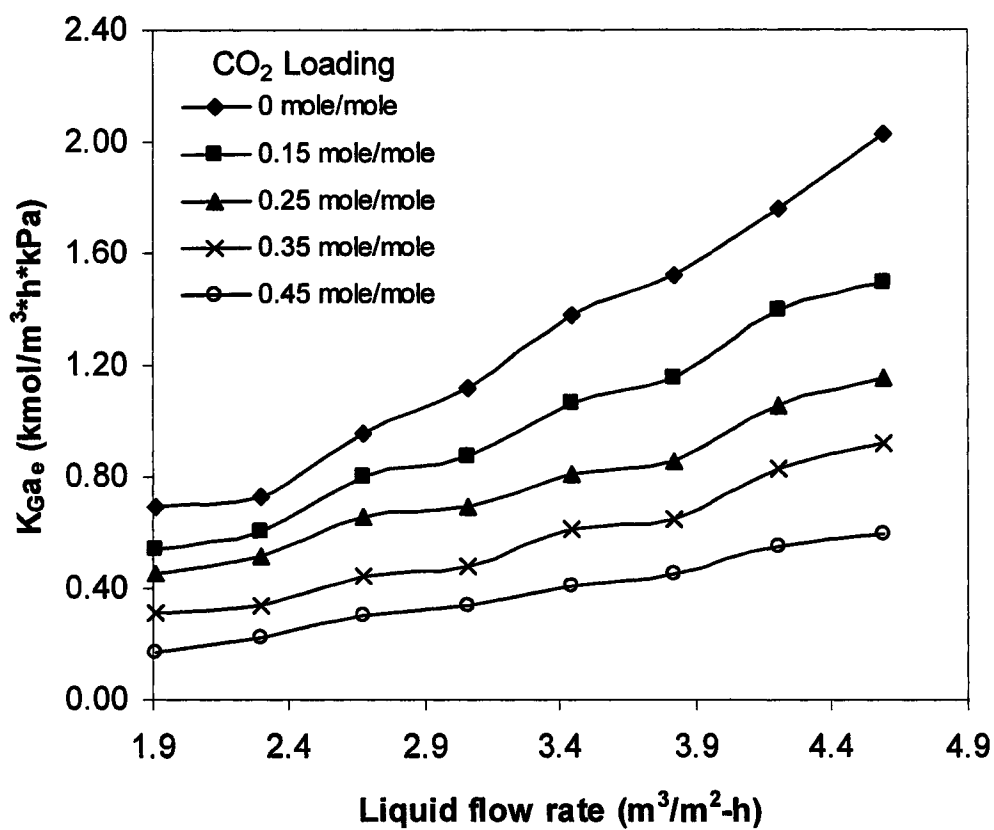


**Figure 4.6:** Effect of liquid flow rate on overall mass transfer of P-28 nozzle at different CO<sub>2</sub> loadings ( $P_{CO_2}=15$  kPa,  $[MEA] =5M$ , Gas flow rate= $382$  m<sup>3</sup>/m<sup>2</sup>-h).

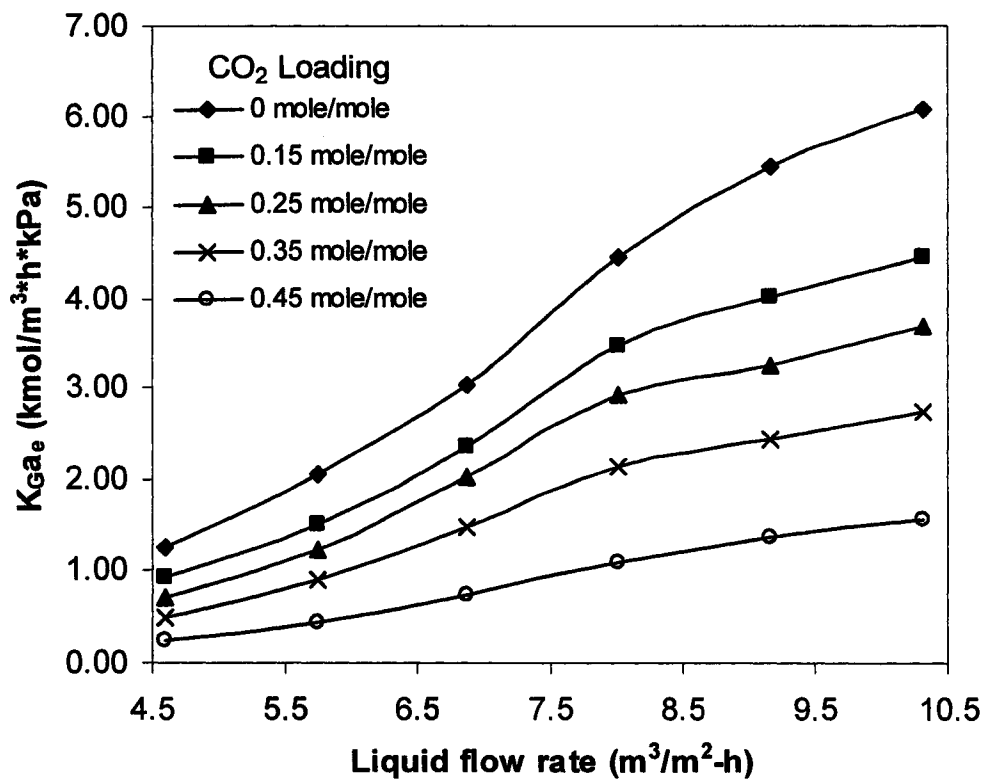


**Figure 4.7:** Effect of liquid flow rate on overall mass transfer of P-40 nozzle at different CO<sub>2</sub> loadings ( $P_{CO_2}=15$  kPa,  $[MEA] =5M$ , Gas flow rate= $382$  m<sup>3</sup>/m<sup>2</sup>-h).

#### 4.1.4 Effect of MEA Concentration

The effect of the solvent concentration was tested in this study. The change in the MEA concentration apparently has an impact on the CO<sub>2</sub> absorption efficiency. Figure 4.8 shows that as the concentration increased from 3 kmol/m<sup>3</sup> to 5 kmol/m<sup>3</sup> and to 7 kmol/m<sup>3</sup> so did the  $K_G a_e$  value. The reason for this behavior is that the increasing concentration yielded a higher amount of the active molecules available to diffuse towards the gas-liquid interface and react with the dissolved molecules. The active MEA concentration in the bulk liquid can be estimated using the relationship between the CO<sub>2</sub> loading and the total concentration of the aqueous solution:

$$C_{activeMEA} = \left( \frac{\alpha_{CO_2,eq} - \alpha_{CO_2}}{\alpha_{CO_2,eq}} \right) C_{total} \quad (4.1)$$

where  $C_{activeMEA}$  is concentration of active MEA,  $C_{total}$  is concentration of aqueous solution,  $\alpha_{CO_2}$  is CO<sub>2</sub> loading, and  $\alpha_{CO_2,eq}$  is CO<sub>2</sub> loading at equilibrium condition.

The finding that the  $K_G a_e$  increased as the MEA concentration increased from 3 kmol/m<sup>3</sup> to 7 kmol/m<sup>3</sup> differs from what has been normally observed in the packed column. According to Strigle (1987), the mass transfer coefficient of packed column decreases by 5% for every molarity of MEA increasing beyond 3 kmol/m<sup>3</sup>. The reduction in the  $K_G a_e$  of packed column results from an increase in the viscosity of amine solution, which causes the rate of chemical diffusion to reduce. The increasing viscosity also tends to cause a reduction in the effective mass transfer area ( $a_e$ ) between gas and liquid in the free-flow packed column. However, the increasing  $K_G a_e$  of spray column due to the concentration clearly shows no reduction in the effective area for mass transfer. This can be explained in the spray column in the manner that the viscosity of the liquid

has very little effect on the size of droplets produced. It is believed that the amount of energy to force the liquid through the nozzle will slightly increase but once the liquid droplets are formed and the absorption zone is produced the droplets will stay separate until after the absorption takes place. The droplets will then start to interact again as they pool in the bottom of the spray column and are pumped out to the stripping column but at this point they have made their pass through the absorber and have no more bearing on the absorption process.

#### **4.1.5 Effect of CO<sub>2</sub> Loading**

The CO<sub>2</sub> loading of the solution was tested to see the results on the mass transfer. The loading was tested at points of 0, 0.15, 0.25, 0.35 and 0.45 mole CO<sub>2</sub>/mole MEA. In all instances, Figures 4.5, 4.6 and 4.7 show that as the loading increased the  $K_G a_e$  value decreased. This was the same no matter if the liquid or the gas flow rate was tested against it. This can be explained in the fact that as the CO<sub>2</sub> loading increases the amount of active absorbent decreases, causing the  $K_G a_e$  to decrease. The relationship between the  $K_G a_e$  and CO<sub>2</sub> loading for three nozzles tested is presented in Figure 4.9.

#### **4.1.6 Effect of Nozzle Size**

Three nozzles with different orifice sizes were tested in this study (see Table 3.1). Each nozzle has a different operating range and produced slightly different results in the overall mass transfer coefficient. Table 4.2 shows the ranges that each of the nozzles was tested. Figure 4.10 shows a direct comparison between the P-28 and P-40 nozzles. When the nozzles were run at the same gas flow rate and CO<sub>2</sub> partial pressure, the results are

slightly different. It shows that when the liquid flow rate is at the low end of the flow range for a particular nozzle the  $K_G a_e$  is lower. This is attributed to the fact that the spray is not fully developed and the interfacial area is lower. As the liquid flow rate increases, the spray is more fully developed with the smaller liquid droplets that offer the higher effective area per unit volume, causing the  $K_G a_e$  to increase accordingly. When the spray is not fully developed it travels out of the nozzle in more of a liquid sheet pattern than spray droplets. Once the spray reaches the optimal operating parameters of the nozzle that is when the liquid starts to be atomized and this is when it is ideal for absorption. In effect, as the nozzle size increases the liquid flow through the nozzle increases and this in-turn increases the amount of small liquid droplets being produced, leading to an increase in the interfacial area available for CO<sub>2</sub> absorption.

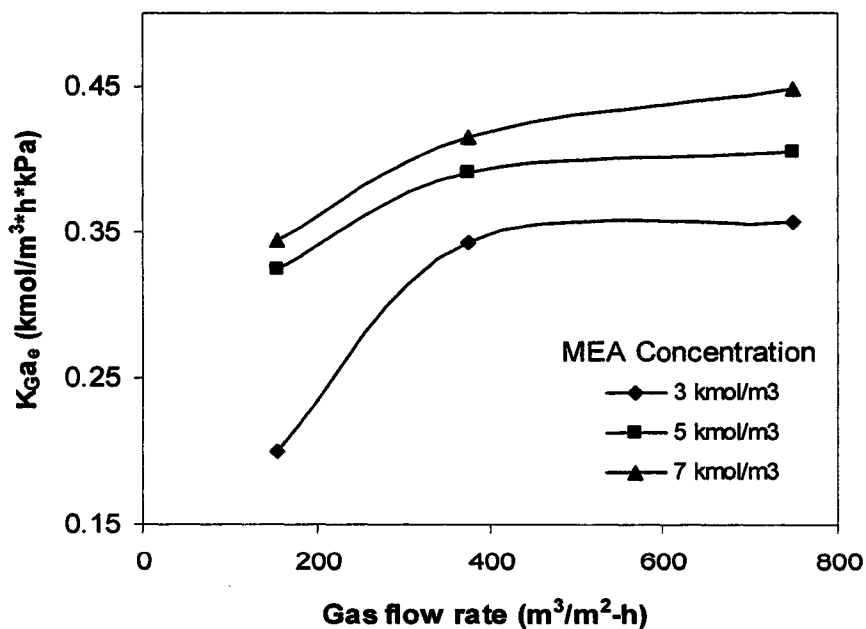
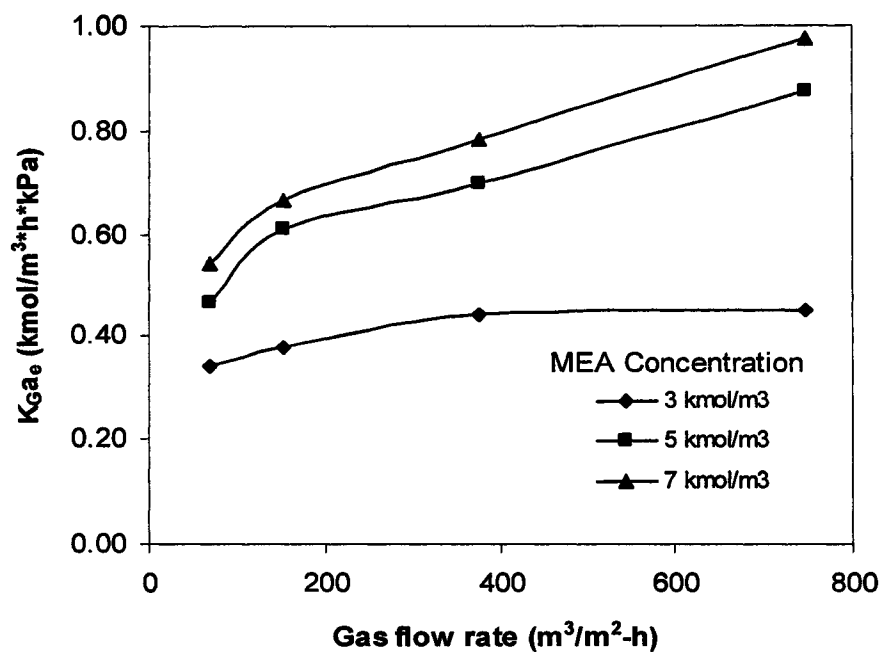


**Figure 4.8:** Effect of the concentration of the MEA on overall mass transfer at  $CO_2$  loadings of 0.00 mole/mole (upper) and 0.25 mole/mole (lower) (Nozzle=P-20,  $P_{CO_2}$ =15 kPa).

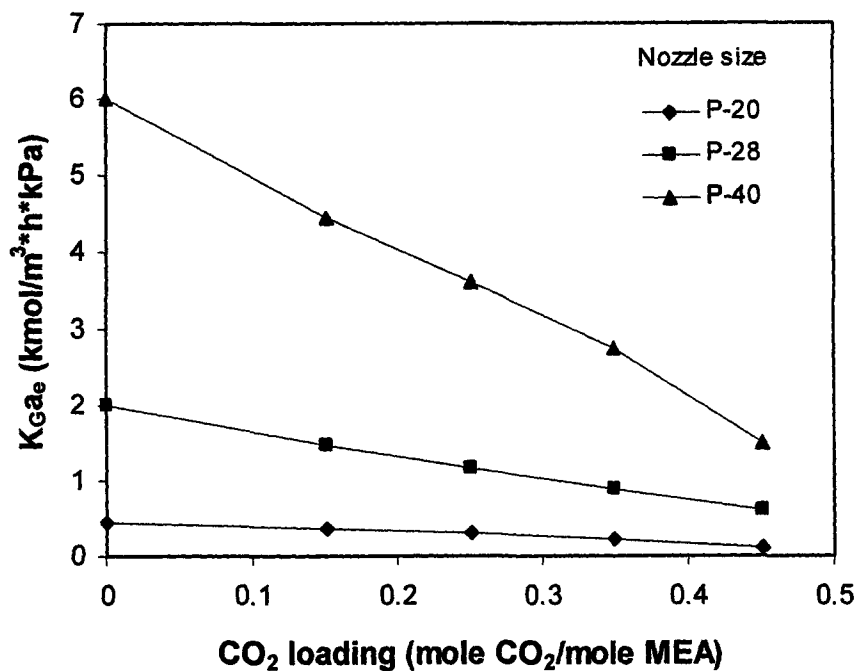


**Figure 4.9:** Effect of CO<sub>2</sub> loading on overall mass transfer for different nozzles (for P-20 nozzle, P<sub>CO<sub>2</sub></sub>=15 kPa, [MEA] =3M, Gas flow rate=76 m<sup>3</sup>/m<sup>2</sup>-h, Liquid flow rate = 1.53 m<sup>3</sup>/m<sup>2</sup>-h; for P-28 nozzle, P<sub>CO<sub>2</sub></sub>=15 kPa, [MEA] =5M, Gas flow rate=382 m<sup>3</sup>/m<sup>2</sup>-h, Liquid flow rate = 4.59 m<sup>3</sup>/m<sup>2</sup>-h; and for P-40 nozzle, P<sub>CO<sub>2</sub></sub>=15 kPa, [MEA] =5M, Gas flow rate=382 m<sup>3</sup>/m<sup>2</sup>-h, Liquid flow rate=10.32 m<sup>3</sup>/m<sup>2</sup>-h).

**Table 4.2:** Operating ranges of spray nozzles tested.

<b>Nozzle</b>	<b>Flow Range <math>\text{m}^3/\text{m}^2\text{-h}</math></b>
P-20	1.26-1.91
P-28	1.91-4.60
P-40	4.59-10.32

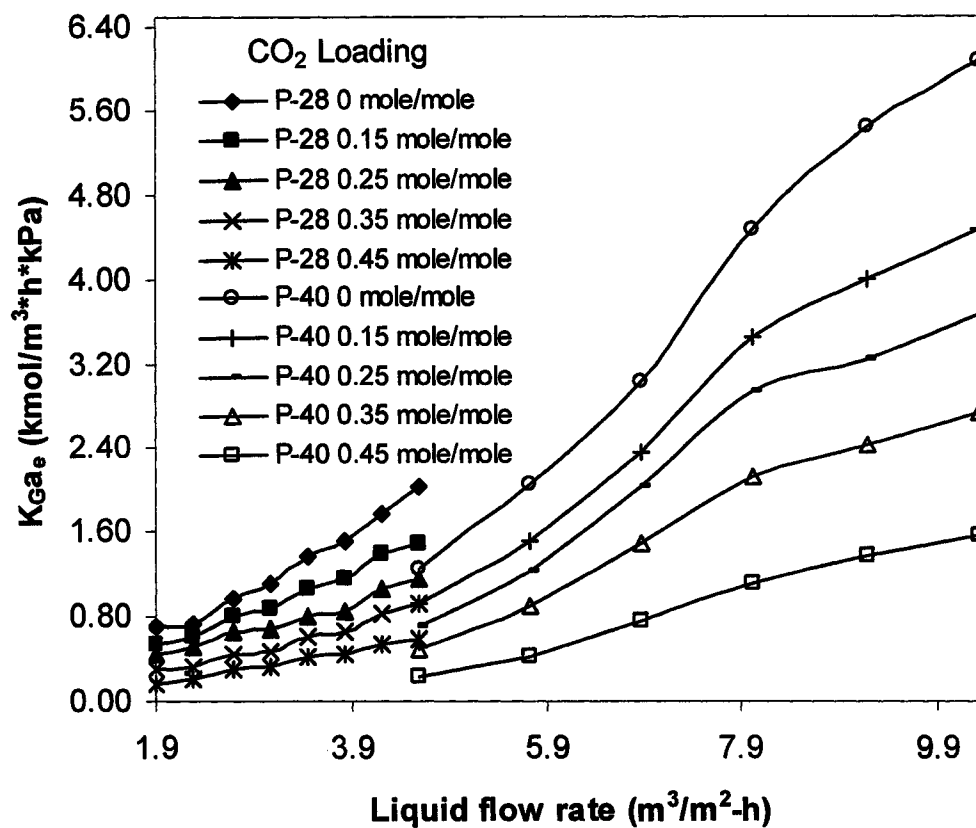


**Figure 4.10:** Effect of the nozzle size on overall mass transfer and liquid flow rate (Gas flow rate=382 m<sup>3</sup>/m<sup>2</sup>-h, P<sub>CO<sub>2</sub></sub>=15% CO<sub>2</sub>, [MEA] =5 kmol/m<sup>3</sup>).

## 4.2 Spray versus Packed Column

The mass transfer performance of spray column obtained from the present study has been directly compared to the performance of conventional packed column. The packed column used two elements of the Mellapak 500Y structured packing, provided by Sulzer Brothers Ltd., Switzerland. This gave a total length of 0.40 m of packing section. The Mellapak 500Y was selected for the comparison because it is one of the best tower packing commercially available in the market. According to the literature (Aroonwilas et al., 1999; Aroonwilas, 2001), the structured packing provided much greater mass transfer performance than the random packing.

In this study, the packed column was compared to the P-40 nozzle spray column as it offered a wider range of liquid flow rate to be tested. Figure 4.11 shows that the spray column offers a much higher overall mass transfer per the area tested. At the CO<sub>2</sub> loading of 0.15 mole/mole, the spray column yielded the  $K_G a_e$  coefficient, which is higher than the coefficient of packed column by a factor of 2 to 7. At the loading of 0.45mole/mole, the spray provided the  $K_G a_e$  coefficient of up to 3 times higher than the coefficient offered by the packed column. This suggests that the use of spray column can considerably improve the efficiency of CO<sub>2</sub> absorption.

The reason for the superior performance of spray column is that the spray nozzle offers a much higher interfacial area than the packing does when the two were tested against each other. The larger area is produced because the absorption liquid is mechanically forced through the small orifice of spray nozzle. This produces very fine droplets that offer a much larger surface area for the gas to contact with. In the packed column, the separation of the liquid takes place by the liquid trickling down the packing.

As it travels by gravity, it slowly breaks apart and stretches out and this is what produces the surface area for mass transfer. One disadvantage is that as the viscosity of the liquid increases it is harder to break apart the bonds of the absorption liquid and therefore the liquid cannot be pulled apart as much. This produces the decrease in surface area in the packed column.

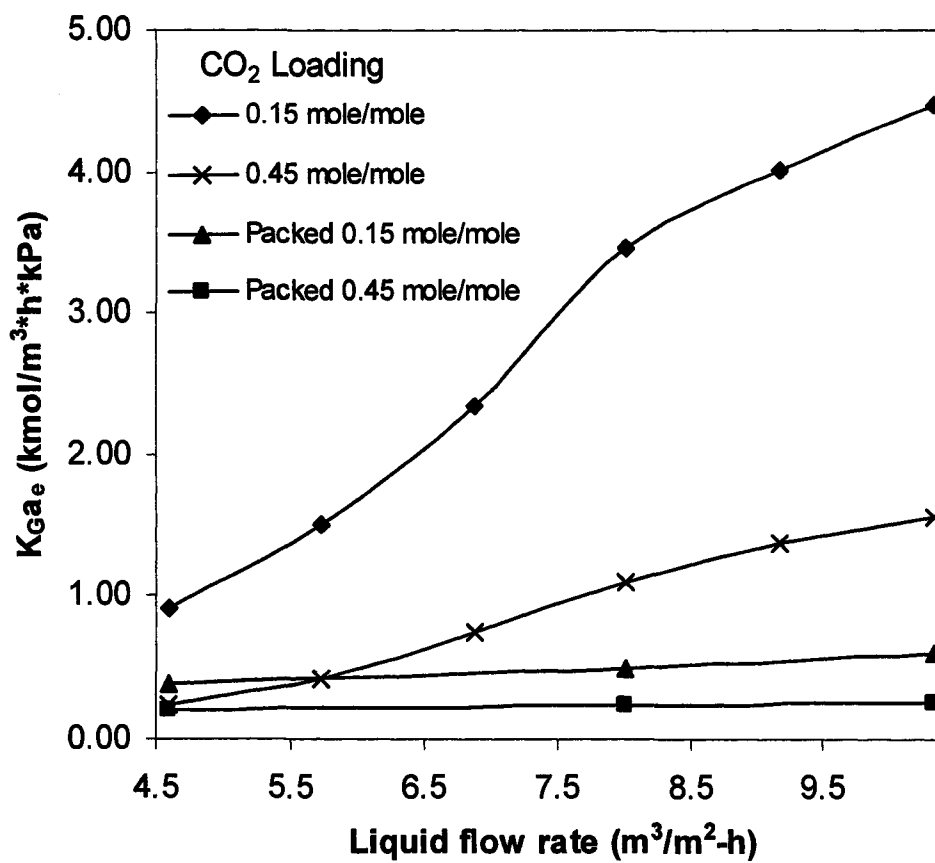


**Figure 4.11:** Mass transfer performance comparison between the packed column and spray column at the same operating conditions.

## Chapter Five

### Theoretical Analysis of Data

This chapter presents the theoretical analysis of the overall mass transfer  $K_G a_e$  that was obtained earlier from the absorption experiments. The analysis was carried out to extract the information on fundamental mass transfer characteristics of spray, i.e. the effective mass transfer area ( $a_e$ ) and the gas-phase mass transfer coefficient ( $k_G$ ). The following sections explain the process taken to determine each value.

#### 5.1 Effective Mass Transfer Area

The analysis of effective mass transfer area was based on the basic relationship between the overall mass transfer coefficient and the individual phase coefficients presented earlier as Equation (2.16):

$$\frac{1}{K_G a_e} = \left( \frac{1}{k_G a_e} \right) + \left( \frac{H}{I k_L^\circ a_e} \right) \quad (2.16)$$

The term  $I k_L^\circ$  can be rewritten as the liquid mass transfer coefficient with chemical reaction  $k_L$ . Therefore, Equation (2.16) can be written in the form:

$$\frac{1}{K_G a_e} = \left( \frac{1}{k_G a_e} \right) + \left( \frac{H}{k_L a_e} \right) \quad (5.1)$$

From this equation, plotting a series of the known ( $1/K_G a_e$ ) against the corresponding ( $H/k_L$ ) ratio at a given liquid flow rate would provide a straight line as illustrated in Figure 5.1. The data points in the plot are of the different CO<sub>2</sub> loadings of the liquid solution tested experimentally. The effective mass transfer area can be analyzed directly

from the calculation of the slope of the straight line, which represents the reciprocal of the area ( $1/a_e$ ).

To apply the above approach for  $a_e$  analysis, the ( $H/k_L$ ) ratio or individual values of Henry's constant ( $H$ ) and liquid mass transfer coefficient ( $k_L$ ) must be known. In this study, the Henry's constant for CO<sub>2</sub>-MEA absorption system was determined from an empirical equation proposed by Weiland (1994):

$$\log(H) = (h_+ + h_- + h_g)I + \log(\sum m_i H'_i) \quad (5.2)$$

where  $h_+$  = van Krevelen coefficient for cations

$h_-$  = van Krevelen coefficient for anions

$h_g$  = coefficient for dissolving gas

$I$  = ionic strength

$H'_i$  = Henry's constant for pure components (water or MEA)

$m_i$  = mass fraction of water or MEA

The liquid mass transfer coefficient ( $k_L$ ) was calculated using the equation for first-order or pseudo-first-order reaction (Perry and Green, 1984):

$$k_L = \sqrt{D_{CO_2,L} (k_2 C_{MEA})} \quad (5.3)$$

where  $D_{CO_2,L}$  = diffusion coefficient of CO<sub>2</sub> in aqueous solution

$C_{MEA}$  = concentration of active MEA in aqueous solution

The  $D_{CO_2,L}$  was found from the following equations (Versteeg, 1988):

$$D_{CO_2,L} = D_{CO_2,water} \left( \frac{1}{\left( \frac{\mu_L}{\mu_{water}} \right)} \right)^{0.8} \quad (5.4)$$

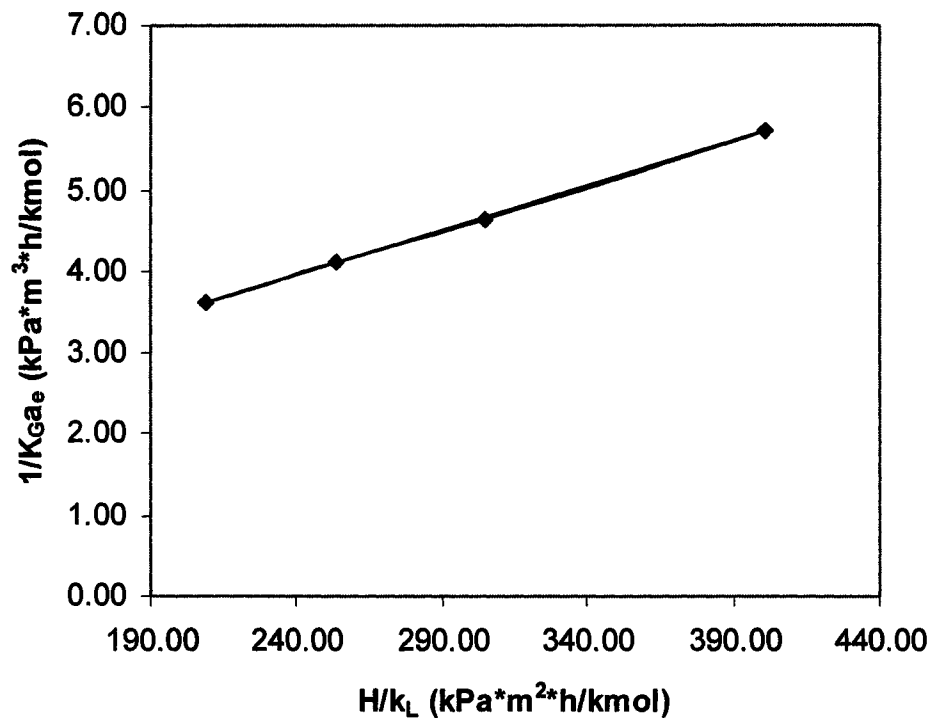


**Figure 5.1:** Linear relationship between  $(1/K_{Ga_e})$  and  $(H/k_L)$  for analysis of effective mass transfer area.

$$D_{CO_2, water} = 2.35 \times 10^{-6} \exp\left(\frac{-2119}{T}\right) \quad (5.5)$$

where  $D_{CO_2, water}$  = diffusion coefficient of CO<sub>2</sub> in water  
 $\mu_L$  = viscosity of aqueous solution  
 $\mu_{water}$  = viscosity of water  
 $T$  = absolute temperature

The viscosity ratio ( $\mu_L/\mu_{water}$ ) was calculated from an empirical equation reported by Weiland (1998) as functions of MEA weight percent concentration ( $w$ ), CO<sub>2</sub> loading ( $\alpha_{CO_2}$ ), and absolute temperature ( $T$ ):

$$\frac{\mu_L}{\mu_{water}} = \exp\left[\frac{(21.186 w + 2373) [\alpha_{CO_2} (0.01015 w + 0.0093 T - 2.2589) + 1] w}{T^2}\right] \quad (5.6)$$

The values for rate constant ( $k_2$ ) and concentration of active MEA in the aqueous solution ( $C_{MEA}$ ) were found from the following equations:

$$\log(k_2) = 10.99 - \frac{2152}{T} \quad (5.7)$$

$$C_{MEA} = \left(\frac{0.5 - \alpha_{CO_2}}{0.5}\right) C_{solution} \quad (5.8)$$

Figure 5.2 shows calculated values of effective mass transfer area, which were produced by P-28 nozzle at different liquid flow rates. It was found that the effective area varied significantly as the liquid flow rate was changed, i.e. it increased by more than 4 times when the flow rate increased from 1.9 to 4.6 m<sup>3</sup>/m<sup>2</sup>\*h. The increase in effective area with the liquid flow rate is a result of two main contributors; (i) a reduction in size of

spray droplet providing an increasing surface area of droplet per unit volume, and (ii) an increase in the number of spray droplets dispersed in the gas phase.

Figure 5.3 illustrates the extent of the two contributors causing the effective area to increase. When the reduction in size of spray droplet is considered to be the only contributor, the increase in effective area is presented by the dotted line. Note that the variation in effective area in this case was estimated by using an equation developed by Mugele (1960) that correlates the maximum drop diameter ( $D_m$ ) as a function of nozzle orifice diameter ( $d_o$ ), physical properties of the liquid, and the relative velocity of the dispersed liquid with respect to the continuous gas phase ( $u_r$ ):

$$D_m = 57 d_o \left( \frac{d_o \rho_L u_r}{\mu_L} \right)^{-0.48} \left( \frac{\mu_L u_r}{\sigma} \right)^{-0.18} \quad (5.9)$$

where  $\rho_L$  and  $\sigma$  are the density and surface tension of liquid, respectively. By taking into account the increasing number of spray droplet with liquid flow rate, the increase in effective area is presented in the solid line which provides a good agreement with the experimental data (closed circles).

Figure 5.4 shows the effective mass transfer area produced by P-28 nozzle at two different MEA concentrations, i.e. 3 kmol/m<sup>3</sup> and 5 kmol/m<sup>3</sup>. It was found that the effective area in both cases is comparable. This means the concentration of liquid solution has very little effect when compared to others process parameters such as liquid flow rate.

The effect of nozzle size on the effective area is demonstrated in Figure 5.5. It appears that at a given liquid flow rate the smaller nozzle P-28 provides a higher effective area than that of the larger nozzle P-40. This can be attributed to the fully developed

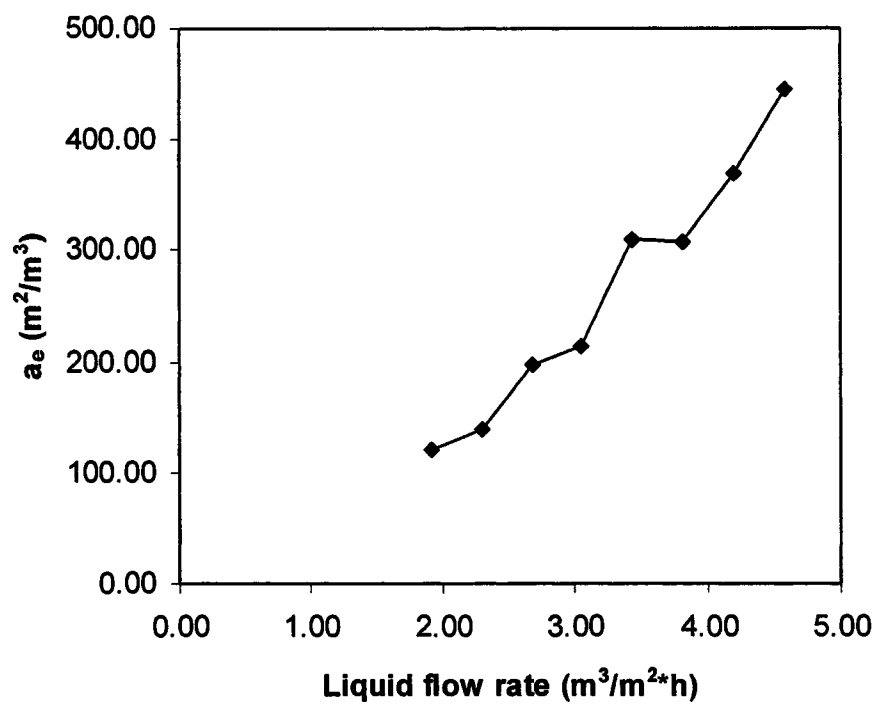


**Figure 5.2:** An increase in effective mass transfer area with liquid flow rate for P-28 nozzle (Gas flow rate=382 m<sup>3</sup>/m<sup>2</sup>-h, P<sub>CO2</sub>=15% CO<sub>2</sub>, [MEA] =3 kmol/m<sup>3</sup>)

spray cone for the smaller nozzle (P-28) that adds a greater surface area due to more uniform drops being produced. It should however be noted that the larger nozzle requires less energy to overcome a relatively low pressure-drop across the orifice. This means that the larger nozzle P-40 is capable of handling a wider range of liquid flow rate (see Table 4.2), thus offering a much higher effective area than that of the smaller nozzles P-20 and P-28. The P-40 nozzle produces larger spray droplet sizes than the others so one would imply that the area would be less. However, the higher liquid flow rate passing through the P-40 nozzle increases the overall area available for gas-liquid contact.

As mentioned in Chapter 4, the spray column offers a much higher overall mass transfer per the area tested. The P-40 nozzle required only approximately 0.1 m of space to absorb the CO<sub>2</sub>. This is about 75% less than the packed column. The reason for this is that the spray column offers a much higher effective mass transfer area than the packed column does when the two were tested against each other. The comparison of effective area between the two columns is given in Table 5.1.

## 5.2 Gas-Phase Mass Transfer Coefficient ( $k_G$ )

The gas-phase mass transfer coefficient can be analyzed from Equation (5.1) showing the relationship between the overall coefficient ( $K_G a_e$ ) and the individual phase coefficients ( $k_G a_e$  and  $k_L a_e$ ). By rearranging this equation, the individual mass transfer coefficient ( $k_G$ ) can be expressed as

$$\frac{1}{k_G} = \left\{ \left( \frac{1}{K_G a_e} \right) * (a_e) - \frac{H}{k_L} \right\} \quad (5.10)$$

From this equation, the  $k_G$  value was produced. The effective mass transfer area ( $a_e$ ) was obtained earlier as described in the previous section.

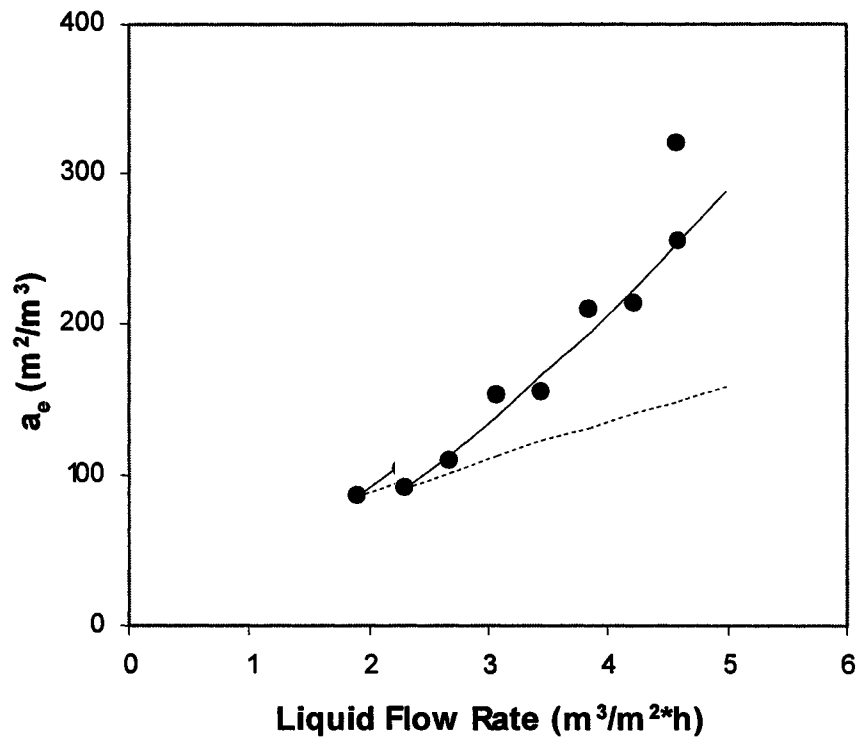


**Figure 5.3:** Contribution of reduction in droplet size and number of spray droplet to effective mass transfer area.

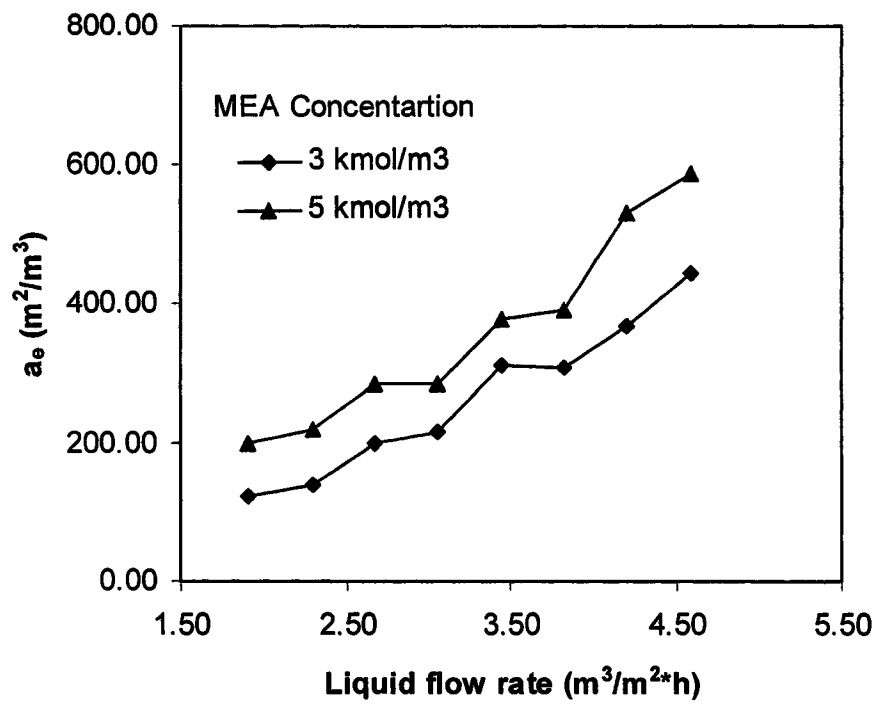


**Figure 5.4:** Effective mass transfer area at different MEA concentrations (Nozzle P-28, Gas flow rate= $382 \text{ m}^3/\text{m}^2\cdot\text{h}$ ,  $P_{\text{CO}_2}=15\%$ ).

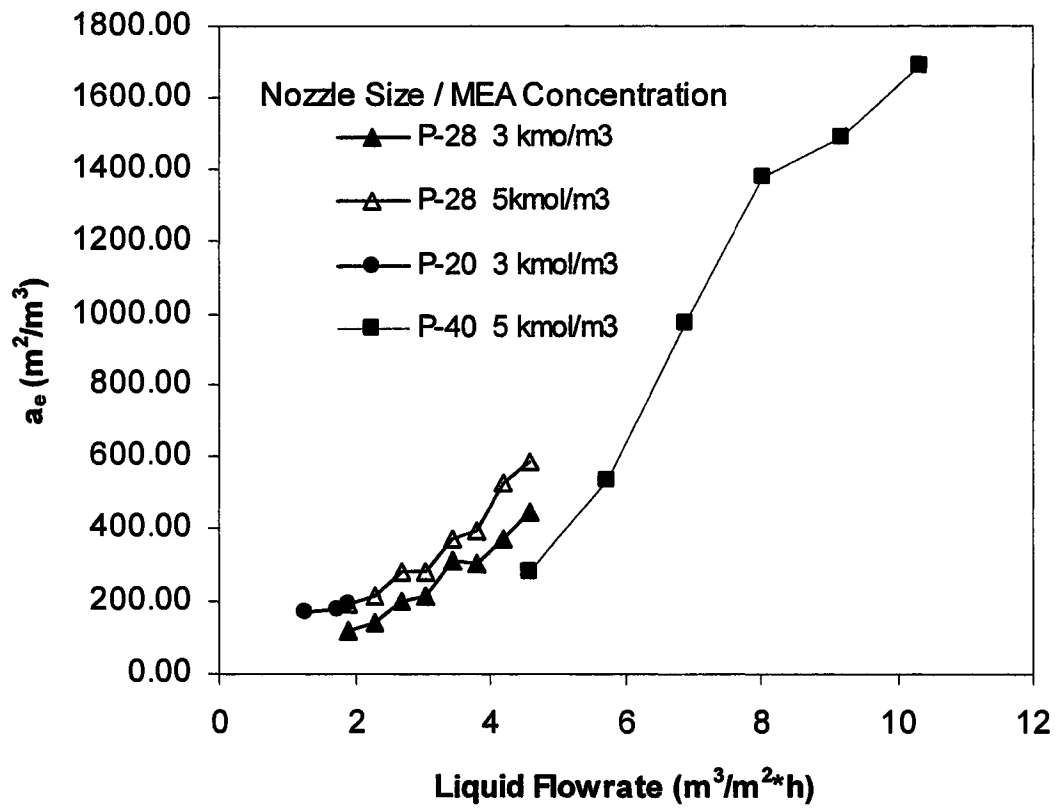


**Figure 5.5:** Effect of nozzle size on effective mass transfer area (Gas flow rate= $382 \text{ m}^3/\text{m}^2\cdot\text{h}$ ,  $P_{\text{CO}_2}=15\%$ ).

**Table 5.1:** Comparison of packed column and spray column with [MEA] = 5 kmol/m<sup>3</sup>, gas flow rate = 382 m<sup>3</sup>/m<sup>2</sup>\*h, 15 kPa CO<sub>2</sub>.

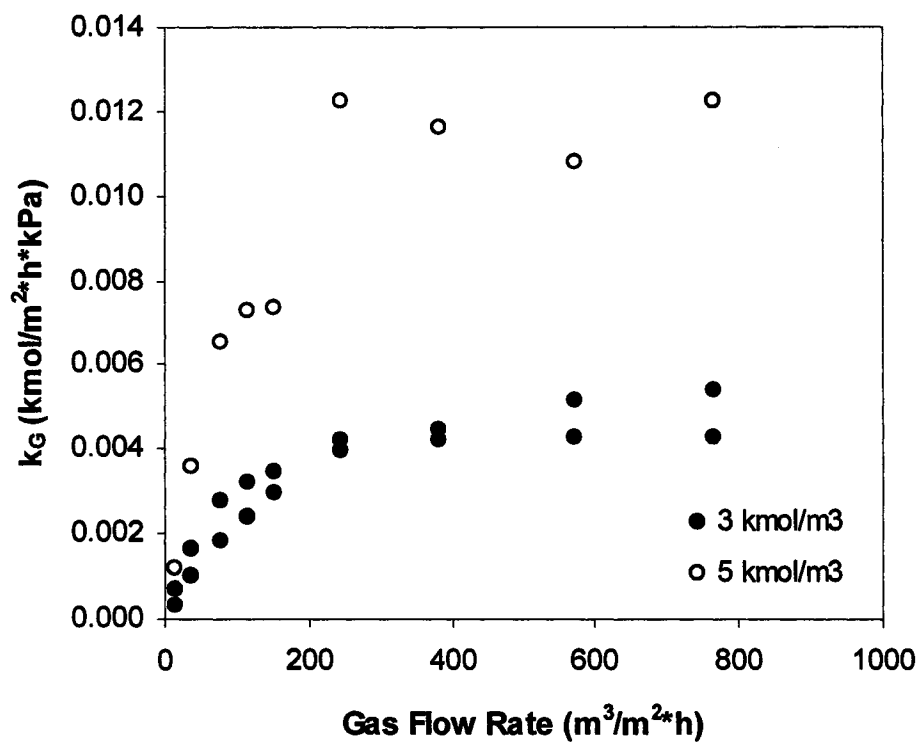
	P-40 Spray Nozzle	Packed Column
Liquid Flowrate (m <sup>3</sup> /m <sup>2</sup> *h)	Area (m <sup>2</sup> /m <sup>3</sup> )	
4.59	280.27	174.84
5.73	533.18	Not Tested
6.88	974.57	Not Tested
8.03	1379.72	248.96
9.17	1484.52	Not Tested
10.32	1685.73	252.48

Figure 5.6 shows calculated values of individual coefficient ( $k_G$ ) of P-28 nozzle presented as a function of gas flow rate. It was found that the  $k_G$  coefficient varied significantly with the gas flow rate of up to 245 m<sup>3</sup>/m<sup>2</sup>\*h. The coefficient then remained nearly unchanged under the high gas flow rate condition. The variation of the individual  $k_G$  coefficient with gas flow rate was found to follow the trend produced by the well-recognized equation of Onda et al (1968).

$$\frac{k_G RT}{a_t D_G} = C_1 \left( \frac{G}{a_t \mu_G} \right)^{0.7} \left( \frac{\mu_G}{\rho_G D_G} \right)^{1/3} (a_t D_p)^{-2.0} \quad (5.11)$$

- where  $D_G$  = gas-phase diffusion coefficient  
 $a_t$  = surface area of packing  
 $D_p$  = equivalent diameter of packing  
 $\mu_G$  = viscosity of gas stream  
 $\rho_G$  = density of gas stream  
 $G$  = gas flow rate  
 $C_1$  = constant for equation

Figure 5.7 shows that the  $k_G$  coefficient obtained from this study is proportional to  $G^{0.7}$  as suggested by the above equation.



**Figure 5.6:** Gas-phase mass transfer coefficient of P-28 nozzle.

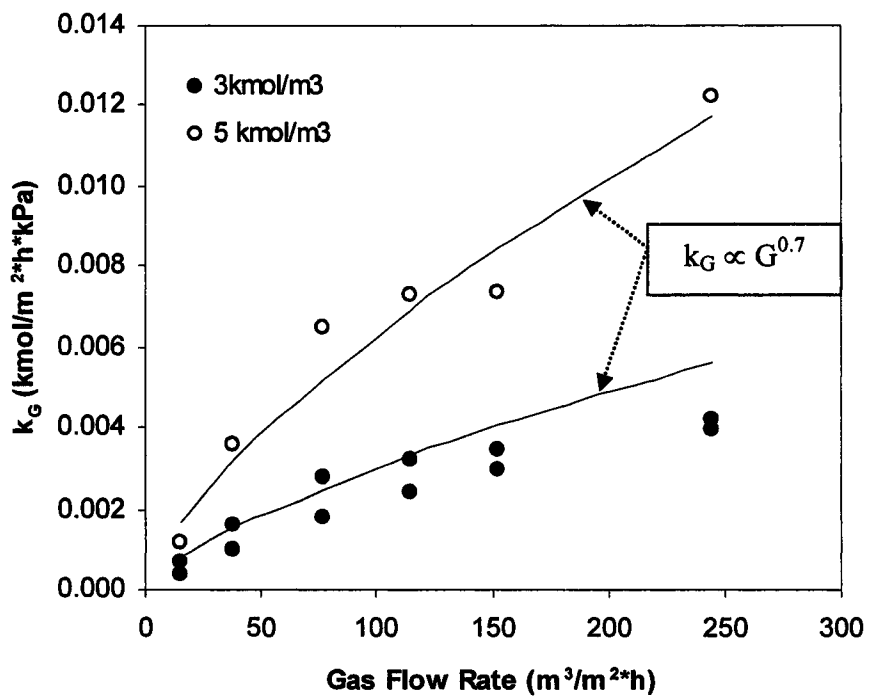


**Figure 5.7:** Gas-phase mass transfer coefficient and Onda et al correlation.

## Chapter Six

### Conclusion and Future Work

#### 6.1 Conclusions

The study was undertaken to determine the mass transfer performance and the viability of a spray column for the removal of CO<sub>2</sub> from gas streams. The performance was tested experimentally with an aqueous solution of MEA as the solvent, and reported in terms of the overall mass transfer coefficient  $K_{Ga_e}$ . The following principal conclusions can be drawn from the study.

The mass transfer coefficient  $K_{Ga_e}$  of the spray column was found to vary significantly with the tested variables. The  $K_{Ga_e}$  value becomes lower as the partial pressure of CO<sub>2</sub> in the gas-phase is increased. This is supported by the overall mass transfer equation. The  $K_{Ga_e}$  value increases with the increasing gas flow rate, and then remains constant when the gas flow rate exceeds 300 m<sup>3</sup>/m<sup>2</sup>-h. The  $K_{Ga_e}$  value also increases with an increase in liquid flow rate. This behavior is a result of the increasing effective mass transfer area available for gas-liquid contact within the spray column. The  $K_{Ga_e}$  value was found to increase with an increase in MEA concentration of liquid solvent from 3 to 7 kmol/m<sup>3</sup>. This finding is the opposite of what commonly takes place in the packed column. The  $K_{Ga_e}$  value is lower as the CO<sub>2</sub> loading of the liquid is increased. It was also found that the different nozzle sizes offer different ranges of  $K_{Ga_e}$  value. This is due to the difference in hydrodynamic capacity of each spray nozzle. Among all process variables tested, the liquid flow rate is the most influential variable that causes the variation in mass transfer performance of the spray column.

The fundamental mass transfer characteristics including effective mass transfer area ( $a_e$ ) and gas-phase mass transfer coefficient ( $k_G$ ) were analyzed from the experimental results. Each spray nozzle provides an individual range of effective area for mass transfer process. The P-40 nozzle produces the highest range of effective area, followed by P-28 and P-20 nozzles, respectively. Even though the P-40 nozzle having the largest orifice size offers the largest droplets, it allows at the same time for a higher rate of liquid to be dispersed throughout the gas space, thus resulting in more gas-liquid contact. The same can be said when comparing the P-28 and P-20 nozzles. The effective area is also most affected by the liquid flow rate while the gas flow rate and MEA concentration have small effects on the effective area produced. The individual mass transfer coefficient  $k_G$  was found to increase with the increasing gas flow rate, especially at the low range. The increase in  $k_G$  coefficient closely follows the trend derived from the Onda et al correlation. For the high range of gas flow rate, the  $k_G$  coefficient tends to remain constant as the performance of the spray column is primarily controlled by liquid-phase mass transfer.

The performance of spray column was directly compared with that of packed column. The comparison was carried out experimentally under identical conditions. It was found that the spray column is capable of removing more CO<sub>2</sub> from gas streams than the packed column by a factor of 2 to 7. Along with the higher performance, a much cheaper cost can be associated with the spray column due to the simplicity of the column and its internals (Appendix B).

## **6.2 Recommendations for Future Work**

As stated throughout the thesis, there is very little published information on the spray column for use in CO<sub>2</sub> removal application. The information obtained in this study gives a valid basis to further pursue the spray column a viable option in the removal of CO<sub>2</sub> from gas streams. Future work in this area should include the testing of other absorption solvents that can also be compared to that of a packed column. Other work can extend in the area of attempting to measure the drop size generated from the nozzles, and finding correlations that will aid in further study. Since it is a newer technology, the future work possibilities are endless but a lot can already be learned from all the data that has been produced from the packed column and the work can be streamlined to get immediate results. As more data is produced it will give a profound understanding where the spray column will fit in terms of efficiency and affordability.

## References

1. Aroonwilas, A. (1996). *High Efficiency Structured Packing for CO<sub>2</sub> Absorption Using 2-Amino-2-methyl-1-propanol (AMP): M.A.Sc. Thesis*, University of Regina, Regina, Saskatchewan, Canada.
2. Aroonwilas, A.; Veawab, V., Tontiwachwuthikul, P. (1999). Behavior of the Mass-Transfer Coefficient of Structured Packings in CO<sub>2</sub> Absorbers with Chemical Reactions. *Industrial Engineering Chemical Research*. **38**, 2044-2050.
3. Aroonwilas, A. (2001). *Mass Transfer with Chemical Reaction in Structured Packing for CO<sub>2</sub> Absorption Process: Ph.D. Thesis*, University of Regina, Regina, Saskatchewan, Canada.
4. Aroonwilas, A., Tontiwachwuthikul, P., and Chakma, A. (2001). Effects of operating and design parameters on CO<sub>2</sub> absorption in columns with structured packings. *Separation and Purification Technology*. **24**, 403-411.
5. Association of Official Analytical Chemists (AOAC): [www.aoac.org](http://www.aoac.org), 2006.
6. Astarita, G.; Savage, D. W. and Bistrot, A. (1983). *Gas Treating with Chemical Solvents*, John Wiley & Sons, New York.
7. Austgen, D. M. and Rochelle, G. T. (1989). Model of Vapor-Liquid Equilibria for Aqueous Acid Gas-Alkanolamine Systems using the Electrolyte-NRTL Equation. *Industrial Engineering Chemical Research*. **28(7)**, 1060-1073.
8. BETE Industrial Spray Nozzles: [www.bete.com](http://www.bete.com), 2006.
9. Blauwhoff, P. M. M.; Versteeg, G. F. and van Swaaij, W. P. M. (1984). A Study on the Reaction between CO<sub>2</sub> and Alkanolamines in Aqueous Solutions. *Chemical Engineering Science*. **39(2)**, 207-225.
10. Bravo, J. L. (1997). Select Structured Packing or Trays? *Chemical Engineering Progress*. **93(7)**, 36-41.
11. Canada and the Kyoto Protocol. [www.climatechange.gc.ca/cop/cop6\\_hague/english/overview\\_e.html](http://www.climatechange.gc.ca/cop/cop6_hague/english/overview_e.html). February 7, 2006.
12. DeCoursey, W. J, and Thring, R. W. (1989). Effects of Unequal Diffusivities on Enhancement Factors for Reversible and Irreversible Reaction. *Chemical Engineering Science*. **44(8)**, 1715.

13. Dimiccoli, A.; Di Serio, M. and Santacesaria, E. (2000). Mass Transfer and Kinetics in Spray-Tower-Loop Absorbers and Reactors. *Industrial Engineering Chemical Research*. **39(11)**, 4082-4093.
14. DOE – Fossil Energy: Carbon Capture and Separation: [www.fossil.energy.gov/programs/sequestration/capture](http://www.fossil.energy.gov/programs/sequestration/capture), March 3, 2006.
15. Drew, T. B. and Hoopes, J. W. Jr. (1956). *Advances in Chemical Engineering: Volume 1*, Academic Press, Inc., New York.
16. DuPart, M. S.; Bacon, T. R. and Edwards, D. J. (1993). Part 2 – Understanding Corrosion in Alkanolamine Gas Treating Plants. *Hydrocarbon Processing*. **72(5)**, 89-94.
17. Feldkamp, M.; Neumann, J. and Feldkamp, H. (2003). Influence of Droplet Collision on the Design of Flue-Gas Desulfurization Scrubbers in Power Plant Technology. *Chemical Engineering Technology*. **26(9)**, 956-959.
18. Fukunaka, Y.; Inada, A., Ogawa, A. and Asaki, Z. (1992). Absorption of CO<sub>2</sub> Gas into Falling Droplets of Aqueous NaOH Solution. *Metallurgical Review of MMIJ*. **9(1)**, 33-50.
19. Geankoplis, C. J. (1993). *Transport Processes and Unit Operations: 3<sup>rd</sup> Edition*, PTR Prentice-Hall Inc., New Jersey.
20. Greenhouse Gases, Climate Change and the Canadian Environmental Protection Act, 1999. [www.ec.gc.ca/press/2005/050902\\_b\\_e.htm](http://www.ec.gc.ca/press/2005/050902_b_e.htm). February 7, 2006.
21. Higbie, R. (1935). The Rate of Absorption of a Pure Gas into a Still Liquid During Short Periods of Exposure. *Transactions of American Institute of Chemical Engineers*. **31**, 365-389.
22. Hikita, H.; Asai, S., Ishikawa, H. and Honda, M. (1977). The Kinetics of Reactions of Carbon Dioxide with Monoethanolamine, Diethanolamine and Triethanolamine by a Rapid Mixing Method. *Chemical Engineering Journal*. **13**, 7-12.
23. IEA Greenhouse Gas R&D Programme, *Putting Carbon Back into the Ground*, February 2001, ISBN 1 898373 28 0.
24. Installation and Operating Instructions for Sulzer Columns C-803: [www.sulzer.com](http://www.sulzer.com), 2005.
25. Kohl, A. and Nielsen, R. (1997). *Gas Purification: 5<sup>th</sup> Edition*, Gulf Publishing Company, Houston, Texas.

26. Levenspiel, O. (1999). *Chemical Reaction Engineering: 3<sup>rd</sup> Edition*, John Wiley & Sons, New York.
27. Marland, G.; Boden T.A. and Andres, R.J. (2005) Global, Regional, and National CO<sub>2</sub> Emissions. *In Trends: A compendium of data on global change*. U.S. Department of Energy.
28. Mehta, K. C. and Sharma, M. M. (1970). Mass Transfer in Spray Columns. *British Chemical Engineering*. **15(11)**, 1440-1444.
29. Mugele, R. A. (1960). Maximum Stable Droplets in Dispersoids. *AIChEJ.* **6(3)**, 3-8.
30. Nguyen, K. D. and Spink, D. R. (1993). Turbotak Technology in FGD Scrubbers to Control SO<sub>2</sub> Emissions. *International Pittsburgh Coal Conference*. **10**, 812-817.
31. Nicholls, M. P.; Cumming, I. W. and Cloete, F. L. D. (1998). Performance of a Co-current Spray Gas-Liquid Contacting Stage. *ICHEME Research Event*.
32. Onda, K.; Takeuchi, H. and Okumoto, Y. (1968). Mass Transfer Coefficients between Gas and Liquid phases in Packed Column. *Journal Chemical Engineering of Japan*. **1(1)**, 56-62.
33. Overview of Climate Change Research. [www.exploratorium.edu/climate](http://www.exploratorium.edu/climate), September 19, 2005.
34. Perry, R.H. and Green, D. (1984). *Perry's Chemical Engineers' Handbook: 6<sup>th</sup> Edition*, McGraw-Hill Book Company, New York.
35. Reeve, D. A. (2000). The Capture and Storage of Carbon Dioxide Emissions. *Office of Energy Research and Development*.
36. Santacesaria, E.; Di Serio, M. and Tesser, R. (2005). Gas-Liquid and Gas-Liquid-Solid Reactions Performed in Spray Tower Loop Reactors. *Industrial Engineering Chemical Research*. **44(25)**, 9461-9472.
37. Sartori, G. and Savage, D.W. (1983). Sterically Hindered Amines for CO<sub>2</sub> Removal from Gases. *Industrial Engineering Chemistry Fundamentals*. **22**, 239.
38. Skarupa, R. C.,; Hargrove, O. W. Jr. and Carey, T. R. (1995). *International Pittsburgh Coal Conference*. **12**, 98-103.
39. Strigle, R. F. Jr. (1987) *Random Packings and Packed Towers: Design and Applications*. Gulf Publishing Company, Houston.

40. Taniguchi, I.; Takamura, Y. and Asano, K. (1997). Experimental Study of Gas Absorption with a Spray Column. *Journal of Chemical Engineering of Japan*. **30(3)**, 427-433.
41. Taniguchi, I.; Yokoyama, H. and Asano, K. (1999). Mass Transfer in Absorption of Lean Gas Using Small Spray Column. *Journal of Chemical Engineering of Japan*. **32(1)**, 145-150.
42. The GHG Protocol Initiative. [www.ghgprotocol.org](http://www.ghgprotocol.org). September 28, 2005.
43. Treybal, R. E. (1980). *Mass-Transfer Operations: 3<sup>rd</sup> Edition*. McGraw-Hill, Singapore.
44. Trompiz, C. J. and Fair, J., R. (2000). Entrainment from Spray Distributors for Packed Columns. *Industrial Engineering Chemical Research*. **39**, 1797-1808.
45. Versteeg, G. F. and van Swaaij, W. P. M. (1988). Solubility and Diffusivity of Acid Gases (CO<sub>2</sub>, N<sub>2</sub>O) in Aqueous Alkanolamine Solutions. *Journal Chemical Engineering Data*. **33**, 29-34.
46. Weiland, R. H.; Dingman, J. C., Cronin, D. B. and Browning, G. J. (1998). Density and Viscosity of Some Partially Carbonated Aqueous Alkanolamine Solutions and Their Blends. *Journal Chemical Engineering Data*. **43**, 378-382.
47. Weiland, R. H. and Browning, G. J. (1994). Physical Solubility of Carbon Dioxide in Aqueous Alkanolamines via Nitrous Oxide Analogy. *Journal Chemical Engineering Data*. **39**, 817-822.
48. Weiss, S.; Ruhland, F., Kind, R. (1990). Flue Gas Desulphurization by Absorption with Lime. *Inzynieria Chemiczna I Procesowa*. **11(1)**, 157-169.
49. Yeh, N. K. and Rochelle, G. T. (2003). Liquid-Phase Mass Transfer in Spray Contactors. *AIChE Journal*. **49(9)**, 2363-2373.

**Appendix A**  
Data from spray column with nozzles P-20, P-28, P-40 and  
packed column with Mellapak 500Y

### Appendix A1 – P-20 Nozzle Data

Nozzle	Gas Flow m <sup>3</sup> /m <sup>2</sup> *h	Liquid Flow m <sup>3</sup> /m <sup>2</sup> *h	P <sub>CO2</sub> In %	P <sub>CO2</sub> Out %	Conc. mol MEA/L	Loading In mol/mol	Loading Out mol/mol	Mass Balance %	K <sub>ga</sub> kmol/m <sup>3</sup> *h*kPa
P-20	38.22	1.53	5.35	1.10	3	0.0099	0.0248	-3.10	0.2778
P-20	38.22	1.53	5.60	1.46	3	0.1487	0.1587	-34.02	0.2488
P-20	38.22	1.53	5.35	1.58	3	0.2504	0.2628	-9.42	0.2306
P-20	38.22	1.53	5.35	2.07	3	0.3495	0.3619	3.34	0.1893
P-20	38.22	1.53	5.35	3.16	3	0.4561	0.4661	22.31	0.1158
P-20	76.43	1.53	5.60	1.82	3	0.0099	0.0397	4.27	0.4492
P-20	76.43	1.53	5.48	2.31	3	0.1487	0.1735	3.11	0.3611
P-20	76.43	1.53	5.35	2.67	3	0.2504	0.2727	9.32	0.2974
P-20	76.43	1.53	5.35	3.16	3	0.3495	0.3719	32.81	0.2311
P-20	76.43	1.53	5.60	4.25	3	0.4561	0.4661	-4.92	0.1280
P-20	114.65	1.53	5.48	2.55	3	0.0099	0.0446	1.79	0.4966
P-20	114.65	1.53	5.48	3.16	3	0.1487	0.1785	9.38	0.3683
P-20	114.65	1.53	5.60	3.40	3	0.2504	0.2777	5.38	0.3362
P-20	114.65	1.53	5.60	4.01	3	0.3495	0.3719	18.52	0.2293
P-20	114.65	1.53	5.48	4.74	3	0.4561	0.4661	13.34	0.1034
P-20	152.87	1.53	5.48	3.16	3	0.0099	0.0545	14.26	0.5666
P-20	152.87	1.53	5.48	3.52	3	0.1487	0.1884	20.08	0.4598
P-20	152.87	1.53	5.48	3.89	3	0.2504	0.2777	1.16	0.3606
P-20	152.87	1.53	5.48	4.25	3	0.3495	0.3768	30.96	0.2684
P-20	152.87	1.53	5.48	4.86	3	0.4561	0.4661	-5.42	0.1311
P-20	244.59	1.53	5.35	3.64	3	0.0099	0.0645	19.58	0.6837
P-20	244.59	1.53	5.48	4.01	3	0.1487	0.1884	0.89	0.5590
P-20	244.59	1.53	5.48	4.25	3	0.2504	0.2826	-1.91	0.4555
P-20	244.59	1.53	5.48	4.50	3	0.3495	0.3818	22.27	0.3570
P-20	244.59	1.53	5.48	5.11	3	0.4561	0.4661	-0.36	0.1308
P-20	382.17	1.53	5.48	4.13	3	0.0000	0.0843	25.06	0.6818
P-20	382.17	1.53	5.48	4.37	3	0.1487	0.1091	-19.34	0.5456
P-20	382.17	1.53	5.35	4.50	3	0.2529	0.2876	-2.96	0.4245
P-20	382.17	1.53	5.48	4.74	3	0.3520	0.3768	-19.47	0.3526
P-20	382.17	1.53	5.48	5.11	3	0.4561	0.4760	28.33	0.1770
P-20	573.25	1.53	5.60	4.62	3	0.0000	0.1091	23.65	0.6938
P-20	573.25	1.53	5.35	4.62	3	0.1487	0.2132	16.89	0.5317
P-20	573.25	1.53	5.48	4.86	3	0.2529	0.3074	12.97	0.4292
P-20	573.25	1.53	5.48	4.99	3	0.3520	0.3867	14.13	0.3645
P-20	573.25	1.53	5.48	5.23	3	0.4561	0.1091	2.04	0.1849
P-20	764.33	1.53	5.48	4.74	3	0.0000	0.1289	-5.32	0.7003
P-20	764.33	1.53	5.48	4.86	3	0.1487	0.2479	8.22	0.5775
P-20	764.33	1.53	5.48	4.99	3	0.2529	0.3173	12.78	0.4573
P-20	764.33	1.53	5.72	5.35	3	0.3520	0.4066	-8.03	0.3769
P-20	764.33	1.53	5.48	5.23	3	0.4561	0.4809	20.82	0.2688

**Appendix A1 – P-20 Nozzle Data (Continued)**

Nozzle	Gas Flow m <sup>3</sup> /m <sup>2</sup> h	Liquid Flow m <sup>3</sup> /m <sup>2</sup> h	P <sub>coz</sub> In %	P <sub>coz</sub> Out %	Conc. mol MEAL	Loading In mol/mol	Loading Out mol/mol	Mass Balance %	K <sub>ga</sub> kmol/m <sup>2</sup> h <sup>0.5</sup> kPa
P-20	15.29	1.53	10.45	1.10	3	0.0099	0.0248	21.56	0.1190
P-20	15.29	1.53	10.45	1.34	3	0.1487	0.1587	-17.03	0.1139
P-20	15.29	1.53	10.21	1.46	3	0.2504	0.2628	8.12	0.1104
P-20	15.29	1.53	10.45	2.07	3	0.3495	0.3619	11.82	0.0996
P-20	15.29	1.53	10.45	4.01	3	0.4561	0.4661	14.13	0.0691
P-20	38.22	1.53	10.33	2.31	3	0.0099	0.0397	-3.96	0.2754
P-20	38.22	1.53	10.21	2.91	3	0.1487	0.1735	-12.45	0.2424
P-20	38.22	1.53	10.33	3.52	3	0.2504	0.2777	2.44	0.2160
P-20	38.22	1.53	10.33	4.50	3	0.3495	0.3719	-3.15	0.1747
P-20	38.22	1.53	10.45	6.70	3	0.4561	0.4760	30.62	0.1018
P-20	76.43	1.53	10.33	4.01	3	0.0099	0.0595	-3.67	0.4033
P-20	76.43	1.53	10.33	4.86	3	0.1487	0.1834	-22.72	0.3321
P-20	76.43	1.53	10.45	5.72	3	0.2504	0.2925	7.35	0.2728
P-20	76.43	1.53	10.21	6.45	3	0.3495	0.3818	2.82	0.2115
P-20	76.43	1.53	10.33	8.41	3	0.4561	0.4710	-9.50	0.1005
P-20	114.65	1.53	10.33	5.60	3	0.0099	0.0694	-0.85	0.4233
P-20	114.65	1.53	10.21	6.21	3	0.1487	0.1983	-2.78	0.3490
P-20	114.65	1.53	10.33	7.07	3	0.2504	0.2975	12.00	0.2717
P-20	114.65	1.53	10.33	7.80	3	0.3495	0.3867	13.05	0.2041
P-20	114.65	1.53	10.21	9.13	3	0.4561	0.4710	4.61	0.0841
P-20	152.87	1.53	10.33	6.45	3	0.0099	0.0793	-2.54	0.4768
P-20	152.87	1.53	10.45	7.31	3	0.1487	0.2082	2.03	0.3689
P-20	152.87	1.53	10.45	7.92	3	0.2504	0.3024	10.03	0.2895
P-20	152.87	1.53	10.33	8.53	3	0.3495	0.3917	24.26	0.2023
P-20	152.87	1.53	10.33	9.61	3	0.4561	0.4710	8.87	0.0784
P-20	244.59	1.53	10.09	7.31	3	0.0099	0.0992	9.92	0.5243
P-20	244.59	1.53	10.21	7.80	3	0.1487	0.2082	-16.11	0.4425
P-20	244.59	1.53	10.33	8.53	3	0.2504	0.3124	15.82	0.3189
P-20	244.59	1.53	10.33	9.01	3	0.3495	0.3966	19.64	0.2289
P-20	244.59	1.53	10.45	9.85	3	0.4561	0.4760	10.16	0.1015
P-20	382.17	1.53	10.33	8.41	3	0.0099	0.1091	11.97	0.5311
P-20	382.17	1.53	10.33	8.65	3	0.1487	0.2330	8.58	0.4596
P-20	382.17	1.53	10.21	9.01	3	0.2529	0.3223	24.98	0.3247
P-20	382.17	1.53	10.21	9.25	3	0.3520	0.4016	11.41	0.2572
P-20	382.17	1.53	10.33	9.97	3	0.4561	0.4760	18.23	0.0946
P-20	573.25	1.53	10.21	8.89	3	0.0099	0.1537	12.89	0.5307
P-20	573.25	1.53	10.21	9.13	3	0.1487	0.2479	28.69	0.4295
P-20	573.25	1.53	10.21	9.37	3	0.2529	0.3471	13.21	0.3305
P-20	573.25	1.53	10.21	9.61	3	0.3520	0.4066	-7.95	0.2337
P-20	573.25	1.53	10.33	10.09	3	0.4561	0.4760	19.92	0.0927
P-20	764.33	1.53	10.09	9.13	3	0.0099	0.1934	13.21	0.5166
P-20	764.33	1.53	10.21	9.37	3	0.1487	0.2777	12.36	0.4447
P-20	764.33	1.53	10.21	9.61	3	0.2529	0.3619	-9.63	0.3143
P-20	764.33	1.53	10.33	9.85	3	0.3520	0.4462	-4.65	0.2478
P-20	764.33	1.53	10.33	10.15	3	0.4561	0.4809	1.02	0.0935

**Appendix A1 – P-20 Nozzle Data (Continued)**

Nozzle	Gas Flow m <sup>3</sup> /m <sup>2</sup> h	Liquid Flow m <sup>3</sup> /m <sup>2</sup> h	P <sub>co2</sub> In %	P <sub>co2</sub> Out %	Conc. mol MEAL	Loading In mol/mol	Loading Out mol/mol	Mass Balance %	K <sub>g,a</sub> kmol/m <sup>2</sup> h <sup>2</sup> kPa
P-20	15.29	1.53	15.26	1.70	3	0.0000	0.0198	5.10	0.1250
P-20	15.29	1.53	15.26	2.31	3	0.1487	0.1686	9.31	0.1160
P-20	15.29	1.53	15.37	3.16	3	0.2504	0.2677	0.44	0.1048
P-20	15.29	1.53	15.37	4.37	3	0.3520	0.3669	-5.57	0.0897
P-20	15.29	1.53	15.37	6.45	3	0.4512	0.4661	13.92	0.0682
P-20	38.22	1.53	15.26	4.62	3	0.0000	0.0496	11.35	0.2517
P-20	38.22	1.53	15.26	5.48	3	0.1487	0.1884	-3.99	0.2239
P-20	38.22	1.53	15.37	6.82	3	0.2504	0.2826	-12.09	0.1856
P-20	38.22	1.53	15.37	8.65	3	0.3520	0.3818	1.17	0.1377
P-20	38.22	1.53	15.37	11.16	3	0.4512	0.4710	4.79	0.0811
P-20	76.43	1.53	15.48	7.92	3	0.0000	0.0793	16.56	0.3268
P-20	76.43	1.53	15.37	9.37	3	0.1487	0.2082	8.58	0.2489
P-20	76.43	1.53	15.59	10.81	3	0.2504	0.2925	-5.24	0.1894
P-20	76.43	1.53	15.48	11.75	3	0.3520	0.3867	-0.89	0.1446
P-20	76.43	1.53	15.26	13.03	3	0.4512	0.4710	-6.71	0.0854
P-20	114.65	1.53	15.37	9.73	3	0.0000	0.0843	6.44	0.3545
P-20	114.65	1.53	15.04	11.16	3	0.1487	0.2132	16.80	0.2366
P-20	114.65	1.53	15.15	11.75	3	0.2504	0.2975	-3.40	0.2037
P-20	114.65	1.53	15.15	12.80	3	0.3520	0.3867	1.53	0.1375
P-20	114.65	1.53	15.26	13.93	3	0.4512	0.4710	1.51	0.0760
P-20	152.87	1.53	15.80	11.52	3	0.0000	0.1041	17.47	0.3646
P-20	152.87	1.53	15.26	12.22	3	0.1487	0.2132	2.20	0.2579
P-20	152.87	1.53	15.48	13.14	3	0.2504	0.3024	6.06	0.1927
P-20	152.87	1.53	15.48	13.37	3	0.3520	0.3966	0.48	0.1731
P-20	152.87	1.53	15.48	14.38	3	0.4512	0.4760	6.12	0.0890
P-20	244.59	1.53	15.26	12.10	3	0.0000	0.1091	5.72	0.4237
P-20	244.59	1.53	15.04	12.91	3	0.1487	0.2231	6.12	0.2817
P-20	244.59	1.53	15.48	13.48	3	0.2504	0.3223	8.29	0.2576
P-20	244.59	1.53	15.04	13.60	3	0.3520	0.4016	3.36	0.1883
P-20	244.59	1.53	15.04	14.38	3	0.4512	0.4760	12.01	0.0855
P-20	382.17	1.53	15.48	13.37	3	0.0000	0.1289	18.46	0.4239
P-20	382.17	1.53	15.59	13.71	3	0.1487	0.2529	6.96	0.3734
P-20	382.17	1.53	15.48	13.82	3	0.2529	0.3471	9.66	0.3295
P-20	382.17	1.53	15.48	14.27	3	0.3520	0.3917	-22.34	0.2380
P-20	382.17	1.53	15.37	14.93	3	0.4561	0.4760	-13.33	0.0859
P-20	573.25	1.53	15.26	13.82	3	0.0000	0.1339	21.64	0.4252
P-20	573.25	1.53	15.15	13.82	3	0.1487	0.2777	26.88	0.3940
P-20	573.25	1.53	15.37	14.16	3	0.2529	0.3818	-16.54	0.3543
P-20	573.25	1.53	15.37	14.49	3	0.3520	0.4314	17.21	0.2549
P-20	573.25	1.53	15.26	14.93	3	0.4561	0.4809	-2.28	0.0957
P-20	764.33	1.53	15.37	14.27	3	0.0000	0.1388	21.90	0.4317
P-20	764.33	1.53	15.37	14.38	3	0.1487	0.3074	14.96	0.3871
P-20	764.33	1.53	15.37	14.49	3	0.2529	0.4016	2.06	0.3428
P-20	764.33	1.53	15.48	14.82	3	0.3520	0.4661	-4.26	0.2537
P-20	764.33	1.53	15.15	14.93	3	0.4561	0.4809	8.89	0.0862

## Appendix A1 – P-20 Nozzle Data (Continued)

Nozzle	Gas Flow m <sup>3</sup> /m <sup>2</sup> *h	Liquid Flow m <sup>3</sup> /m <sup>2</sup> *h	P <sub>CO2</sub> In %	P <sub>CO2</sub> Out %	Conc. mol MEA/L	Loading In mol/mol	Loading Out mol/mol	Mass Balance %	K <sub>Gas</sub> kmol/m <sup>3</sup> *h*kPa
P-20	76.43	1.26	15.48	9.01	3	0.0000	0.0744	4.12	0.2636
P-20	76.43	1.26	15.37	10.45	3	0.1487	0.2082	7.92	0.1930
P-20	76.43	1.26	15.48	11.52	3	0.2504	0.2975	4.67	0.1507
P-20	76.43	1.26	15.48	12.57	3	0.3520	0.3867	3.66	0.1080
P-20	76.43	1.26	15.26	13.60	3	0.4512	0.4710	2.60	0.0612
P-20	76.43	1.41	15.48	8.41	3	0.0000	0.0744	7.46	0.2937
P-20	76.43	1.41	15.37	9.85	3	0.1487	0.2082	8.61	0.2201
P-20	76.43	1.41	15.48	11.28	3	0.2504	0.2925	-0.62	0.1606
P-20	76.43	1.41	15.48	12.10	3	0.3520	0.3867	0.79	0.1266
P-20	76.43	1.41	15.26	13.37	3	0.4512	0.4710	1.51	0.0700
P-20	76.43	1.53	15.48	7.92	3	0.0000	0.0793	16.56	0.3399
P-20	76.43	1.53	15.37	9.37	3	0.1487	0.2082	8.58	0.2588
P-20	76.43	1.53	15.48	10.81	3	0.2504	0.2925	-2.93	0.1930
P-20	76.43	1.53	15.48	11.75	3	0.3520	0.3867	-0.89	0.1504
P-20	76.43	1.53	15.26	13.03	3	0.4512	0.4710	-6.71	0.0889
P-20	76.43	1.64	15.48	7.68	3	0.0000	0.0744	14.11	0.3789
P-20	76.43	1.64	15.37	9.25	3	0.1487	0.2082	14.58	0.2839
P-20	76.43	1.64	15.48	10.45	3	0.2504	0.2925	-2.66	0.2248
P-20	76.43	1.64	15.48	11.52	3	0.3520	0.3867	0.50	0.1723
P-20	76.43	1.64	15.26	13.03	3	0.4512	0.4710	0.29	0.0952
P-20	76.43	1.76	15.48	7.43	3	0.0000	0.0645	2.86	0.4241
P-20	76.43	1.76	15.37	8.77	3	0.1487	0.2033	4.69	0.3347
P-20	76.43	1.76	15.48	9.85	3	0.2504	0.2925	-6.31	0.2754
P-20	76.43	1.76	15.48	11.40	3	0.3520	0.3867	4.55	0.1916
P-20	76.43	1.76	15.26	12.68	3	0.4512	0.4710	-6.68	0.1193
P-20	76.43	1.91	15.48	7.07	3	0.0000	0.0645	7.36	0.4489
P-20	76.43	1.91	15.37	8.28	3	0.1487	0.2082	16.26	0.3647
P-20	76.43	1.91	15.48	9.49	3	0.2504	0.2925	-3.92	0.2961
P-20	76.43	1.91	15.48	10.93	3	0.3520	0.3867	2.39	0.2165
P-20	76.43	1.91	15.26	12.68	3	0.4512	0.4710	1.43	0.1193

**Appendix A1 – P-20 Nozzle Data (Continued)**

<b>Nozzle</b>	<b>Gas Flow</b> m <sup>3</sup> /m <sup>2</sup> *h	<b>Liquid Flow</b> m <sup>3</sup> /m <sup>2</sup> *h	<b>P<sub>CO2</sub> In</b> %	<b>P<sub>CO2</sub> Out</b> %	<b>Conc.</b> mol MEA/L	<b>Loading In</b> mol/mol	<b>Loading Out</b> mol/mol	<b>Mass Balance</b> %	<b>K<sub>Ga<sub>e</sub></sub></b> kmol/m <sup>3</sup> *h*kPa
P-20	382.17	1.53	15.48	13.37	3	0.0000	0.1289	18.46	0.4239
P-20	382.17	1.53	15.59	13.71	3	0.1487	0.2529	6.96	0.3734
P-20	382.17	1.53	15.48	13.82	3	0.2529	0.3471	9.66	0.3295
P-20	382.17	1.53	15.48	14.27	3	0.3520	0.3917	-25.01	0.2380
P-20	382.17	1.53	15.37	14.93	3	0.4561	0.4760	-13.33	0.0859
P-20	382.17	1.53	15.48	12.22	5	0.0149	0.1190	4.57	0.7002
P-20	382.17	1.53	15.48	13.60	5	0.2499	0.3213	22.22	0.3914
P-20	382.17	1.53	15.37	14.82	5	0.4492	0.4685	12.65	0.1119
P-20	382.17	1.53	15.48	13.37	7	0.0149	0.2350	13.68	0.7821
P-20	382.17	1.53	15.26	14.27	7	0.2499	0.3272	25.75	0.4160
P-20	382.17	1.53	15.26	14.93	7	0.4492	0.4685	-5.61	0.1593
P-20	382.17	1.26	15.26	13.48	3	0.0248	0.1487	11.56	0.3727
P-20	382.17	1.26	15.80	14.38	3	0.2529	0.3619	21.02	0.2880
P-20	382.17	1.26	15.26	14.93	3	0.4512	0.4760	19.14	0.0672
P-20	382.17	1.53	15.48	13.37	3	0.0000	0.1289	18.46	0.4239
P-20	382.17	1.53	15.59	13.71	3	0.1487	0.2529	6.96	0.3734
P-20	382.17	1.53	15.48	13.82	3	0.2529	0.3471	9.66	0.3295
P-20	382.17	1.53	15.48	14.27	3	0.3520	0.3917	-23.65	0.2380
P-20	382.17	1.53	15.37	14.93	3	0.4561	0.4760	-13.33	0.0859
P-20	382.17	1.76	15.26	13.14	3	0.0248	0.1388	20.49	0.4478
P-20	382.17	1.76	15.80	14.16	3	0.2529	0.3570	15.67	0.3348
P-20	382.17	1.76	15.26	14.82	3	0.4512	0.4760	24.53	0.0900
P-20	382.17	1.91	15.37	12.91	3	0.0248	0.1388	13.14	0.5206
P-20	382.17	1.91	15.80	13.93	3	0.2529	0.3520	27.40	0.3824
P-20	382.17	1.91	15.26	14.71	3	0.4512	0.4760	8.27	0.1129

### Appendix A2 – P-28 Nozzle Data

Nozzle	Gas Flow m <sup>3</sup> /m <sup>2</sup> *h	Liquid Flow m <sup>3</sup> /m <sup>2</sup> *h	P <sub>CO2</sub> In %	P <sub>CO2</sub> Out %	Conc. mol MEA/L	Loading In mol/mol	Loading Out mol/mol	Mass Balance %	K <sub>Ga</sub> <sub>2</sub> kmol/m <sup>3</sup> *h*kPa
P-28	382.17	1.91	15.48	12.91	3	0.0099	0.1388	22.34	0.6777
P-28	382.17	1.91	15.69	13.82	3	0.1537	0.2529	27.37	0.4817
P-28	382.17	1.91	15.48	14.05	3	0.2529	0.3272	24.89	0.3683
P-28	382.17	1.91	15.59	14.49	3	0.3520	0.4115	29.97	0.2781
P-28	382.17	1.91	15.59	14.82	3	0.4512	0.4958	39.33	0.1954
P-28	382.17	2.29	15.59	13.03	3	0.0099	0.1289	35.53	0.6724
P-28	382.17	2.29	15.69	13.71	3	0.1537	0.2429	29.91	0.5120
P-28	382.17	2.29	15.48	13.93	3	0.2529	0.3223	29.87	0.3982
P-28	382.17	2.29	15.59	14.38	3	0.3520	0.4016	18.14	0.3071
P-28	382.17	2.29	15.59	14.82	3	0.4512	0.4859	30.04	0.1949
P-28	382.17	2.68	15.48	12.91	3	0.0099	0.1289	28.11	0.8132
P-28	382.17	2.68	15.69	13.60	3	0.1537	0.2330	27.62	0.6510
P-28	382.17	2.68	15.48	13.82	3	0.2529	0.3173	24.31	0.5140
P-28	382.17	2.68	15.59	14.27	3	0.3520	0.4016	26.33	0.4035
P-28	382.17	2.68	15.59	14.60	3	0.4512	0.4859	17.96	0.3031
P-28	382.17	3.06	15.48	12.68	3	0.0099	0.1190	13.56	0.8910
P-28	382.17	3.06	15.69	13.48	3	0.1537	0.2231	21.24	0.6880
P-28	382.17	3.06	15.48	13.71	3	0.2529	0.3173	1.23	0.5504
P-28	382.17	3.06	15.59	14.16	3	0.3520	0.3966	19.93	0.4388
P-28	382.17	3.06	15.59	14.49	3	0.4512	0.4859	21.31	0.3381
P-28	382.17	3.44	15.48	12.45	3	0.0099	0.1140	16.53	1.0778
P-28	382.17	3.44	15.48	13.25	3	0.1537	0.2231	26.79	0.7765
P-28	382.17	3.44	15.48	13.60	3	0.2529	0.3074	26.03	0.6523
P-28	382.17	3.44	15.59	13.93	3	0.3520	0.3966	16.91	0.5670
P-28	382.17	3.44	15.59	14.38	3	0.4512	0.4859	24.05	0.4149
P-28	382.17	3.82	15.48	11.98	3	0.0099	0.1091	39.79	1.2577
P-28	382.17	3.82	15.48	13.03	3	0.1537	0.2231	37.74	0.8609
P-28	382.17	3.82	15.48	13.37	3	0.2529	0.3074	25.30	0.7348
P-28	382.17	3.82	15.59	13.82	3	0.3520	0.3966	21.77	0.6071
P-28	382.17	3.82	15.59	14.38	3	0.4512	0.4809	18.14	0.4144
P-28	382.17	4.20	15.48	11.75	3	0.0099	0.1091	14.93	1.5185
P-28	382.17	4.20	15.48	12.91	3	0.1537	0.2231	12.68	1.0166
P-28	382.17	4.20	15.37	13.14	3	0.2529	0.3074	30.93	0.8805
P-28	382.17	4.20	15.59	13.71	3	0.3520	0.3966	26.06	0.7285
P-28	382.17	4.20	15.59	14.27	3	0.4512	0.4809	19.11	0.5106
P-28	382.17	4.59	15.48	11.63	3	0.0099	0.1091	5.23	1.5710
P-28	382.17	4.59	15.48	12.57	3	0.1537	0.2231	9.65	1.1630
P-28	382.17	4.59	15.37	12.80	3	0.2529	0.3074	24.22	1.0247
P-28	382.17	4.59	15.59	13.48	3	0.3520	0.3966	23.04	0.8207
P-28	382.17	4.59	15.59	14.16	3	0.4512	0.4809	19.93	0.5553

## Appendix A2 – P-28 Nozzle Data (Continued)

Nozzle	Gas Flow m <sup>3</sup> /m <sup>2</sup> *h	Liquid Flow m <sup>3</sup> /m <sup>2</sup> *h	P <sub>CO2</sub> In %	P <sub>CO2</sub> Out %	Conc. mol MEA/L	Loading In mol/mol	Loading Out mol/mol	Mass Balance %	K <sub>ga</sub> kmol/m <sup>3</sup> *h*kPa
P-28	382.17	1.91	15.69	13.03	5	0.0134	0.0982	28.55	0.6989
P-28	382.17	1.91	15.69	13.60	5	0.1473	0.2053	11.10	0.5425
P-28	382.17	1.91	15.59	13.82	5	0.2499	0.3034	21.77	0.4551
P-28	382.17	1.91	15.48	14.27	5	0.3525	0.3927	32.86	0.3094
P-28	382.17	1.91	15.48	14.82	5	0.4552	0.4775	35.43	0.1676
P-28	382.17	2.29	15.69	12.91	5	0.0134	0.0892	32.50	0.7309
P-28	382.17	2.29	15.69	13.37	5	0.1473	0.2053	20.62	0.6044
P-28	382.17	2.29	15.59	13.60	5	0.2499	0.3034	29.88	0.5160
P-28	382.17	2.29	15.48	14.16	5	0.3525	0.3882	29.89	0.3388
P-28	382.17	2.29	15.48	14.60	5	0.4552	0.4775	21.84	0.2252
P-28	382.17	2.68	15.69	12.68	5	0.0134	0.0848	34.74	0.9548
P-28	382.17	2.68	15.69	13.14	5	0.1473	0.2053	28.48	0.8006
P-28	382.17	2.68	15.59	13.48	5	0.2499	0.3034	10.32	0.6562
P-28	382.17	2.68	15.48	14.05	5	0.3525	0.3882	5.63	0.4422
P-28	382.17	2.68	15.48	14.49	5	0.4552	0.4775	26.33	0.3052
P-28	382.17	3.06	15.69	12.22	5	0.0134	0.0848	34.18	1.1139
P-28	382.17	3.06	15.69	12.91	5	0.1473	0.2053	35.10	0.8771
P-28	382.17	3.06	15.59	13.37	5	0.2499	0.2990	8.65	0.6934
P-28	382.17	3.06	15.48	13.93	5	0.3525	0.3838	29.87	0.4781
P-28	382.17	3.06	15.48	14.38	5	0.4552	0.4775	29.92	0.3404
P-28	382.17	3.44	15.69	11.87	5	0.0134	0.0848	9.63	1.3741
P-28	382.17	3.44	15.69	12.68	5	0.1473	0.2008	29.92	1.0609
P-28	382.17	3.44	15.59	13.25	5	0.2499	0.2945	2.31	0.8122
P-28	382.17	3.44	15.48	13.71	5	0.3525	0.3838	27.83	0.6118
P-28	382.17	3.44	15.48	14.27	5	0.4552	0.4775	32.86	0.4177
P-28	382.17	3.82	15.69	11.52	5	0.0134	0.0803	31.88	1.5137
P-28	382.17	3.82	15.69	12.45	5	0.1473	0.2008	34.43	1.1486
P-28	382.17	3.82	15.59	13.14	5	0.2499	0.2900	32.83	0.8542
P-28	382.17	3.82	15.48	13.60	5	0.3525	0.3838	33.67	0.6526
P-28	382.17	3.82	15.48	14.16	5	0.4552	0.4775	35.31	0.4575
P-28	382.17	4.20	15.69	11.40	5	0.0134	0.0803	12.83	1.7561
P-28	382.17	4.20	15.69	12.22	5	0.1473	0.2008	6.32	1.3924
P-28	382.17	4.20	15.59	12.91	5	0.2499	0.2856	19.06	1.0567
P-28	382.17	4.20	15.48	13.37	5	0.3525	0.3838	31.56	0.8270
P-28	382.17	4.20	15.48	14.05	5	0.4552	0.4775	5.66	0.5597
P-28	382.17	4.59	15.69	10.81	5	0.0134	0.0803	36.39	2.0287
P-28	382.17	4.59	15.69	11.98	5	0.1473	0.1963	30.02	1.4943
P-28	382.17	4.59	15.59	12.68	5	0.2499	0.2856	19.92	1.1539
P-28	382.17	4.59	15.48	13.14	5	0.3525	0.3838	29.86	0.9213
P-28	382.17	4.59	15.48	13.93	5	0.4552	0.4730	11.32	0.6046

**Appendix A2 – P-28 Nozzle Data (Continued)**

Nozzle	Gas Flow m <sup>3</sup> /m <sup>2</sup> h	Liquid Flow m <sup>3</sup> /m <sup>2</sup> h	P <sub>CO2</sub> in %	P <sub>CO2</sub> Out %	Conc. mol MEA/L	Loading In mol/mol	Loading Out mol/mol	Mass Balance %	K <sub>ea</sub> kmol/m <sup>3</sup> h <sup>0.5</sup> kPa
P-28	76.43	2.29	15.48	11.75	3	0.0099	0.1091	15.35	0.4771
P-28	76.43	2.68	15.48	11.63	3	0.0099	0.1091	29.22	0.5332
P-28	76.43	3.06	15.69	13.82	3	0.1537	0.2529	27.37	0.5826
P-28	76.43	3.44	15.69	13.71	3	0.1537	0.2429	29.91	0.6239
P-28	76.43	3.82	15.69	13.60	3	0.1537	0.2330	27.62	0.6559
P-28	76.43	4.20	15.69	13.48	3	0.1537	0.2231	21.24	0.0001
P-28	15.29	1.91	15.59	1.46	3	0.0099	0.0248	-5.55	0.1687
P-28	38.22	1.91	15.48	3.40	3	0.0099	0.0496	-0.89	0.3871
P-28	76.43	1.91	15.48	6.33	3	0.0099	0.0744	-0.47	0.5421
P-28	114.65	1.91	15.37	8.65	3	0.0099	0.0892	6.26	0.5676
P-28	152.87	1.91	15.37	10.45	3	0.0099	0.1041	17.72	0.5659
P-28	244.59	1.91	15.15	11.28	3	0.0099	0.1091	-0.90	0.6912
P-28	382.17	1.91	15.37	12.91	3	0.0099	0.1686	12.66	0.6508
P-28	573.25	1.91	15.48	13.82	3	0.0099	0.1735	14.66	0.6329
P-28	764.33	1.91	15.80	14.49	3	0.0099	0.1785	15.00	0.6582
P-28	15.29	4.59	15.15	0.98	3	0.0099	0.0149	-23.92	0.2655
P-28	38.22	4.59	15.26	2.07	3	0.0099	0.0248	-17.01	0.6800
P-28	76.43	4.59	15.69	3.76	3	0.0099	0.0397	-13.37	1.1601
P-28	114.65	4.59	15.37	5.35	3	0.0099	0.0545	-0.25	1.4190
P-28	152.87	4.59	15.37	7.07	3	0.0099	0.0645	0.56	1.5891
P-28	244.59	4.59	15.37	8.89	3	0.0099	0.0744	-5.38	1.8458
P-28	382.17	4.59	15.37	10.93	3	0.0099	0.0892	6.91	1.8549
P-28	573.25	4.59	15.26	12.10	3	0.0099	0.1339	7.55	1.8960
P-28	764.33	4.59	15.59	13.14	3	0.0099	0.1388	6.32	1.9112
P-28	764.33	1.91	15.80	14.49	3	0.0099	0.1785	12.89	0.6582
P-28	15.29	1.91	15.80	14.49	3	0.0535	0.1785	-10.23	0.6582
P-28	38.22	1.91	15.37	4.25	5	0.0535	0.0773	6.87	0.3454
P-28	76.43	1.91	15.37	6.70	5	0.0535	0.0922	4.71	0.5093
P-28	114.65	1.91	15.26	8.65	5	0.0535	0.0982	1.39	0.5602
P-28	152.87	1.91	15.26	10.21	5	0.0535	0.1041	3.02	0.5865
P-28	244.59	1.91	15.26	11.52	5	0.0535	0.1101	-3.05	0.6626
P-28	382.17	1.91	15.48	12.91	5	0.0535	0.1190	3.52	0.6777
P-28	573.25	1.91	15.37	13.48	5	0.0535	0.1309	11.97	0.7286
P-28	764.33	1.91	15.37	13.93	5	0.0535	0.1487	13.22	0.7382
P-28	15.29	4.59	15.48	0.86	5	0.0535	0.0595	47.13	0.2711
P-28	38.22	4.59	15.37	1.70	5	0.0535	0.0654	7.10	0.7129
P-28	76.43	4.59	15.37	3.64	5	0.0535	0.0744	3.33	1.1613
P-28	114.65	4.59	15.26	5.23	5	0.0535	0.0833	10.97	1.4333
P-28	152.87	4.59	15.26	6.70	5	0.0535	0.0863	-1.96	1.6652
P-28	244.59	4.59	15.26	8.41	5	0.0535	0.0952	-3.05	1.9887
P-28	382.17	4.59	15.37	10.57	5	0.0535	0.1190	17.55	2.0230
P-28	573.25	4.59	15.37	11.98	5	0.0535	0.1309	21.39	2.0316
P-28	764.33	4.59	15.37	12.80	5	0.0535	0.1309	6.55	2.0379

## Appendix A3 – P-40 Nozzle Data

Nozzle	Gas Flow m <sup>3</sup> /m <sup>2</sup> *h	Liquid Flow m <sup>3</sup> /m <sup>2</sup> *h	P <sub>CO2</sub> In %	P <sub>CO2</sub> Out %	Conc. mol MEAL	Loading In mol/mol	Loading Out mol/mol	Mass Balance %	K <sub>GA<sub>0</sub></sub> kmol/m <sup>3</sup> *h*kPa
P-40	382.17	4.59	15.48	11.28	5	0.0089	0.0535	5.55	1.2588
P-40	382.17	4.59	15.48	12.33	5	0.1517	0.1830	-2.54	0.9182
P-40	382.17	4.59	15.48	13.03	5	0.2544	0.2811	6.25	0.7044
P-40	382.17	4.59	15.48	13.71	5	0.3525	0.3748	21.74	0.5006
P-40	382.17	4.59	15.48	14.60	5	0.4507	0.4596	-2.53	0.2447
P-40	382.17	5.73	15.48	11.16	5	0.0089	0.0491	15.65	2.0400
P-40	382.17	5.73	15.48	12.22	5	0.1517	0.1785	0.83	1.5005
P-40	382.17	5.73	15.48	12.80	5	0.2544	0.2767	1.47	1.2172
P-40	382.17	5.73	15.48	13.48	5	0.3525	0.3704	8.21	0.8919
P-40	382.17	5.73	15.48	14.49	5	0.4507	0.4596	8.28	0.4343
P-40	382.17	6.88	15.48	10.93	5	0.0089	0.0446	17.26	3.0315
P-40	382.17	6.88	15.48	11.87	5	0.1517	0.1740	-8.57	2.3464
P-40	382.17	6.88	15.48	12.33	5	0.2544	0.2767	4.42	2.0203
P-40	382.17	6.88	15.48	13.14	5	0.3525	0.3704	11.31	1.4740
P-40	382.17	6.88	15.48	14.27	5	0.4507	0.4596	6.29	0.7490
P-40	382.17	8.03	15.48	10.21	5	0.0089	0.0402	4.31	4.4696
P-40	382.17	8.03	15.48	11.28	5	0.1517	0.1740	-7.64	3.4617
P-40	382.17	8.03	15.48	11.87	5	0.2544	0.2767	6.67	2.9333
P-40	382.17	8.03	15.48	12.80	5	0.3525	0.3704	13.65	2.1310
P-40	382.17	8.03	15.48	14.05	5	0.4507	0.4596	4.90	1.1151
P-40	382.17	9.17	15.48	9.25	5	0.0089	0.0402	1.90	5.4317
P-40	382.17	9.17	15.48	10.69	5	0.1517	0.1740	-6.87	4.0124
P-40	382.17	9.17	15.48	11.52	5	0.2544	0.2767	11.53	3.2479
P-40	382.17	9.17	15.48	12.45	5	0.3525	0.3704	15.49	2.4264
P-40	382.17	9.17	15.48	13.71	5	0.4507	0.4596	-2.61	1.3888
P-40	382.17	10.32	15.48	8.65	5	0.0089	0.0402	5.20	6.0677
P-40	382.17	10.32	15.48	10.21	5	0.1517	0.1740	-4.20	4.4696
P-40	382.17	10.32	15.48	11.04	5	0.2544	0.2767	12.72	3.6796
P-40	382.17	10.32	15.48	12.10	5	0.3525	0.3704	16.98	2.7288
P-40	382.17	10.32	15.48	13.48	5	0.4507	0.4596	-2.61	1.5748

## Appendix A4 – Packed Column Data

Nozzle	Gas Flow m <sup>3</sup> /m <sup>2</sup> *h	Liquid Flow m <sup>3</sup> /m <sup>2</sup> *h	P <sub>CO2</sub> In %	P <sub>CO2</sub> Out %	Conc. mol MEA/L	Loading In mol/mol	Loading Out mol/mol	Mass Balance %	K <sub>Ga</sub> <sub>o</sub> kmol/m <sup>3</sup> *h*kPa
Packed	382.17	4.59	15.48	7.07	5	0.1517	0.2276	-6.21	0.3931
Packed	382.17	4.59	15.59	8.04	5	0.2544	0.3525	33.74	0.3405
Packed	382.17	4.59	15.69	10.21	5	0.3525	0.4239	30.55	0.2315
Packed	382.17	4.59	15.48	10.57	5	0.4507	0.5132	27.39	0.2114
Packed	382.17	8.03	15.48	5.48	5	0.1517	0.2097	7.37	0.4943
Packed	382.17	8.03	15.59	6.21	5	0.2544	0.3168	22.24	0.4496
Packed	382.17	8.03	15.69	8.53	5	0.3525	0.4016	22.38	0.3177
Packed	382.17	8.03	15.48	10.09	5	0.4507	0.4909	31.31	0.2334
Packed	382.17	10.32	15.48	4.01	5	0.1517	0.2008	3.45	0.6002
Packed	382.17	10.32	15.59	5.48	5	0.2544	0.2990	4.93	0.4978
Packed	382.17	10.32	15.69	7.68	5	0.3525	0.3882	3.25	0.3650
Packed	382.17	10.32	15.48	9.49	5	0.4507	0.4819	18.94	0.2633

**Appendix B**  
**Economics of spray and packed column**

	<b>Spray Column</b>	<b>Packed Column</b>	<b>Packed Column</b>	<b>Spray Column</b>	<b>Packed Column</b>	<b>Packed Column</b>
		<b>Random Packing</b>	<b>Structured Packing</b>		<b>Random Packing</b>	<b>Structured Packing</b>
<b>Column Height (m)</b>	0.40	0.40	0.40	8.0	8.0	8.0
<b>Column diameter (m)</b>	0.10	0.10	0.10	2.0	2.0	2.0
<b>Nozzles Required</b>	1	-	-	11	-	-
<b>Cost per Nozzle (US\$)</b>	40	-	-	40	-	-
<b>US\$ Cost per m<sup>3</sup></b>	-	3,045	10,660	-	3,045	10,660
<b>Total Volume (m<sup>3</sup>)</b>	0.00314	0.00314	0.00314	25.133	25.133	25.133
<b>Total Cost (US\$)</b>	40	9.57	33.49	440.00	76529.13	267914.80

Packed column calculation based on 2" stainless steel Pall rings @ \$86.20/ft<sup>3</sup> and cost of structured packing \$258.60/ft<sup>3</sup>. Costs shown are for internals only.